(EXAMINER'S COPY)

DESIGN AND IMPLEMENTATION OF A THYRISTOR CONTROLLED SERIES CAPACITOR FOR RESEARCH LABORATORY APPLICATION

By

Ronnie Happy-Boy Mazibuko

BScEng

Submitted in fulfillment of the academic requirements for the degree of Master of Science in Engineering, in the Department of Electrical Engineering, University of Natal, Durban, South Africa.

September 2003

I hereby declare that all the material incorporated into this thesis is my own original and unaided work except where specific reference is made by name or in the form of a numbered reference. The work contained herein has not been submitted for a degree at any other university.

Signed: _____

R H Mazibuko

ABSTRACT

The power transfer capability of a transmission line is determined by the magnitude of the voltage at each end of the line, angle difference of these voltages and the impedance of the line. This impedance is mainly inductive. Traditionally, fixed series capacitor banks have been used for series compensation. However, due to instability problems associated with loading transmission line close to their thermal limits, researchers have looked at other alternatives to line compensation by static devices such as fixed series capacitors. Flexible AC Transmission Systems (FACTS) has allowed power utilities to use existing transmission line networks close to their thermal limits without compromising stability of the power system. A FACTS series compensator is capable of influencing the transmission of power in a transmission line by dynamic control of the series compensating reactance inserted in the line. There are several different devices under the FACTS family, however, in this thesis only the Thyristor-Controlled Series Capacitor (TCSC) was considered. A TCSC comprises a fixed capacitor in parallel with a thyristor-controlled reactor (TCR). By varying the firing angle $\propto$ of the thyristors, the TCSC can be made to act in variable inductive or capacitive reactance mode. The thesis' overall objective was to design a practical TCSC for use in a research laboratory for further research initiatives.

This thesis looks at different issues that need to be considered when designing and rating a TCSC compensator. In particular, the thesis examines the effects of different sizes of TCSC components on the rating of the device, the effects of harmonics on the TCSC ratings, sizing of TCSC's variable reactance, and the response time of TCSC to a step change in the firing angle.

A mathematical model of a TCSC in a single-machine infinite bus (SMIB) system was developed and subsequently used in the initial design of the TCSC. Studies that were done using mathematical model of the TCSC module confirmed the ability of the

TCSC controller to dynamically control the capacitive compensating reactance in the transmission line. The thesis then describes the development of a laboratory-scale TCSC for research investigations. Measured results from the laboratory demonstrate the ability of the TCSC series compensator to provide rapid control of series reactance of a transmission line. A detailed mathematical model of the SMIB equipped with TCSC module was developed, using parameter values of the laboratory scale prototype, to investigate power oscillation damping. Time-domain simulation results are presented in this thesis to demonstrate its ability to damp power swings in an electrical network.

ACKNOWLEDGEMENTS

The work presented in this thesis was carried out under the supervision of Dr. Bruce S. Rigby and Professor Ronald G. Harley both of the Department of Electrical Engineering, University of Natal, Durban. I would like to thank Dr. Rigby for his support, guidance throughout the course of this thesis, and for his efforts during the correction of this thesis. I would also like to thank Professor Harley for affording me the opportunity to carry out this research work.

In addition, I would like to thank the following people:

The workshop staff for their input during TCSC circuit design

My family for their support, patience and their best wishes

My friends for their support

Eskom and University of Natal for providing much needed financial support

The staff and postgraduate students of Electrical and Electronic Engineering, unfortunately too many to mention by name.

God for making everything possible

TABLE OF CONTENTS

Abstract i

Acknowledgements iii

List of Figures and Tables ix

List of Symbols xiv

CHAPTER ONE INTRODUCTION

1.1 Background 1.1

1.2 FACTS Series Compensators 1.3

1.3 Thyristor-Controlled Series Capacitor 1.3

1.4 Objectives Of The Thesis 1.4

1.5 Thesis Layout 1.6

1.6 Research Publications 1.7

CHAPTER TWO GENERAL OPERATION OF THE TCSC

2.1 Introduction 2.1

2.2 The world's first multi-module TCSC system [2] 2.2

2.3 Operating principles of a TCSC 2.4

2.4 Factors considered when selecting the inductor of the reactor loop 2.9

2.4.1 Introduction 2.9

2.4.2 Firing region 2.10

2.4.3 The Reactance Order 2.13

2.4.4 Operating Capability of the TCSC 2.14

2.4.5 Rating the TCSC Components 2.16

2.4.6 Harmonic Performance of the TCSC 2.17

2.4.7 Transient Response of the TCSC 2.19

2.4.8 Frequency Response of the TCSC 2.23

2.5 Some common applications of the TCSC 2.24

2.5.1 Power Swing Damping 2.24

2.5.2 Mitigation of Subsynchronous Resonance 2.26

2.6 Conclusion 2.6

CHAPTER 3 MATHEMATICAL MODELING FOR COMPUTER SIMULATION OF TCSC

3.1 Introduction 3.1

3.2 Trigger circuit for the TCR 3.2

3.3 Sizing of TCSC Variable Reactance Range 3.6

3.4 TCSC Design and Rating 3.7

3.4.1 Sizing the TCSC's Internal Capacitor 3.7

3.4.2 Determining the TCSC's Maximum Reactance Order 3.8

3.4.3 Sizing the TCSC Inductor 3.8

3.4.4 Rating the TCSC's Circuit Components 3.18

3.5 Harmonic Analysis of the TCSC 3.20

3.5.1 TCSC Harmonic Voltage 3.20

3.5.2 Harmonic Analysis of the Line Current 3.22

3.6 Conclusion 3.24

4. DEVELOPMENT OF A LABORATORY PROTOTYPE TCSC

4.1 Introduction 4.1

4.2 Practical Implementation 4.2

4.2.1 Hardware Description 4.2

4.3 Practical Results 4.10

4.3.1 Practical TCSC Characteristics 4.10

4.3.2 Comparison of Simulated and Measured Results 4.12

4.4 Conclusion 4.24

5. APPLICATION OF THE TCSC TO DAMP POWER SYSTEM OSCILLATIONS ON A SMIB SYSTEM

5.1 Introduction 5.1

5.2 Application of the TCSC in Power System Oscillation Damping 5.2

5.3 Results of the Power Oscillation Damping Study 5.3

5.3.1 Trigger Circuit Control Strategy 5.3

5.4 Conclusion 5.9

6. CONCLUSION

6.1 Introduction 6.1

6.2 Factors that Influence the Design of the TCSC 6.1

6.3 Mathematical Models to Study the Performance of the TCSC 6.2

6.4 Development of the Laboratory-Scale TCSC 6.3

6.5 Power Oscillation Damping using the TCSC 6.4

6.6 Suggestions for Further Work 6.4

APPENDICES

APPENDIX A PARAMETERS OF A SIMPLE EMTDC CIRCUIT USED DURING THE TCSC DESIGN STAGE

A.1 Parameters of a Simple Circuit with a TCSC Device A.1

A.1.1 Derivation of the Per-Unit System A.1

A.1.2 Transmission Line Impedance A.1

A.1.3 TCSC Device A.1

APPENDIX B MODIFIED TRIGGER CIRCUIT FOR THE CONTROL OF A THYRISTOR CONTROLLED SERIES CAPACITOR

APPENDIX C ADDITIONAL SIMULATION DETAILS AND RESULTS FROM CHAPTER FOUR

APPENDIX D EMTDC SIMULATION MODEL FOR POWER OSCILLATION DAMPING STUDY

D.1 Parameters of a Detailed EMTDC Circuit _____ D.1

D 1.1 Generator Parameters (per unit unless stated) _____ D.1

D 1.2 Turbine Model _____ D.2

D 1.3 Transmission Line and TCSC Parameters (per phase) _____ D.2

D 1.4 Infinite Bus-Bar _____ D.3

REFERENCES _____ **R.1**

LIST OF FIGURES AND TABLES

FIGURES **PAGE**

Fig. 1.1 Two-machine power system diagram.....1.1

Fig. 1.2 Two-machine power system diagram with series compensating capacitors.....1.2

Fig. 1.3 Diagram of a TCSC module.....1.4

Fig. 2.1 One-line diagram of Slatt TCSC.....2.1

Fig. 2.2 TCSC Module in series with a conventional capacitor.....2.4

Fig. 2.3 The reactance vs delay firing angle characteristic of the TCSC.....2.4

Fig. 2.4 TCSC diagram operating under thyristor blocked mode.....2.5

Fig. 2.5 TCSC diagram operating under thyristor bypassed mode.....2.6

Fig. 2.6 TCSC module under capacitive vernier operation mode.....2.7

Fig. 2.7 Current waveforms during the vernier operating mode.....2.8

Fig. 2.8 TCSC characteristic curves' variations with three sizes of the reactor.....2.9

Fig. 2.9 Figure 2.9: Typical simulation results of the current and voltage waveforms of the TCSC for different reactor sizes at the same firing angle.....2.10

Fig. 2.10 Characteristics of the TCSC showing resonance region and α_{min}.....2.11

Fig. 2.11 TCSC characteristic curve showing the reactance range of the device.....2.12

Fig. 2.12 Typical TCSC V-I capability characteristic.....2.13

Fig. 2.13 Typical TCSC X-I capability characteristics.....2.14

Fig. 2.14 3^{rd} Harmonic voltage of the TCSC capacitor in pu of fundamental as a function of the firing angle.....2.17

Fig. 2.15 5^{th}, 7^{th} and 9^{th} TCSC capacitor voltage harmonics in pu of fundamental as a function of the firing angle.....2.18

Fig. 2.16 Transient response of V_{TCSC} to a step change of $\propto$.....2.19

Fig. 2.17 Transient response of V_{TCSC} to a step change of $\propto$.....2.20

Fig. 2.18 Transient response of V_{TCSC} to a step-down and step-up action of $\propto$.....2.21

Fig. 2.19 Typical frequency response of a transmission line compensated with a TCSC.....2.22

Fig. 2.20 Power system oscillation damping: conventional capacitor vs bang-bang controlled TCSC.....2.24

Fig. 3.1 TCR trigger circuit and the TCSC.....3.3

Fig. 3.2 Trigger pulses and the illustration of the firing delay time.....3.4

Fig. 3.3 Time-domain results of the TCR trigger circuit.....3.5

Fig. 3.4 TCSC characteristic curves' variations with three sizes of the reactor.....3.9

Fig. 3.5 EMTDC/PSCAD time-domain simulation results of the TCSC with the $X_{TCR} = 0.8\ \Omega$. The simulation was done at X_{ORDER} of 1 (A), X_{ORDER} of 2 (B) and X_{ORDER} of 3 (C).....3.11

Fig. 3.6 EMTDC/PSCAD time-domain simulation results of the TCSC with the $X_{TCR} = 1.2\ \Omega$ .The simulation was done at X_{ORDER} of 1 (A), X_{ORDER} of 2 (B) and X_{ORDER} of 3 (C).....3.12

Fig. 3.7 EMTDC/PSCAD time-domain simulation results of the TCSC with the X_{TCR} = 1.6 Ω. The simulation was done at X_{ORDER} of 1 (A), X_{ORDER} of 2 (B) and X_{ORDER} of 3 (C).....3.13

Fig. 3.8 EMTDC/PSCAD time-domain simulation results of the TCSC with the X_{TCR} = 0.8 Ω (A), 1.2 Ω (B) and 1.6 Ω (C). The simulation was done at X_{ORDER} of 1.....3.15

Fig. 3.9 EMTDC/PSCAD time-domain simulation results of the TCSC with the X_{TCR} = 0.8 Ω (A), 1.2 Ω (B) and 1.6 Ω (C). The simulation was done at X_{ORDER} of 2.....3.16

Fig. 3.10 EMTDC/PSCAD time-domain simulation results of the TCSC with the X_{TCR} = 0.8 Ω (A), 1.2 Ω (B) and 1.6 Ω (C). The simulation was done at X_{ORDER} of 3.....3.17

Fig. 3.11 Harmonic generated in pu of fundamental as a function of alpha....3.20

Fig. 4.1 Diagram of the laboratory-scale TCSC 4.4

Fig. 4.2 The three-phase TCSC circuit.....4.5

Fig. 4.3 The transmission line simulator.....4.6

Fig. 4.4 Relationship between the variable pot resistance and the firing angle.....4.7

Fig. 4.5 Original and modified synchronizing stage circuit.....4.8

Fig. 4.6 TCSC characteristic curve for a TCR = 0.8 ohms.....4.10

Fig. 4.7 TCSC characteristic curve for a TCR = 1.2 ohms.....4.11

Fig. 4.8 TCSC characteristic curve for a TCR = 1.6 ohms.....4.11

Fig. 4.9 Comparison of phase A time-domain results at reactance order of 1: Xtcr = 0.8Ω.....4.13

Fig. 4.10 Comparison of phase A time-domain results at reactance order of 1.5: Xtcr =0.8Ω.....4.14

Fig. 4.11 Comparison of phase A time-domain results at reactance order of 2: Xtcr = 0.8Ω.....4.15

Fig. 4.12 TCSC response to a 1 Hz modulation of reactance order between 1 and 2. Xtcr = 0.8 Ω.....4.17

Fig. 4.13 TCSC response to a two level modulation of reactance order between 1.5 and 2. Xtcr = 0.8 Ω.....4.18

Fig. 4.14 TCSC response to a two level modulation of reactance order between 1 and 1.5. Xtcr = 0.8 Ω.....4.19

Fig. 4.15 TCSC response to a two level modulation of reactance order between 1 and 2. Xtcr = 0.8 Ω.....4.20

Fig. 4.16 TCSC transient response as the reactance order is changed from 1 to 3.....4.22

Fig. 4.17 TCSC transient response as the reactance order is changed from 3 to 1.....4.22

Fig. 4.18 TCSC transient response as the reactance order is changed from 3 to1 back to 3.....4.23

Fig. 5.1 SMIB transmission system with TCSC module used to investigate power oscillation damping.....5.4

Fig. 5.2 Relationship between the input to the controller and the firing angle.....5.5

Fig. 5.3 Time-domain simulation results of the SMIB system in Figure 5.1 with and without the TCSC.....5.7

Fig. 5.4 Complete Time-domain simulation results of the SMIB system in Figure 5.1 with and without the TCSC.....5.8

TABLE

Table 3.1 Summary of TCSC variable reactance ranges for typical applications in the literature.

Table 3.2 The relationship of X_{TCR} size and the resonant point for a given value of n and X_C = -j2 Ω.

Table 3.3 TCSC component ratings at X_{TCSC} = -j6 Ω with X_{TCR} = j0.8 Ω

Table 3.4 TCSC component ratings at X_{TCSC} = -j6 Ω with X_{TCR} = j1.2 Ω

Table 3.5 TCSC component ratings at X_{TCSC} = -j6 Ω with X_{TCR} = j1.6 Ω

Table 3.6 Harmonics of TCSC voltage at X_{TCR} = 0.8 Ω

Table 3.7 Harmonics of the Line Current at X_{TCR} = 0.8 Ω

LIST OF SYMBOLS

The commonly used symbols and notations adopted in this thesis are listed below. Other symbols used in the text are explained where they first occur.

Acronyms

AC	Alternating Current
AVR	Automatic Voltage Regulator
BPA	Bonneville Power Administration
DC	Direct Current
EMTDC	Electro-Magnetic Transient Direct Current
FACTS	Flexible AC Transmission System
POD	Power Oscillation Damping
SMIB	Single Machine Infinite Bus
SSR	Sub-Synchronous Resonance
TCR	Thyristor Controlled Reactor
TCSC	Thyristor Controlled Series Capacitor

Synchronous generator symbols

R_A	Armature resistance
X_L	Stator leakage reactance
X_{MD}	D-axis unsaturated magnetizing reactance
R_F	Field resistance

X_F	Field leakage reactance
R_D	D-axis damper resistance
X_{KD}	D-axis damper leakage reactance
X_{MFQ}	Field – damp mutual leakage reactance
X_{MQ}	Q-axis magnetizing reactance
R_{KQ}	Q-axis damper resistance
X_{KQ}	Q-axis damper leakage reactance
E_F	Synchronous generator field voltage
H	Inertia constant
P_E	Electrical power output
P_M	Mechanical power output
Q_E	Reactive power output
T_E	Electrical torque output
T_M	Mechanical torque output
V_{TO}	Terminal voltage magnitude at t = 0
ω	Generator speed
ω_O	Generator synchronous speed
θ_{TO}	Terminal voltage phase at t = 0

System symbols

C	Capacitor
L	Inductor
R	Resistance

R_L	Transmission line resistor
X_L	Transmission line reactance
X_{ORDER}	Reactance order
X_{TCSC}	TCSC reactance
$X_{TCSC\ (MIN)}$	TCSC minimum reactance
$X_{TCSC\ (MAX)}$	TCSC maximum reactance
α	Firing delay angle
α_{MAX}	Maximum firing angle
α_{MIN}	Minimum firing angle
α_{RES}	Resonant point firing angle

CHAPTER ONE

INTRODUCTION

1.1 Background

Despite the fact that bulk power transfers are increasing due to an ever-growing number of consumers, the growth of electric power transmission facilities is restricted by several factors such as difficulties in obtaining servitude, cost required to build new transmission networks and the environmental impact of building new networks. The steady-state power transfer capability of an AC transmission line can be explained using the simple two-machine power system diagram of Figure 1.1.

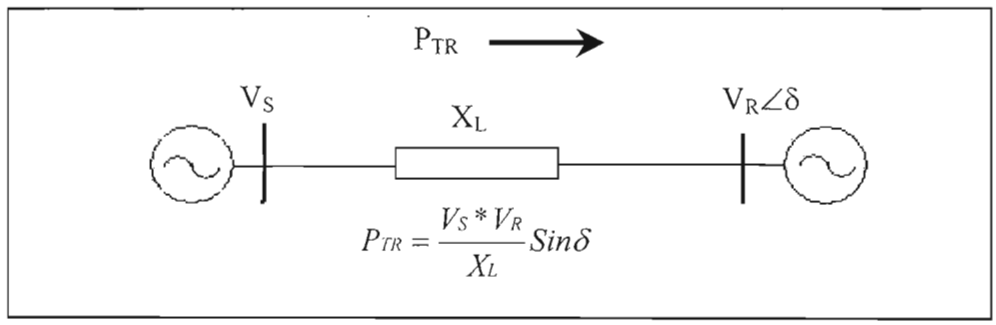

Figure 1.1: Two-machine power system diagram

Figure 1.1 illustrates that the active power P_{TR} transferred from sending bus to the receiving bus is determined by the magnitude of $|V_S|$ and $|V_R|$, the phase difference of the sending end to receiving end voltages as well as the transmission line reactance X_L. Figure 1.2 illustrates capacitive line compensation using a series capacitor. The power transfer capability of the line is increased by inserting

capacitive reactance, X_C, in series with the line inductive reactance, X_L. Equation 1.1 quantifies the magnitude of active power transferred from the sending bus to the receiving bus for a line that has series capacitors.

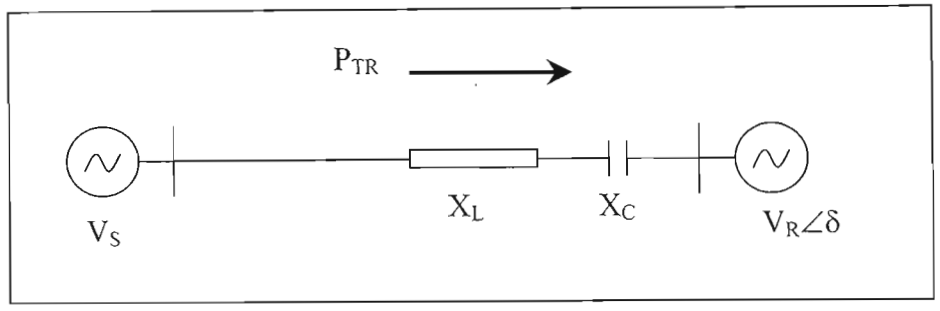

Figure 1.2: Two-machine power system diagram with series compensating capacitors

$$P_{TR} = \frac{V_S * V_R}{X_L - X_C} Sin\delta \quad \text{.....1.1}$$

Historically, several conventional techniques have been studied and used to influence these factors, namely line impedance and the load angle (δ), and hence transmit higher levels of active power over the transmission lines. Transformer tap changing schemes and mechanical switching of conventional series and shunt capacitors are some of the techniques that have traditionally been used to maximise power transfer capabilities of high voltage AC transmission lines. However, since these methods of influencing transmission line characteristics involve mechanical operation of equipment such as circuit breakers, their use is limited for transient and dynamic control of the power system. Another problem associated with the use of conventional series capacitors is that they may lead to system instabilities and sub-harmonic oscillations known as sub synchronous resonance (SSR) [14], [29].

Sub synchronous resonance is described in [29] as the unstable interaction between the electrical resonance(s) of a series capacitor compensated system and mechanical resonance of the flexible distributed mass turbo-generator shaft.

1.2 FACTS Series Compensators

In recent years, power system researchers have been working on alternatives to conventional methods of influencing the factors that determine power transfer capability of the transmission line. These research works by numerous reputable research institutes such as Electrical Power Research Institute (EPRI) coupled with advancements in the field of power-electronics, both have led to the integration of devices such as thyristors into existing methods of power systems control [3], [5]. There are several different types of FACTS devices and they all share, in different degrees, a common aim of enabling long AC transmission lines to be loaded closely to their thermal limits without causing any system instability.

Under steady-state conditions, a FACTS device can be used as a normal conventional compensating device to compensate the transmission line reactance and hence increase power transfer capability of the line. Over and above steady-state compensation, a FACTS device is capable of providing dynamic control of the line's parameters and hence improving system security under fault and post-fault conditions.

1.3 Thyristor-Controlled Series Capacitor

One of the first FACTS compensators to be designed and implemented is the thyristor-controlled series capacitor (TCSC) [5]. As shown in Figure 1.3, a TCSC consists of a conventional capacitor in parallel with thyristor controlled reactor

(TCR). The TCR comprises an inductor in series with a pair of back-to-back thyristors.

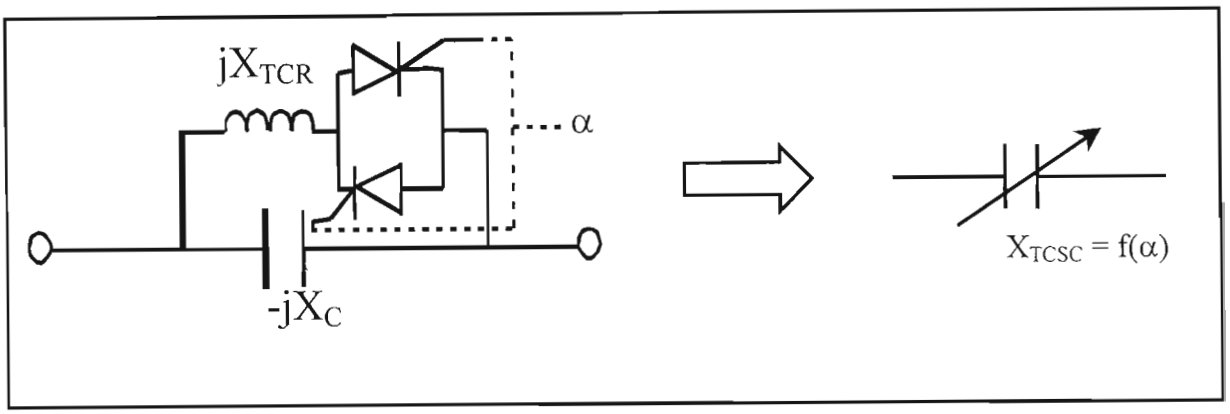

Figure 1.3: Diagram of a TCSC module

The net value of the TCSC reactance can be varied by changing the firing angle, α, of the TCR. The TCSC reactance X_{TCSC} can either be inductive or capacitive depending on the value of the firing angle α.

1.4 Objectives Of The Thesis

The overall objective of this research work was to design and build a three phase TCSC suitable for use in a research laboratory at Natal University. Extensive work has been done on general operation of a TCSC and its ability to damp power system oscillation [22], [27], [34]. However, not so much has been written on techniques that need to be followed when designing a TCSC [19], [28], [36]. The following points are key research topics that are addressed in this thesis.

(a) Operating Region

One of the tasks that was conducted was to identify the range of the firing angles. The firing angle not only determines whether the TCSC reactance is capacitive or inductive, but also determines the magnitude of this reactance.

(b) Rating of TCSC components

Another topic that was investigated was the rating of the TCSC components.

(c) Harmonic analysis

Since the operation of the TCSC involves chopping the current AC waveform, it was expected that harmonics would be generated. Hence, harmonic analysis was conducted to substantiate harmonic contribution by the TCSC to the power system.

(d) Dynamic response of the TCSC

A step change in the firing angle was applied to investigate the transient response of the device.

(e) Practical TCSC module

A three-phase TCSC laboratory scale model was built and tested. The objective in constructing a TCSC was to obtain practical results of the TCSC and hence verify theoretical results from the simulations.

(f) Power swing damping

The last objective was to demonstrate the designed TCSC in a typical application: power oscillation damping was chosen for this research work.

1.5 Thesis Layout

This thesis is made up of six chapters and appendices. A technical literature review, on the subject of series compensation using TCSC, was conducted and it can be found in Chapter Two. Chapter Two also covers background theory on how the TCSC operates. Chapter Two also provides literature review on approaches and implications of selecting capacitor and reactor sizes. Most common applications of the TCSC are also mentioned in Chapter Two.

Chapter Three contains the details on the development of a TCSC's mathematical model for computer simulations. This model also includes the firing angle control scheme, which provides firing pulses for the TCR's thyristors. Time-domain simulations are investigated in this chapter and are also compared in later chapters with the measured results obtained from the laboratory scaled TCSC. Chapter Three also contains the details of the investigation of topics such as rating of the TCSC components, harmonics generated by the TCSC and behavior of TCSC impedance as the firing angle is subjected to a step change.

Chapter Four deals with the development of a laboratory scaled TCSC for practical implementation. The chapter begins by describing different components that were used to construct the hardware TCSC. Subsequent sections of Chapter Four, contain measured results of the performance of the hardware TCSC, which are then compared with results from the mathematical model developed in Chapter Three. These comparisons were performed to ensure that a laboratory scaled TCSC was operating as expected.

A mathematical model, developed in Chapter Three, is expended in Chapter Five with the inclusion of multi-mass model representing turbine shafts as found in the

machine laboratory of the Natal University. The results of this model prove that the TCSC can significantly improve damping of the network, when the network is subjected to a short three-phase fault. Finally, Chapter Six summarises the results of this work and suggests further research that could be undertaken in future

1.6 Research Publication

Some of the findings of this thesis have been presented at a national conference [28].

CHAPTER TWO

GENERAL OPERATION OF THE TCSC

2.1 Introduction

Chapter One of this thesis has briefly outlined the constraints that power utilities need to overcome when transmitting power in AC transmission lines. The benefits of using FACTS devices, such as Thyristor-Controlled Series Capacitor, were also described. One of the main objectives of this thesis work is to determine the methodology which needs to be followed when designing a TCSC device for an AC transmission network, and to demonstrate the capability of the TCSC to damp power oscillations after an occurrence of a major disturbance in a transmission network.

The successful development of the design methodology requires a thorough literature review on the subject of TCSC design. Hence, a comprehensive literature survey was conducted to evaluate some of the considerations and constraints that have been encountered by other researchers in the field of TCSC design. This chapter initially presents a historical experience on the first TCSC modules to be commissioned. The chapter then outlines the operating principle of the TCSC device. This chapter also describes several considerations that need to be addressed when a TCSC is designed. Such considerations include the so-called reactance order (X_{ORDER}), firing region, resonance point and rating of the TCSC components. X_{ORDER} can be defined as the ratio of TCSC effective reactance to that of the internal capacitor reactance.

Another topic that is covered in this chapter is the issue of harmonics. Any switching of an AC waveform will result in the generation of harmonics, hence the effects of this phenomenon on the rating of the different components of the TCSC had to be investigated. The last section of this chapter will outline some common applications of the device. These applications are Power Oscillation Damping (POD) and Sub-Synchronous Resonance (SSR). The literature survey will then form the basis of the design approach that will be followed in the subsequent design methodology covered in latter chapters of the thesis.

2.2 The World's First Multi-Module TCSC System [2]

The Bonneville Power Administration (BPA) thyristor-controlled series capacitor installation was the first of its kind in the world [2]. The pilot site of the TCSC project is Slatt substation on the Slatt-Buckley 500 kV transmission line owned by BPA in Northern Oregon. At the CJ Slatt substation, six identical thyristor-controlled series capacitor modules were applied to each of the three phases. Each phase of the line consisted of the capacitors, current limiting reactors, thyristor switches and protective varistors all at potential of 500 kV (as shown by Figure 2.1 below). Three platforms, for each phase of the line, were specially designed to mount the TCSC system. Communication between platform and ground was achieved by fiber optics. All modules receive continuous signals from the control unit, and these signals establish the operating mode and vernier control for each individual module.

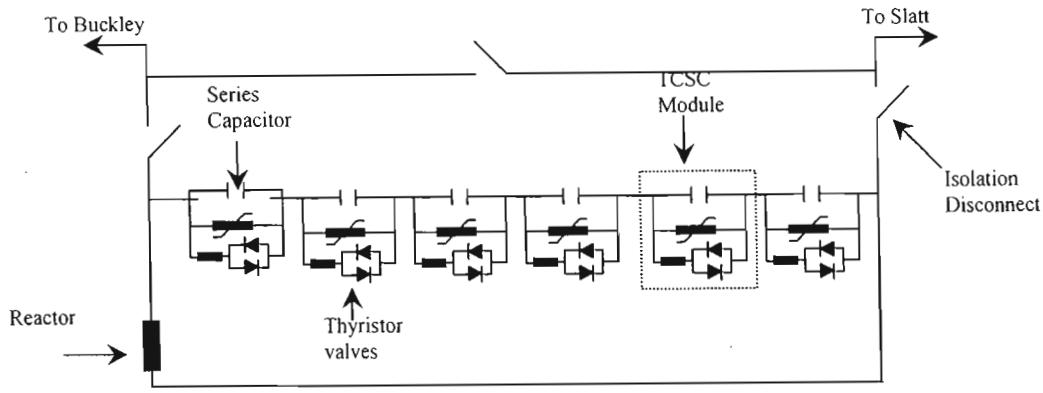

Figure 2.1: One-line diagram of Slatt TCSC [2]

The above Figure 2.1 shows an elementary one-line diagram of a Slatt TCSC on one of the phases of the line. Each TCSC module consists of a back-to-back thyristor in series with a reactor (TCR), and in parallel with a capacitor and a varistor. A bypass switch is connected in parallel with an entire device for use in protective functions. There are also two other isolation switches for TCSC isolation purposes.

Performance Results

- The test results demonstrated TCSC capability of high speed switching for controlling power flow, which in turn allows increased loading of existing transmission lines close to their thermal limits.
- The system damping was also improved after the network was subjected to extreme contingencies.
- It was also shown that the fast-acting TCSC could provide the means of rapidly increasing power transfer upon detection of the critical contingencies, resulting in increased transient stability.
- Sub-Synchronous Resonance (SSR) tests were also performed to demonstrate the ability of the TCSC to greatly reduce a potential SSR problem.
- The Slatt TCSC test also revealed that nearly all harmonic currents are contained within the TCSC loop.

In conclusion, it is the objective of this work to develop a laboratory-scale TCSC in order to carry out research into these and other issues.

2.3 Operating Principles of a TCSC

The basic thyristor-controlled series capacitor scheme consists of the series compensating capacitor shunted by a thyristor-controlled reactor. In practice, several TCSC modules may be connected in series to obtain the desired voltage rating and operating characteristic [2], [5], as shown in Figure 2.1. Another common configuration, as shown in Figure 2.2 below, is to use a hybrid of a conventional series capacitor and TCSC module, connected in series [3].

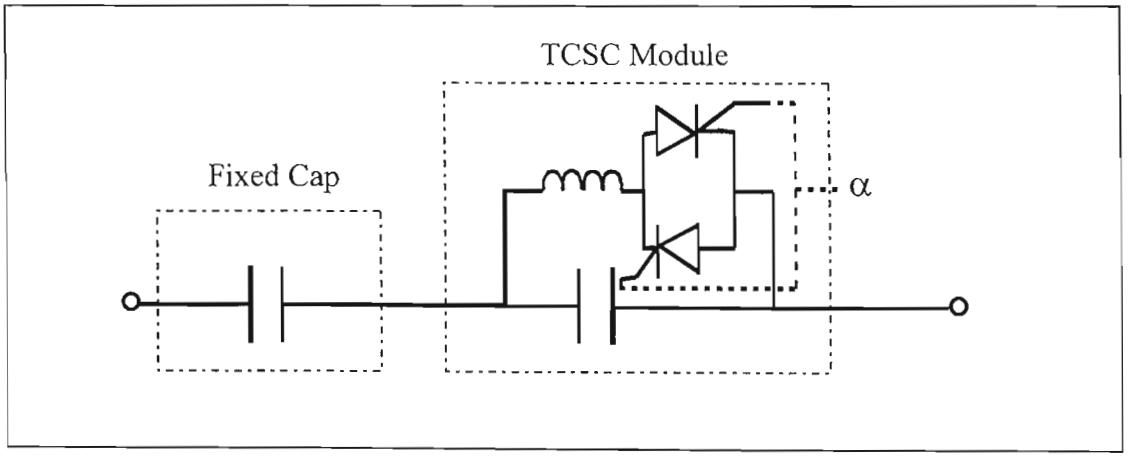

Figure 2.2: TCSC Module in series with a conventional capacitor

Under this arrangement, the conventional series capacitor is used for line compensation and the TCSC is only utilized during contingencies.

The variable reactance of the TCSC is achieved by varying the firing delay angle (α) of the thyristor-controlled reactor.

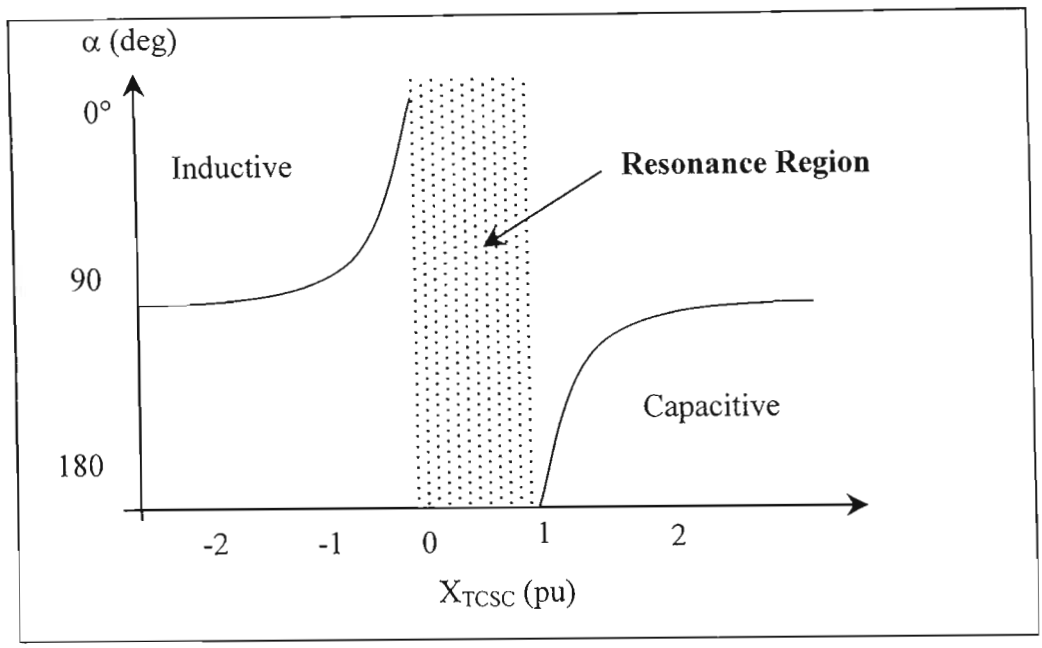

Figure 2.3: The reactance vs delay firing angle characteristic of the TCSC

Figure 2.3 shows the characteristic of the TCSC reactance as a function of the firing angle α.

The TCSC has three basic modes of operation:

- Thyristor blocked,
- Thyristor bypassed and
- Vernier operation.

Thyristor blocked

Under this mode of operation, the thyristors valves are not conducting any current (hence, the term blocked). The TCSC net reactance is effectively the capacitive reactance of the capacitor, $-jX_C$. This mode occurs when the firing angle is 180°. Figure 2.4 shows that no current passes through the thyristors, hence $I_{LINE} = I_{TCSC}$ and $I_{TCR} = 0$.

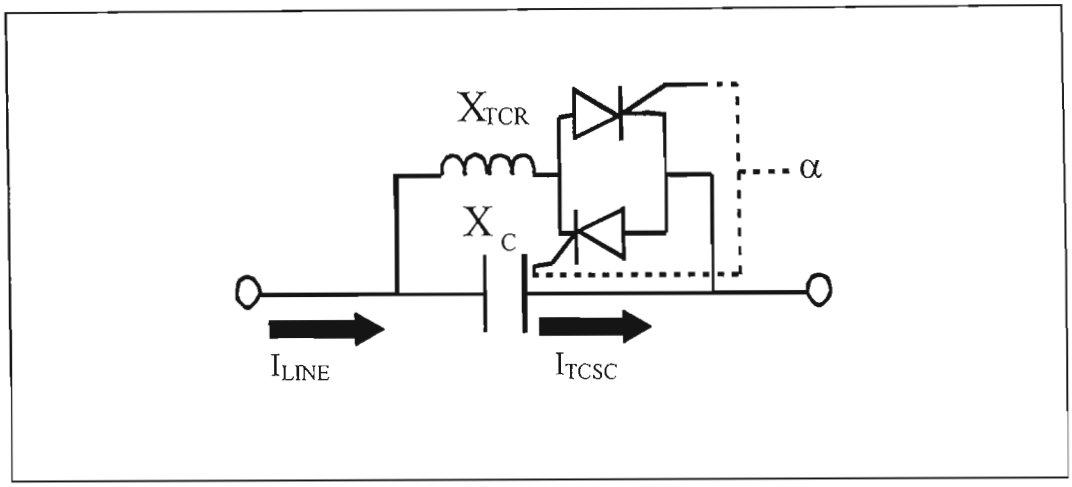

Figure 2.4: TCSC diagram operating under thyristor blocked mode

Thyristor bypassed

Under this mode of operation, the thyristor valves are gated for full conduction. The resulting net TCSC reactance is effectively the parallel combination of $-jX_C$ and jX_{TCR}. This mode occurs when the firing delay angle, α, is equal to 90°. In practice, some current also flows through the capacitor during bypassed operation, but most flows through the thyristor valves and reactor because it is a much lower impedance path.

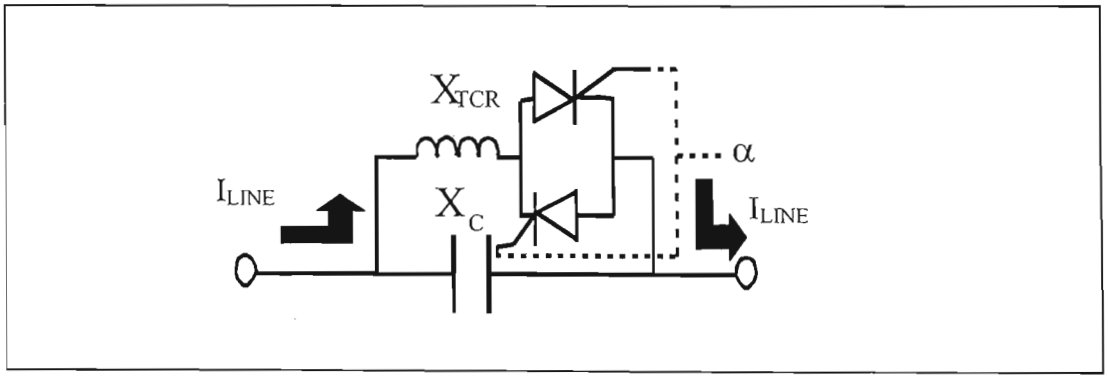

Figure 2.5: TCSC diagram operating under thyristor bypassed mode

Figure 2.5 shows the flow of current under this mode. Depending on the design of the TCSC, most of the line current flows through the TCR branch and hence $I_{LINE} \cong I_{TCR}$ and $I_C \cong 0$.

Vernier operation

This is the most common mode of operation. The vernier operation mode is sub-divided into two categories, namely: inductive vernier mode and capacitive vernier mode. However, only capacitive vernier operation mode will be considered in this thesis.

Under vernier mode, the TCSC reactance can be calculated for each firing angle based on the equation below [23], equation 2.1, that defines the TCSC circuit reactance as a function of the firing angle:

$$X_{TCSC} = \frac{\pi X_{TCR}}{(\sigma - \sin\sigma) + \pi \frac{X_{TCR}}{X_C}} \quad \text{.....(2.1)}$$

where $\sigma = 2\pi - 2\alpha$ (conduction angle)

X_{TCR} = TCR reactance

X_C = fixed capacitor bank reactance

In this mode, the thyristor valves are gated near the end of each half cycle in a manner that can circulate a controlled amount of inductive current through the capacitor, thereby increasing the effective capacitive reactance of the module.

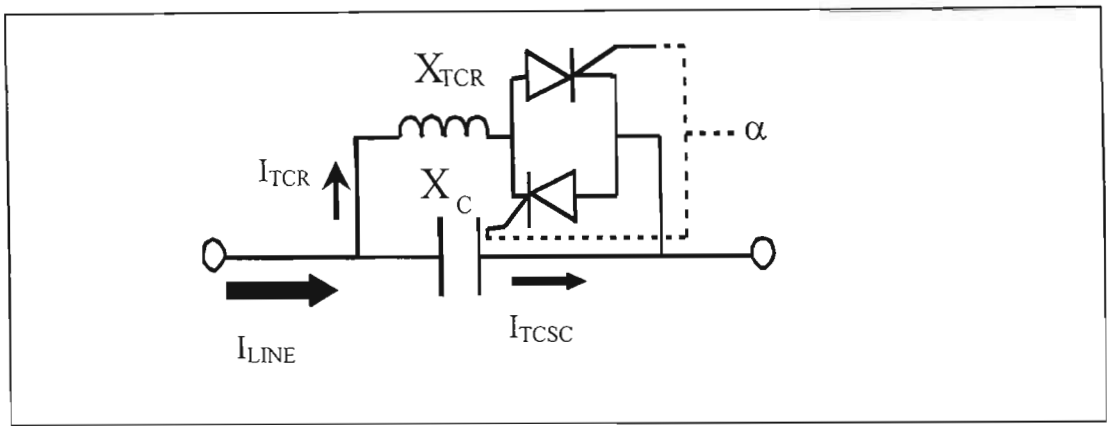

Figure 2.6: TCSC module under capacitive vernier operation mode

Figure 2.6 shows the distribution of currents under capacitive vernier operation mode. From the same figure above, the circuit appears somewhat like that of a parallel L-C tank circuit with variable inductance, such a circuit has a reactance as seen by the AC system at the TCSC terminals:

$$X_{TCSC}(\alpha) = \frac{jX_{TCR}(\alpha) * jX_C}{jX_C - jX_{TCR}(\alpha)} \quad \text{.....(2.2)}$$

Both, equations 2.1 and 2.2, show the relationship of the TCSC impedance with the firing delay angle.

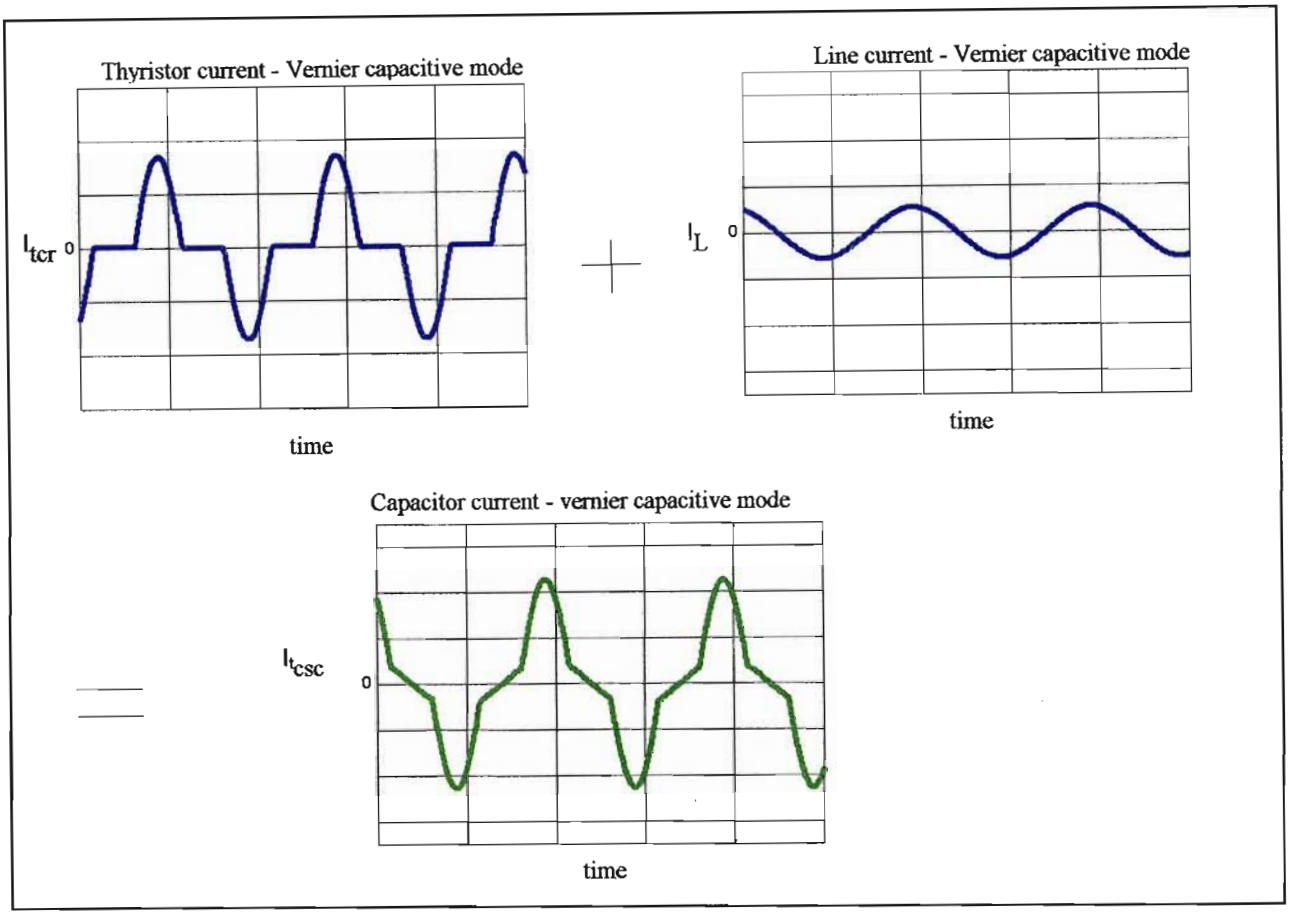

Figure 2.7 : Current waveforms during the vernier operating mode

The above figure 2.7, graphically, shows how the steady-state magnitude of the TCSC current becomes larger than the nominal capacitor current when there is no vernier operation.

2.4 Factors Considered when Selecting the Inductance of the Reactor Loop

2.4.1 Introduction

Section 2.3 has outlined the operating principles of the TCSC device. Different operating modes were explained in this section, and the circuit diagrams showing

the current distribution, including current and voltage waveforms, in the loop were included.

In this section, the intention is to discuss some important design issues that need to be considered when designing a TCSC. These issues include the firing region for vernier capacitive mode, TCSC resonance point, rating of the TCSC components and the ratio of the TCSC maximum reactance to the capacitive reactance of its internal capacitor (X_{ORDER}).

2.4.2 Firing Region

The component sizes of the LC circuit determine the range of the firing region. The bigger the TCR reactance, hence inductor, the more range available for vernier capacitive operation (assuming the same capacitive compensation). Figure 2.8 illustrates this point:

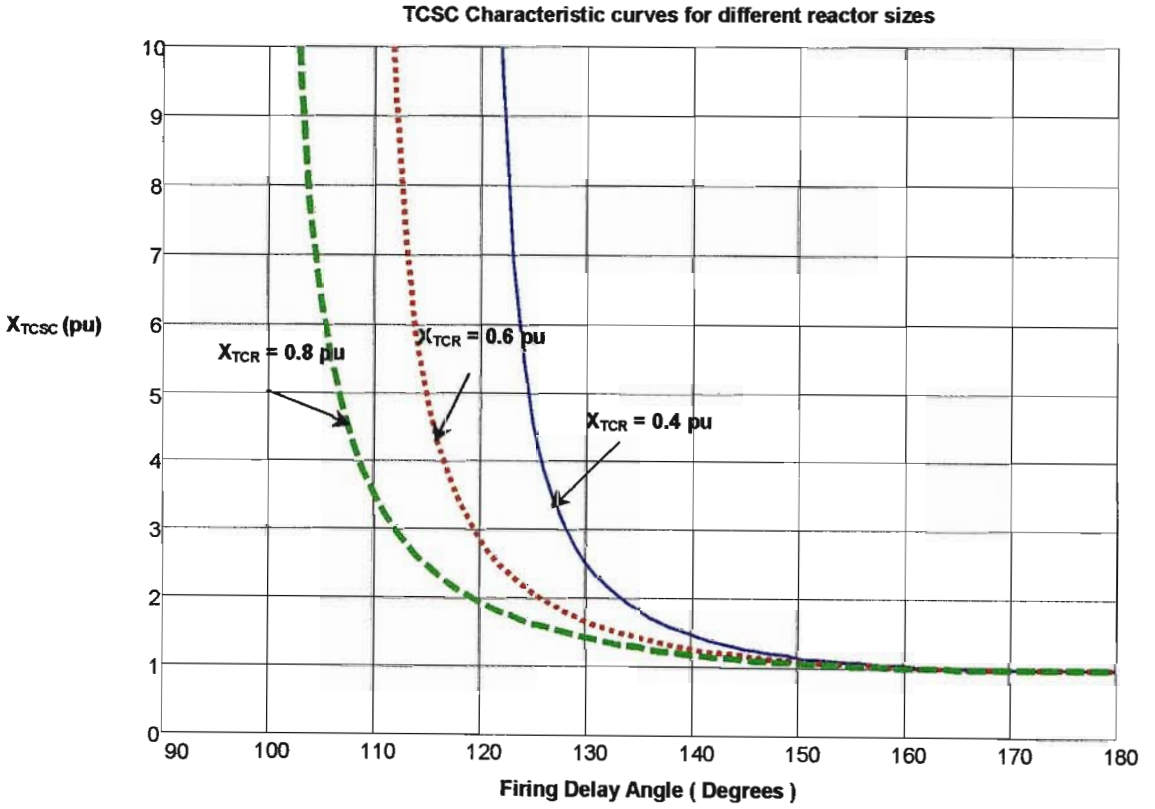

Figure 2.8: TCSC characteristic curves' variations with three sizes of the reactor

The reactors are in per unit values of the internal capacitor of the TCSC. Ideally, the control range should be as large as possible to achieve smoother operating range. However, other factors such as TCSC components' rating (X_{TCR} in particular), hence economics there of, prevents this from being implemented in a practical design [18]. Figure 2.8 also shows that the TCSC reactance increases, as the firing delay angle is decreased from 180 degrees. At a given firing angle, the current flow through the TCR-Capacitor loop decreases as the inductance of the parallel reactor is increased. Figure 2.9 illustrates this point:

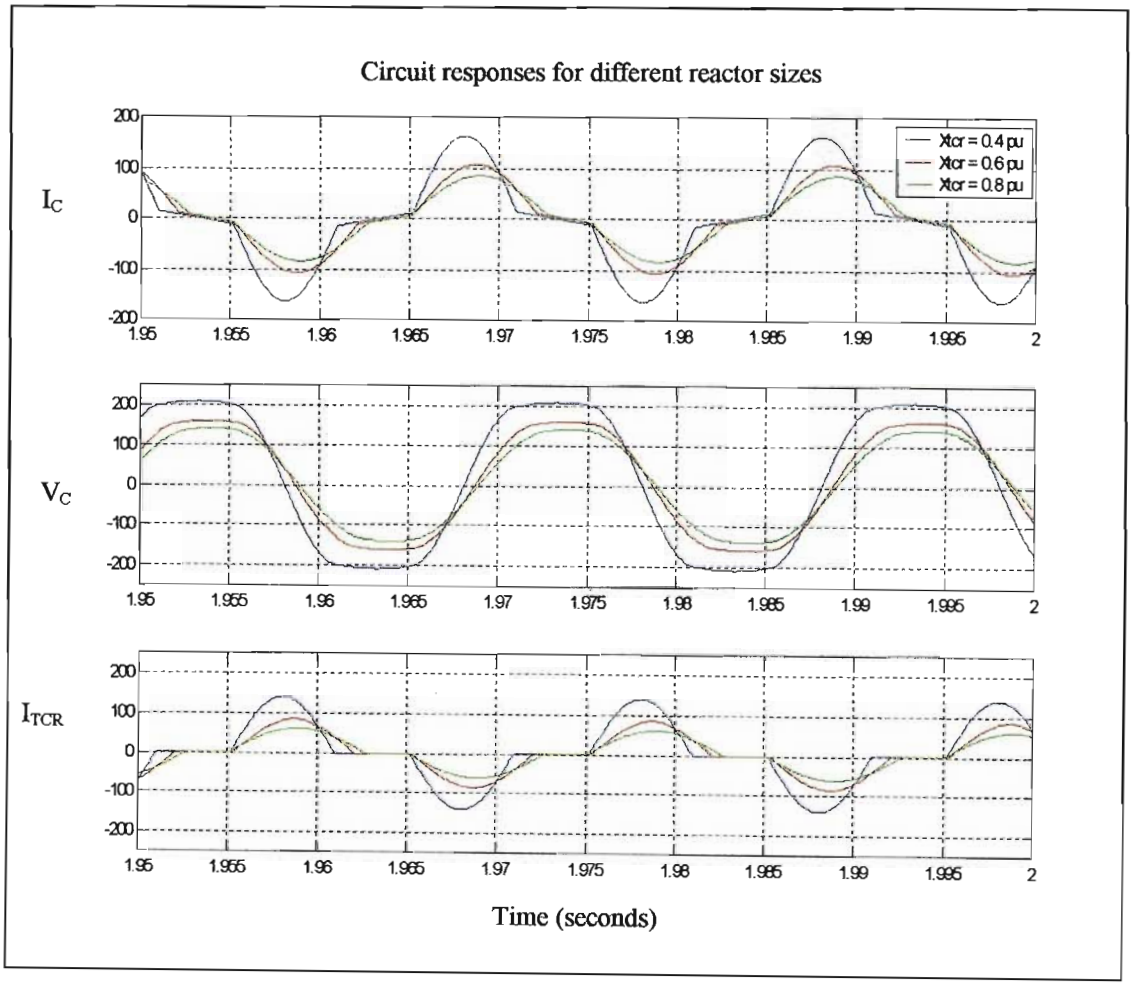

Figure 2.9: Typical simulation results of the current and voltage waveforms of the TCSC for different reactor sizes at the same firing angle

Resonance point

The operating range of the TCSC's firing angles in the capacitive region is from 180 degrees to α_{min}, α_{TCSC} = [180°, α_{min}]. If the TCSC is operated at the firing delay angle of 180 degrees, no current flows through the TCR branch, and hence the effective TCSC reactance is equal to the internal capacitive reactance, $X_{TCSC} = -jX_C$.

However, if the firing angle is any angle within the firing range, [180°, α_{min}], the TCSC reactance is greater than X_C. The actual value of this reactance can be determined by equation 2.1. The exact resonance point of the TCSC is reached when the capacitive reactance equals the inductive reactance of the TCR. At this point, the TCSC reactance becomes infinitely large; hence the TCSC is always operated well below this point. The following figure shows the location of α_{min} and the resonance region where α approaches the resonant point and the TCSC reactance becomes unacceptably large.

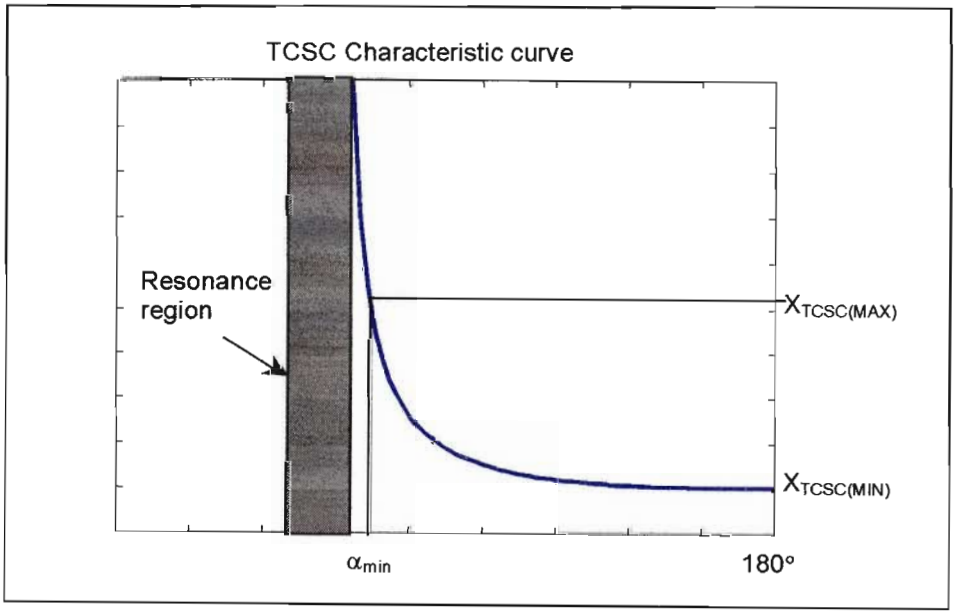

Figure 2.10: Characteristics of the TCSC showing resonance region and α_{min}

As the figure above shows, the operating range of the TCSC is determined once the minimum firing angle is set. For the TCSC with the above characteristics, Figure 2.10, the TCSC reactance range is [$X_{TCSC\,(MIN)}$, $X_{TCSC(MAX)}$].

2.4.3 The Reactance Order

The reactance order (X_{ORDER}) of the TCSC is defined as the ratio of its capacitive reactance to the capacitive reactance of its internal capacitor, with $X_{ORDER} \leq 3$ typically [28]. The following figure illustrates how the X_{ORDER} is determined:

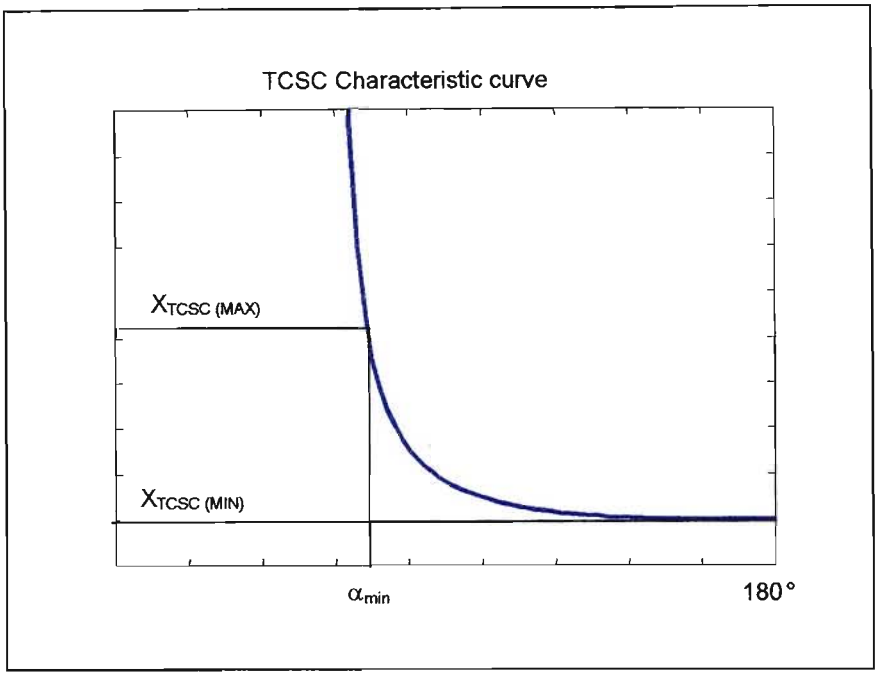

Figure 2.11: TCSC characteristic curve showing the reactance range of the device

Since the minimum reactance of the TCSC is the same as the reactance of the internal capacitor, $X_{TCSC\,(MIN)} = -jX_C$;

$$X_{ORDER} = \frac{X_{TCSC(\alpha)}}{X_{TCSC(MIN)}} \quad \text{.....(2.3)}$$

One of the limiting factors in choosing a larger value of X_{ORDER} is the resonant region. The higher the maximum value of X_{ORDER} is, the more α_{MIN} approaches α_{RES}, with α_{RES} occurring when $|X_{TCR}| = |X_C|$.

2.4.4 Operating Capability of the TCSC

The operating range of the TCSC is dictated by a number of application requirements. This section describes these limits in terms of typical capability curves. One of these limiting factors is the voltage that appears across the TCSC at the minimum firing delay angle, α_{MIN}. An important consideration of this voltage constraint is the duration. The maximum voltage constraint is typically given for three duration: continuous, 30-minutes and a few seconds, as illustrated in Figure 2.12.

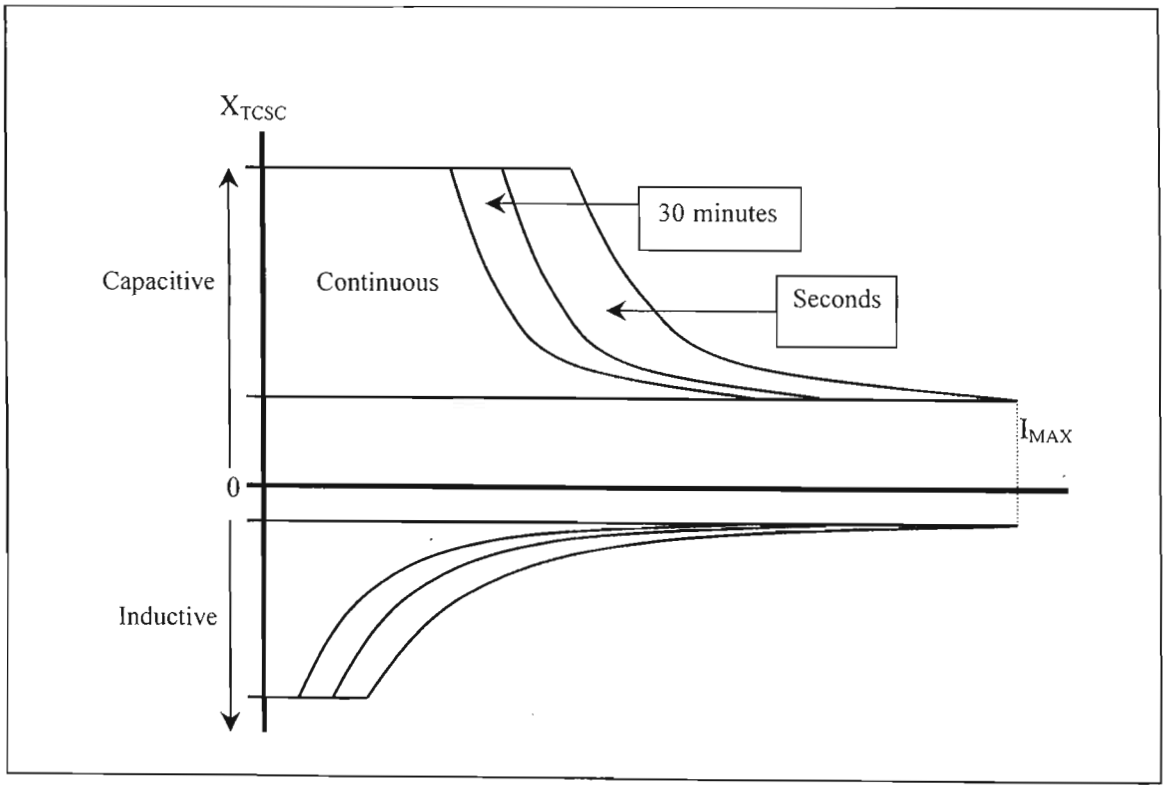

Figure 2.12: Typical TCSC X-I capability characteristic.

Figure 2.12 shows the operating capability characteristics of the TCSC in terms of module voltage versus line current. Given that the control system can operate the TCSC in any combination bypassed or vernier modes, the TCSC can vary its total effective reactance anywhere within the region of the plot. Short-term overload operation is possible at higher levels of line currents. Separate regions are shown

for 30-minutes and seconds overload capabilities. The capability can also be illustrated in terms of reactance versus line current, as shown in Figure 2.13.

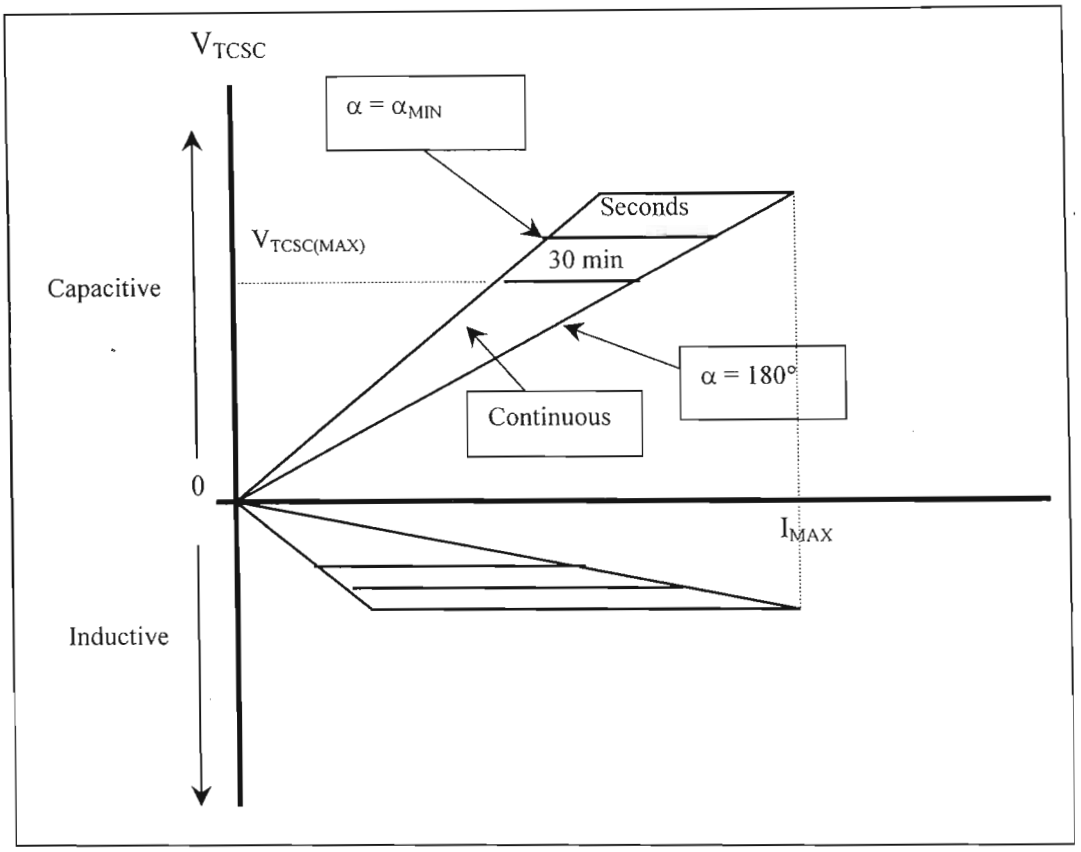

Figure 2.13: Typical TCSC V-I capability characteristics

Figure 2.13 shows the gap in control range between capacitive and inductive operation, as well as the reduction in dynamic range with increasing line current. Other TCSC applications require a relatively smooth control of the reactance. Such a characteristic can be achieved by connecting several TCSC modules in series instead of a single module.

2.4.5 Rating the TCSC Components

One of the critical design factors that needs to be considered when designing a TCSC device is the rating of its components, namely, capacitor, thyristors and the inductor. When designing a TCSC, the added dimension of thyristor control increases the number of factors to be considered, as compared to conventional series compensation. The voltage that appears across the TCSC (hence V_C) and the current through the TCSC set the limits on the operating range of the device.

In the capacitive vernier mode, the circulating loop current adds to the line current and produces higher capacitor currents. This increases voltage drop across the series capacitor, and thus increases the net series compensation as seen from the line. The following are some of the TCSC rating requirements, for both steady-state and transient operation, that need to be considered:

- Current rating,
- Voltage rating and
- MVAR rating

Current rating

The TCSC current ratings are similar to those used for conventional capacitor banks:

I_{RATED} = Continuous line current.

I_{TEMP} = Temporary line current.

t_{TEMP} = Duration of I_{TEMP} (typically 30 minutes).

I_{TRANS} = Capacitor transient current.

Typical values for the temporary and the transient capacitor currents are $I_{TEMP} = 1.35*I_{RATED}$ and $I_{TRANS} = 2*I_{RATED}$ [36].

Voltage rating

The voltage rating of the TCSC is established based on the steady-state and transient performance requirements.

V_{RATED} = Continuous voltage across the TCSC (typically, ≥ X_C*I_{RATED} because of capacitive vernier operating mode).

V_{TEMP} = Maximum temporary voltage across the TCSC (typically, ≥ X_C*I_{TEMP}).

V_{TRANS} = Voltage developed across the TCSC during the transient swings (Typically ≥ X_C*I_{TEMP}).

MVAr Rating

Another important rating parameter, for both capacitor and TCR inductor, is the MVAr. The following MVAr ratings are considered:

Continuous rating:

$MVAr = 3*I_{RATED}*V_{RATED}$

Short-time transient rating:

$MVAr_{trans} = 3*I_{TRANS}*V_{TRANS}$

2.4.6 Harmonic Performance of the TCSC

The TCSC operation with partial conduction of the TCR causes harmonic currents to circulate inside the TCSC loop. These harmonic currents are caused by the TCR harmonic currents that circulate through the series compensation capacitor. The TCR generates all odd harmonics, the magnitudes of which are a function of the delay angle α, as illustrated in Figure 2.14 and Figure 2.15 below.

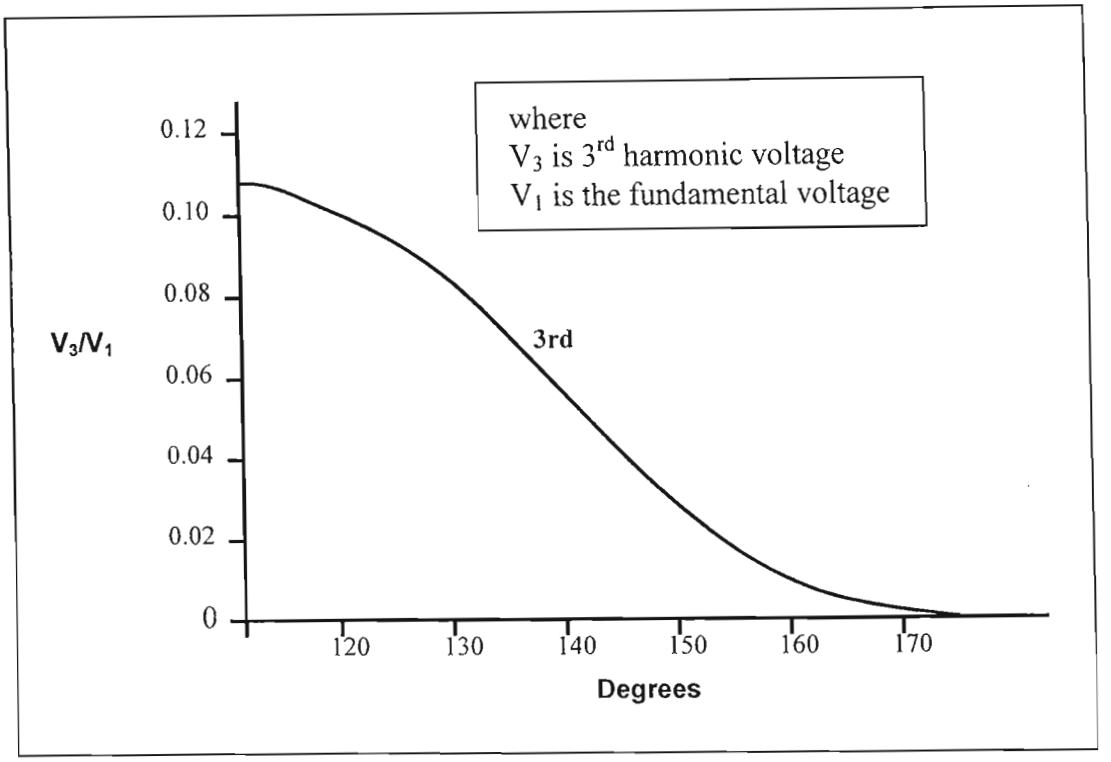

Figure 2.14: 3rd Harmonic voltage of the TCSC capacitor in pu of fundamental as a function of the firing angle

Figure 2.14 shows the per unit magnitude of the 3rd harmonic voltage as a function of the firing delay angle. Harmonics greater than the 3rd are much smaller in relation to the fundamental and have minimal effect on the power system as a whole. This is mainly because the TCSC is usually applied to long, high impedance lines, in which the generated line current harmonics is relatively low [36].

Another important fact about the harmonic currents is that they are confined within the capacitor-TCR loop [16]. This implies that there are no special filters required in the line. However, the TCSC capacitor has to be rated such that it can handle the harmonics (3rd in particular) voltages it will experience under normal operation.

Figure 2.15 shows harmonic currents greater than 3rd as a function of the firing delay angle.

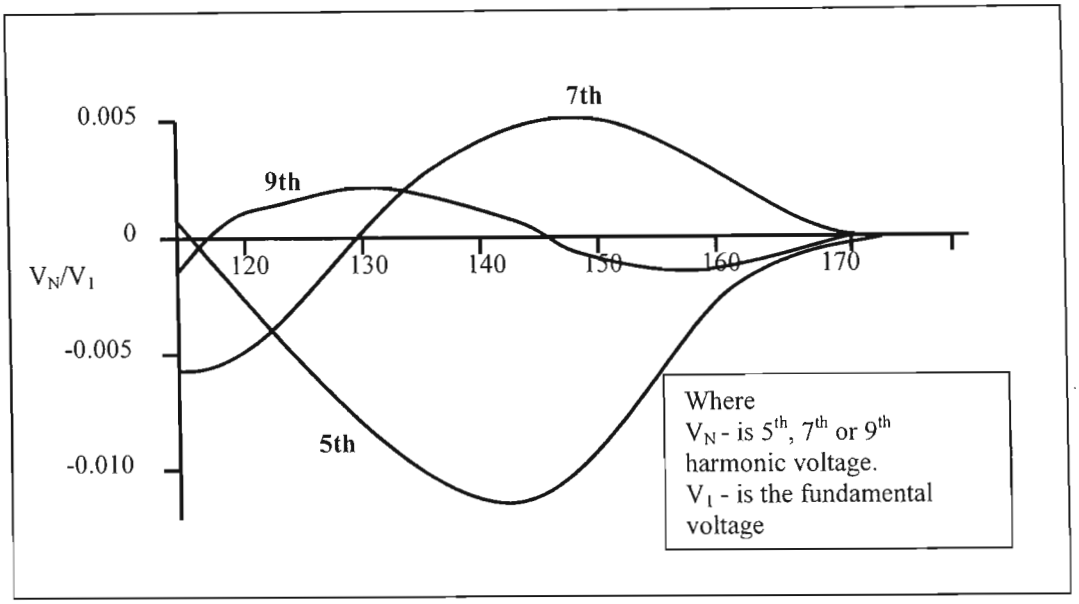

Figure 2.15: 5^{th}, 7^{th} and 9^{th} TCSC capacitor voltage harmonics in pu of fundamental as a function of the firing angle

The above results show the dominance of the third harmonic over the remaining harmonics. As Figure 2.14 illustrates, the 3^{rd} harmonic increases substantially as the firing delay angle is decreased; hence attempts should be made, during design stage, to maintain the magnitude of the 3^{rd} harmonic at tolerable levels.

2.4.7 Transient Response of the TCSC

The transient response of the TCSC's reactance, due to the step change of the firing delay angle, is another important characteristic of the device that need to be looked at during design stages.

Figure 2.16 shows a typical transient response of the TCSC when its commanded reactance is instantaneously changed from a lower reactance to a higher reactance. This can be achieved by instantaneously changing the firing delay angle.

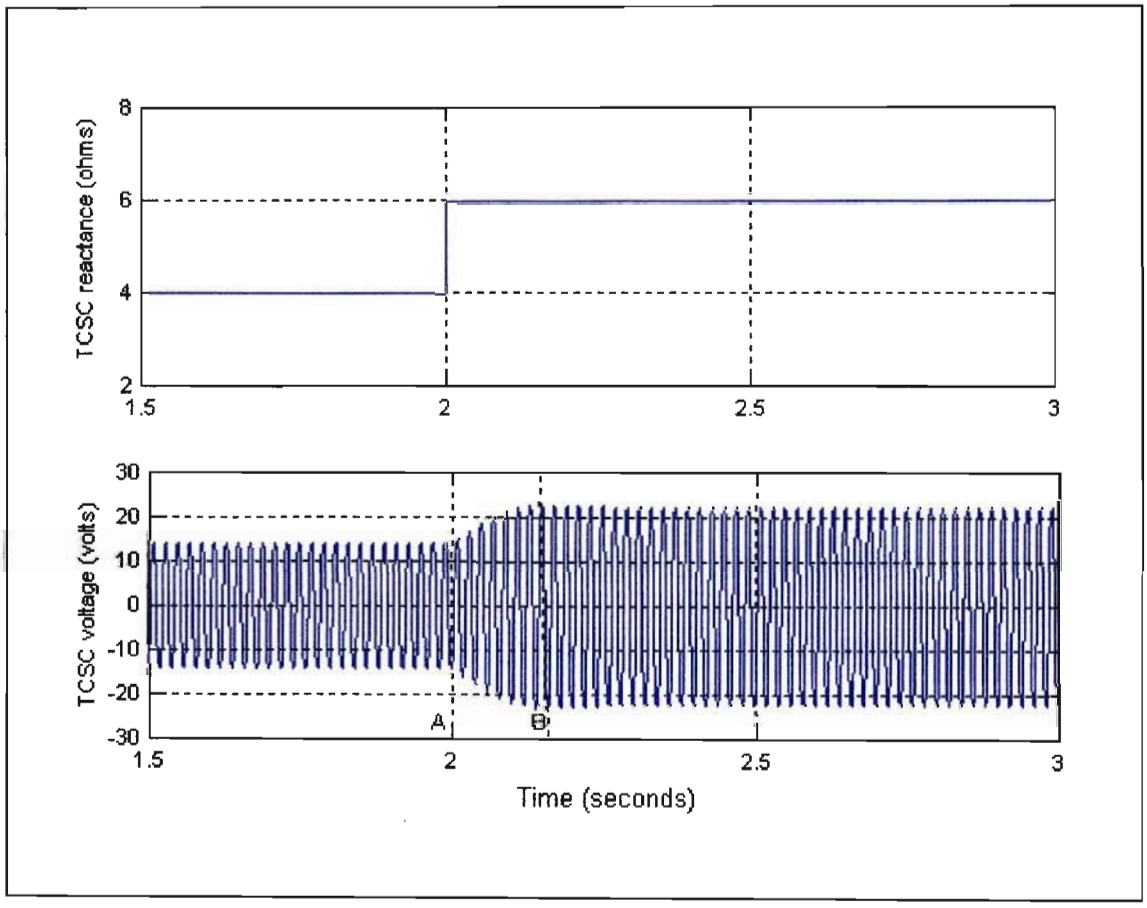

Figure 216: Transient response of V_{TCSC} to a step change of α

Figure 2.16 shows that a step change of the TCSC reactance was applied at t = 2 seconds. The reactance step change resulted to the increase of the voltage across the TCSC. Two vertical lines, A and B, of Figure 2.16 show the duration required for the TCSC voltage to reach the new level. This duration is approximately equal to 8 cycles.

Figure 2.17 shows the transient response of the TCSC voltage, as the commanded reactance is instantaneously decreased. The voltage across the TCSC decreases in response to a step change in TCSC reactance. However, the time duration required for the TCSC voltage to reach a new voltage level is much shorter.

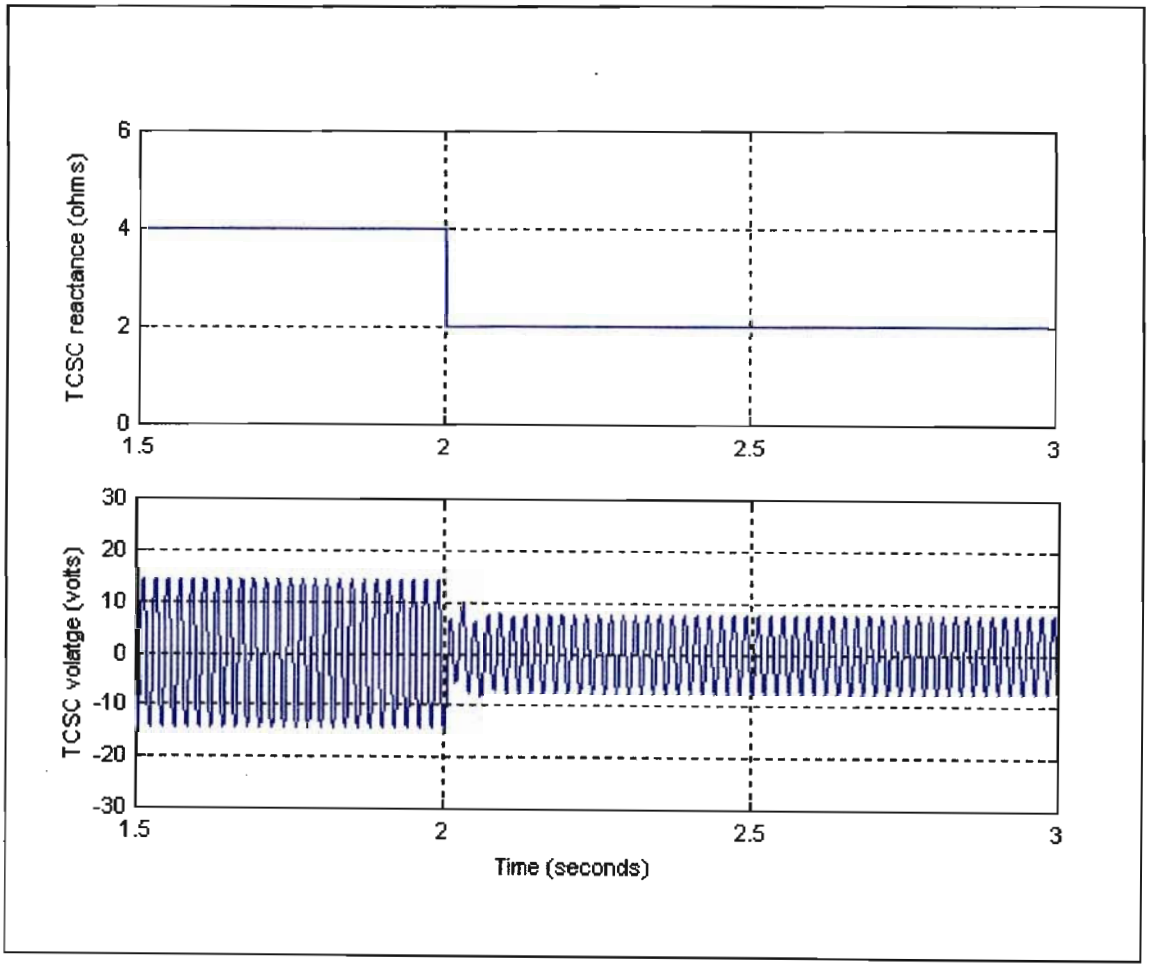

Figure 2.17: Transient response of V_{TCSC} to a step change of α

As can be observed from both Figure 2.16 and Figure 2.17, the response time of the TCSC voltage is asymmetric. When the reactance is increased (as seen in Figure 2.16), the TCSC voltage response time is relatively slow compared to when the reactance is decreased (as seen in Figure 2.17). This can be clearly seen when both step-up and step-down cycles are shown on the same graph, as Figure 2.18 illustrates.

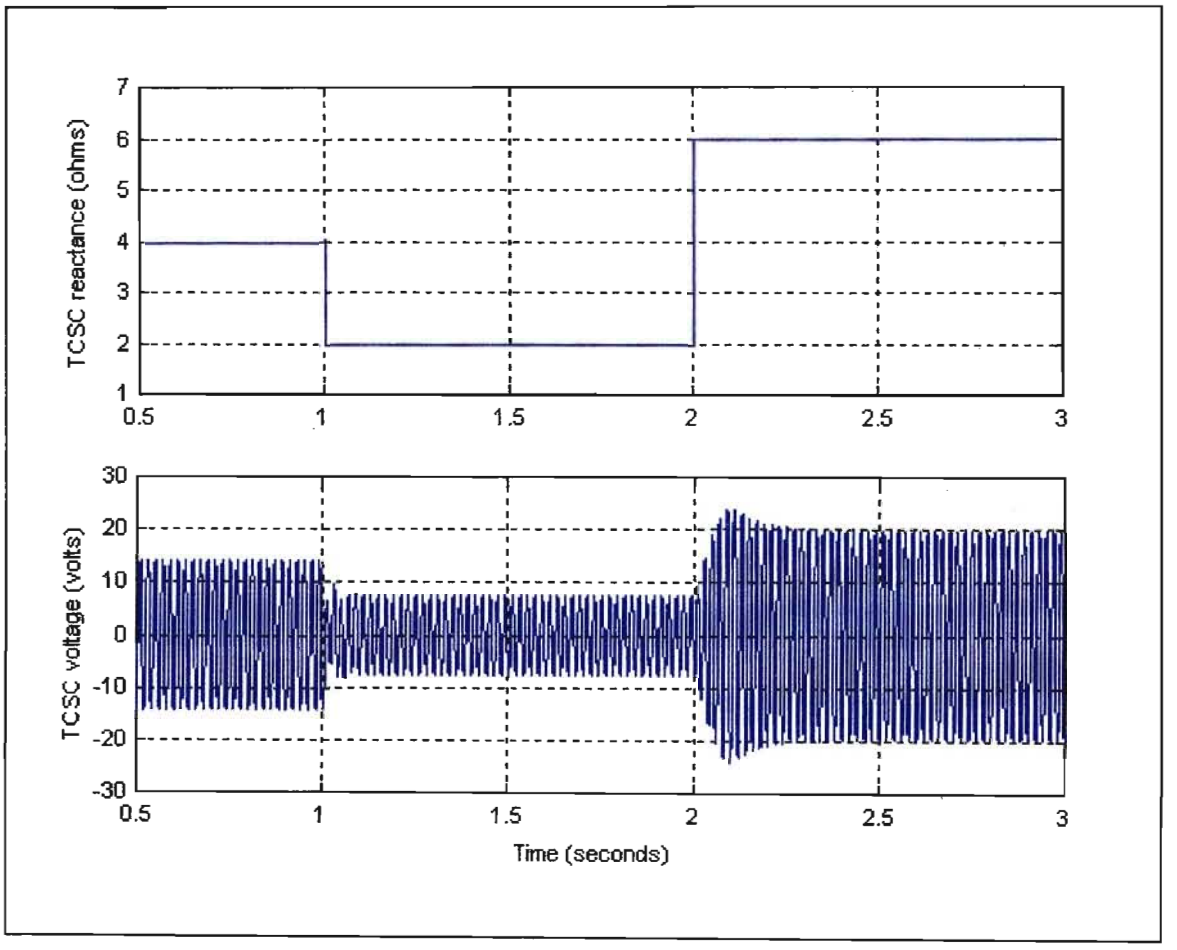

Figure 2.18: Transient response of V_{TCSC} to a step-down and step-up action of α

This behavior is attributed to a physical nature of capacitors. Response time is shorter when the reactance is decreased because the capacitor is simply bypassed and discharges instantaneously. However, when the reactance is increased, the response of the TCSC voltage will be slower because of the initial charge stored by the capacitor [28].

2.4.8 Frequency Response of the TCSC

Another important factor in the TCSC design is its frequency response. Frequency response is a critical factor that needs to be considered, more especially if the TCSC is being used in mitigation of Sub-Synchronous Resonance. Figure 2.19 illustrates a typical frequency response of a transmission line compensated with a TCSC.

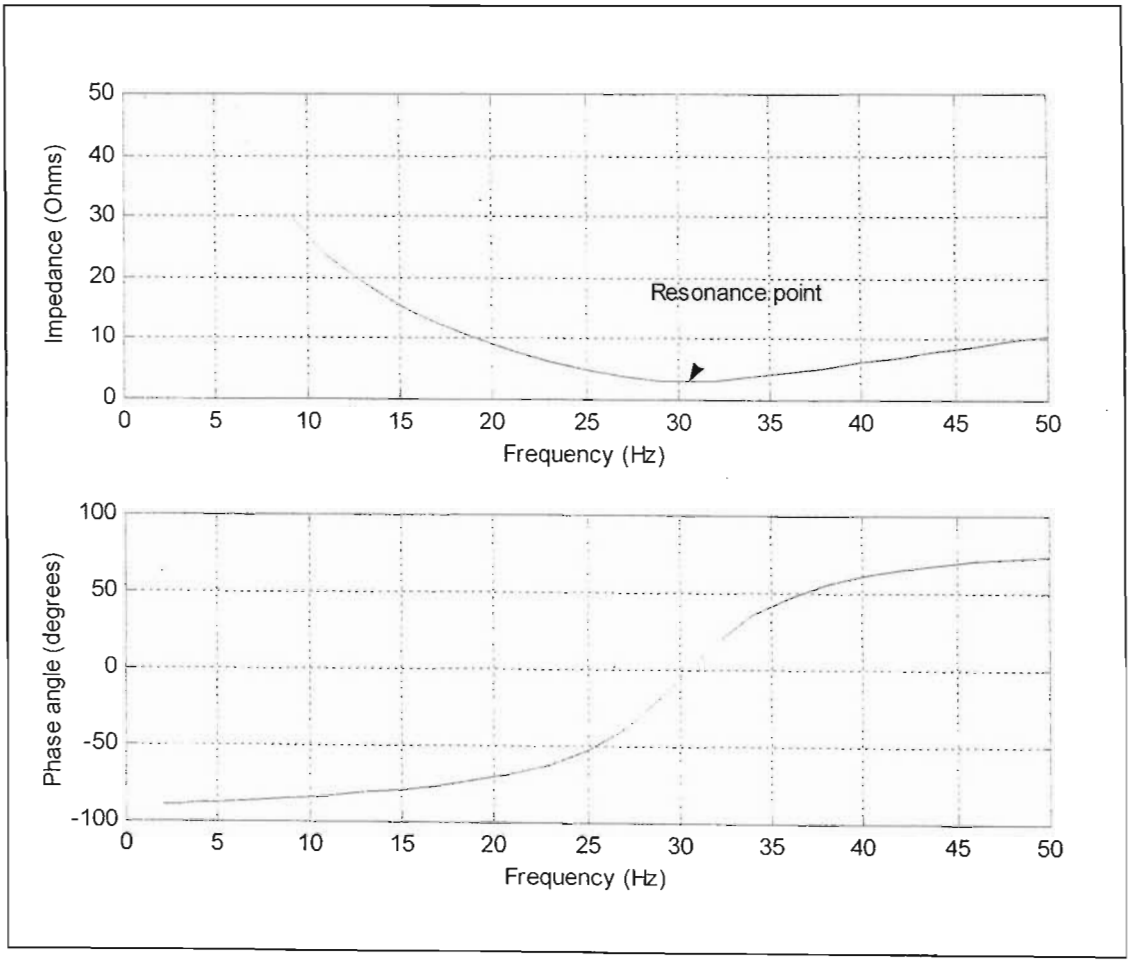

Figure 2.19: Typical frequency response of a transmission line compensated with a TCSC

As Figure 2.19 shows, the frequency response of a transmission line compensated with a TCSC shows similar behavior to a transmission line compensated with conventional fixed capacitors. The figure shows that at the frequency of 30 Hz, the

capacitive reactance of the TCSC is equal to the inductive reactance of the transmission line, hence the existence of a resonance point. However, in the case of the TCSC there is extra resistance at this resonant frequency [32]. This is another advantage of the TCSC, especially if the TCSC is used for power swing damping. This resistive component of the TCSC impedance is usually exploited to provide more positive damping torque when the power system experiences power oscillations.

2.5 Some Common Applications Of The TCSC

The TCSC's high speed switching capability provides a mechanism for controlling line power flow, which permits increased loading of existing transmission lines. This allows for rapid readjustment of line power flow in response to various contingencies, such as damping of power swings and Sub-synchronous resonance (SSR).

The TCSC can also be used as a conventional series capacitor by regulating steady-state power flow within its design limits. This section summarizes some of these typical benefits of the TCSC.

2.5.1 Power Swing Damping

One of the important applications of the TCSC is to damp power oscillations. When damping power oscillations, it is necessary to vary the applied compensation so as to counteract the accelerating or decelerating swings of the power system [10]. When a transient fault occurs, the rotationally oscillating generator accelerates and its rotor speed increases, so the electric power transmitted must be increased to limit the excess kinetic energy picked up by the generator. Conversely, when the generator decelerates, the electrical power transmitted must be decreased.

Figure 2.20 shows a typical machine's speed deviation, due to a transient fault. The figure also shows the benefit of using the TCSC's variable reactance to damp power swing oscillations. The blue curve shows the response of the system using a conventional (fixed) capacitor to compensate for the line inductance. As the graph illustrates, the oscillations are lightly damped. The red curve is the response of the system using a TCSC with the same steady state degree of compensation.

As the figure indicates, the oscillation damping is greatly improved by using a TCSC to vary the series compensation dynamically. In this particular illustration, the TCSC was controlled by a bang-bang type of controller [10]. The bang-bang controller can be defined as a controller with two states of capacitive reactance.

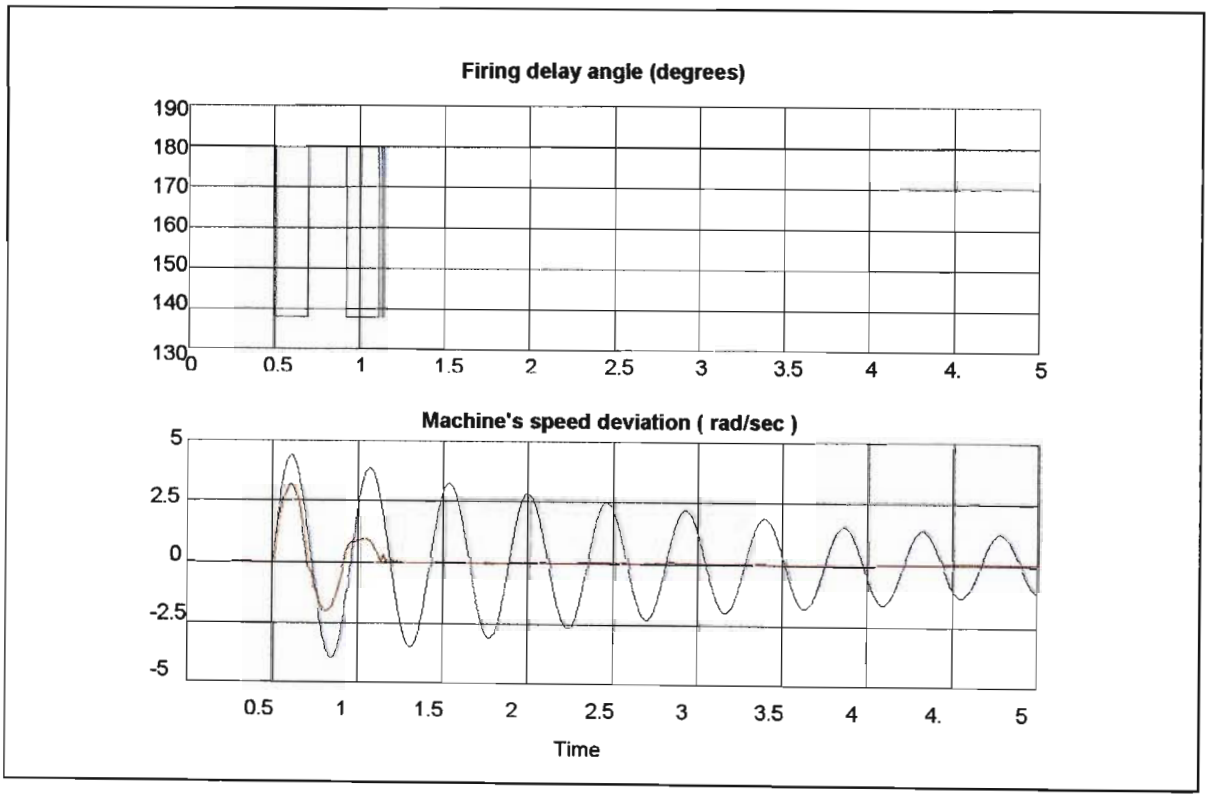

Figure 2.20: Power system oscillation damping: conventional capacitor vs bang-bang controlled TCSC.

The waveforms of Figure 2.20 show the corresponding uncontrolled and controlled oscillations of the machine's speed deviation around its steady state, following an assumed fault that initiated the oscillations. The first waveform, Figure 2.20, shows the TCSC firing delay angle. As the figure shows, this firing angle can either be

180° or 138°. The level of compensation is at the maximum, $\alpha = 138°$, when the speed deviation is positive. Conversely, the compensation level is at the minimum, $\alpha = 180°$, when the speed deviation is negative.

As the figure shows, the bang-bang controller is effective for damping large oscillations. However, damping relatively small power oscillations, continuous variation of the firing delay angle may be a better alternative [10].

2.5.2 Mitigation of Subsynchronous Resonance

Subsynchronous resonance involves oscillatory exchange of energy between a generator and the system below the fundamental system frequency, which is caused by series capacitive compensation. This phenomenon can result in dangerously large power oscillations (at subsynchronous frequencies) between the mechanical system and electrical system.

Computer simulation studies can be used to identify subsynchronous modes of oscillations. When the SSR contingency occurs, the TCSC can then be used to operate at levels that would mitigate the dangers of SSR.

2.6 Conclusion

Designing a TCSC could prove to be complicated task, unless all issues involved are clearly defined and addressed. This chapter has outlined these issues in detail and discussed the design limits associated with them. The review has shown that the choice of reactor and capacitor sizes of the TCSC, not only determines the operating region of the device, but also its operating performance. Rating of the

TCSC components and harmonics contributions are major issues when designing a TCSC. The dominance of the 3rd harmonic voltages was shown.

Chapter Two also discussed both the steady state and transient response of the TCSC. Under steady state conditions, it was shown that when the TCSC (instead of a conventional series capacitor) is fitted in a transmission line a similar resonant condition occurs to conventionally compensated line. However, the additional resistance introduced by the TCSC at resonance frequency, helps to produce positive damping to suppress power swing oscillations as well as to mitigate SSR. Under transient conditions, typical TCSC response curves were shown. The review also discussed the asymmetric nature of the TCSC response due to a step change in the firing delay angle.

Last section of Chapter Two discussed different applications of the TCSC, namely, damping power swings oscillations and mitigation of SSR. A typical response of the TCSC, controlled by a bang-bang type of controller, was shown and different control strategies were also mentioned. The phenomenon of SSR was also explained and the benefit of the TCSC to suppress it was also outlined.

The next chapter, Chapter Three, presents and develops the mathematical models of the TCSC used in the analysis and simulation studies of this thesis.

CHAPTER THREE

MATHEMATICAL MODELING FOR COMPUTER SIMULATION OF TCSC

3.1 Introduction

Chapter Two of this thesis has presented a literature survey that was carried out in order to understand those issues of the TCSC needed to develop the first TCSC hardware for the Machine's laboratory at Natal University. The first TCSC to be developed and applied to a transmission line, at Slatt substation – USA, was briefly discussed and the performance results of the pilot project were discussed.

Chapter Two then described different operating modes of the TCSC. However, most attention was placed on the capacitive vernier mode because the entire design, covered by this thesis, is based on this mode. Different factors, which need to be considered when designing the device, were outlined. These factors include the sizes of the TCSC components, the resonant point and the so-called reactance order. Another important topic that was covered in Chapter Two was the rating of the TCSC's components, namely, the internal capacitor and the reactor. The effect of harmonics was also discussed and their behavior in a transmission line with a TCSC was outlined.

Chapter Two then discussed both the time-domain and frequency responses of a transmission line equipped with the TCSC. Lastly, some common applications of the TCSC were discussed in Chapter Two.

Chapter Three outlines the work that was done during the development of a mathematical simulation model of the TCSC. All simulations were done on the EMTDC and MATLAB simulation platforms [37], [38]. Some issues that are discussed in this chapter include the development of the thyristor trigger circuit, choices of component sizes and some typical simulation results of the TCSC circuit.

3.2 Trigger Circuit for the TCR

The pulses generated by the trigger circuit sequentially trigger the thyristors of the TCR circuit. The firing sequence is the order the thyristors turn on (and off) during operation. Figure 3.1 shows the trigger logic circuit connected to the TCSC. In comparison, if the thyristors were replaced by diodes, then as soon as the voltage across the valve 1 went positive, the diode will turn on. However, if the thyristor is being used, a delay can be introduced on valve 1 by waiting for a period of time before applying a firing pulse. The time from when the voltage goes positive to when the firing pulse is applied is called the firing delay time, as Figure 3.2 illustrates. This delay angle is usually converted to a firing angle, α, using the system frequency.

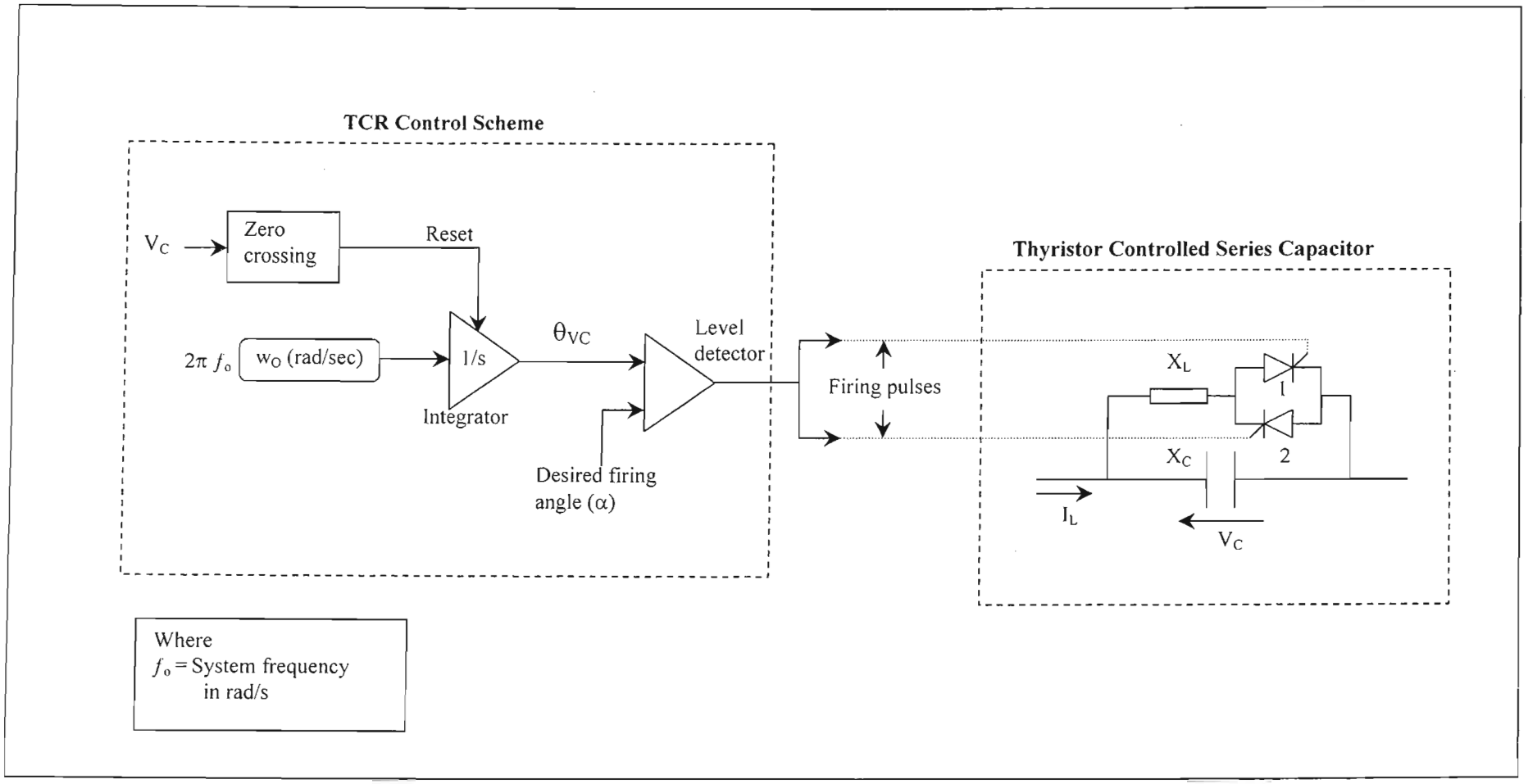

Figure 3.1: TCR trigger circuit and the TCSC

The TCR trigger circuit was designed based on the detection of zero crossing of the commutating capacitor voltage as shown in Figure 3.1. An integration of the fundamental frequency (rad/sec) produces a ramp signal θ_{VC}. A zero crossing outputs a pulse whenever the reference, V_C, goes through zero from a negative to a positive value. This pulse resets the integrator, so the output of the integration block produces a saw-tooth signal, which starts at 0.0 and reaches π radians before being reset.

The desired firing angle, α, is then compared to this ramp signal θ_{VC}. When the ramp is equal or greater then the desired firing angle, the output of the level detector changes its state from low to high (0 to 1). The resultant level is the firing pulse sent to the thyristors. Figure 3.3 shows the EMTDC simulation results of the TCR trigger circuit.

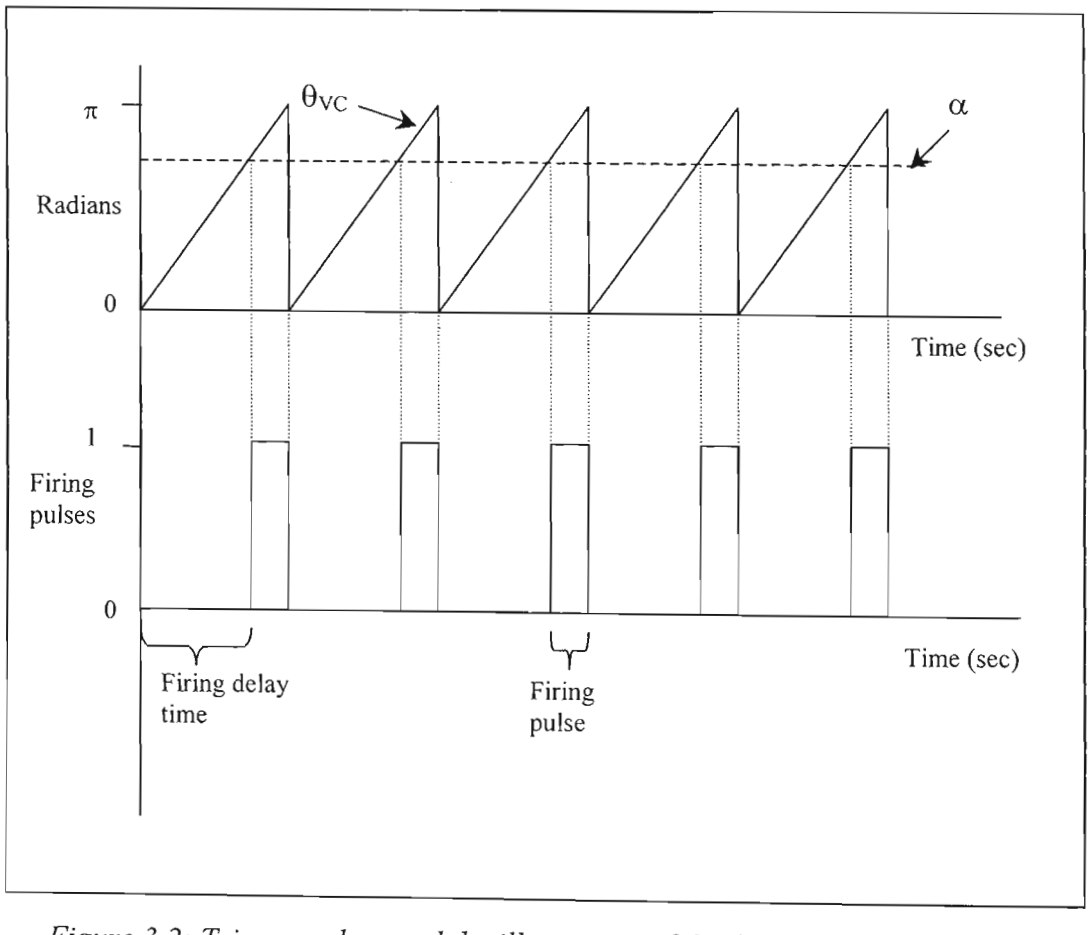

Figure 3.2: Trigger pulses and the illustration of the firing delay time

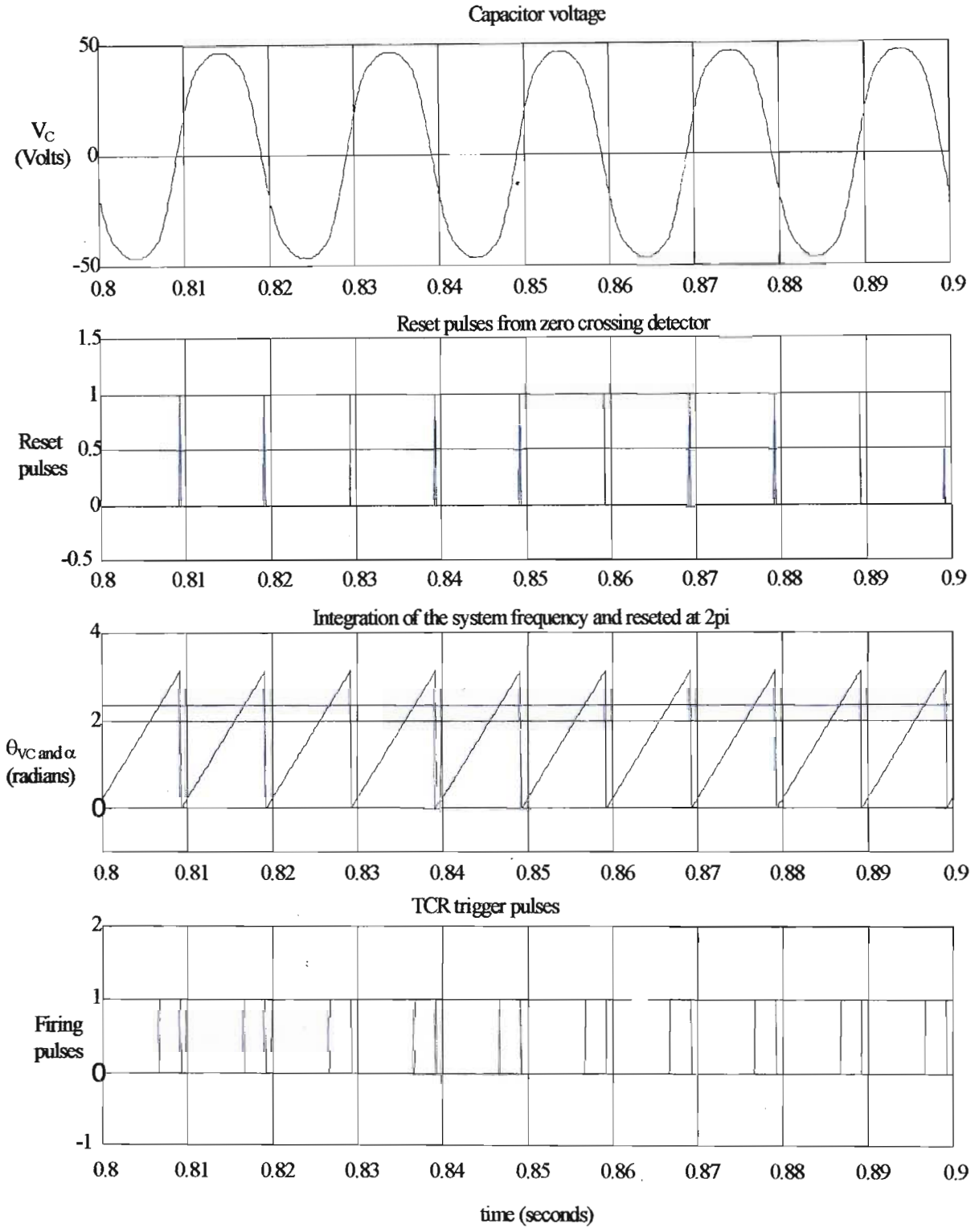

Figure 3.3: Time-domain results of the TCR trigger circuit

The full PSCAD/EMTDC circuit and the parameters of the components that were used to generate the results of Figure 3.3 are found in Appendix A.

3.3 Sizing of TCSC Variable Reactance Range

Since the main function of a TCSC is to provide a controllable capacitive compensating reactance in series with a transmission line, the design of any TCSC installation begins by specifying the range of the compensating reactance values that the device is required to provide for a specific application under consideration.

A literature review [1-5, 23,32] was thus carried out to establish typical variable reactance ranges for the common TCSC applications and results of this review are summarised in Table 3.1. The table shows the typical range of TCSC compensating reactance as a percentage of transmission line reactance in each case.

APPLICATION		VARIABLE REACTANCE RANGE
Local Mode Damping	First Swing	30%
	Small Signal	10%
Inter-Area Mode Damping	Small Signal	20%
Sub-Synchronous Reactance	SSR Damping	Case-Specific

Table 3.1: Summary of TCSC variable reactance ranges for typical applications in the literature.

The literature study revealed that the first swing damping requires the TCSC to provide a larger percentage of variable compensation than does small signal damping, which only needs about 10% variable capacitive reactance. In the case of inter-area modes, damping can be accomplished with only 20% variable compensation. Selection of a TCSC suitable for SSR damping depends entirely on the torsional modes of the system under investigation.

For the torsional modes in the Machine Research Laboratory, SSR is known to manifest itself at compensation levels between 40% and 70% [39] and the base impedance of this system is 16Ω. Therefore, to study the SSR characteristics of a TCSC in this laboratory, and to compare them with those of conventional (fixed) series compensating capacitors, a minimum TCSC reactance of –j6.4Ω is desirable and it should be capable of varying up to –j11.2Ω. By contrast, if the TCSC was to be used for power oscillation damping studies in the laboratory, without any possibility of exciting SSR, one would require a TCSC whose maximum reactance is below 40% of the line reactance.

Taking all these factors into account, it was decided to design a single-module TCSC that would be capable of providing controllable compensation of –j2Ω to –j6Ω (12.5% to 37.5% of system reactance). This compensation range is suitable for a wide range of power oscillation damping studies but below the level of compensation where SSR becomes a concern.

3.4 TCSC Design and Rating

The design procedure that was used in this study is based on that outlined in [19]; briefly, the steps followed in designing the TCSC are as follows:

3.4.1 Sizing the TCSC's Internal Capacitor

The reactance of a TCSC's internal (fixed) capacitor sets the minimum value of capacitive compensating reactance of the device; thus, based on the desired compensation range of the TCSC described above, each phase of the TCSC module required an internal capacitor of reactance –j2Ω at 50Hz, or 1592 μF.

3.4.2 Determining the TCSC's Maximum Reactance Order ($X_{ORDER(MAX)}$)

The reactance order of a TCSC is defined as a ratio of its effective capacitive reactance to the capacitive reactance of its internal capacitor, with $X_{ORDER} \leq 3$ typical. Thus, in this application each TCSC required a $X_{ORDER(max)}$ value of 3, which is within typical range.

3.4.3 Sizing the TCSC Inductor

When sizing the inductor in the thyristor-controlled reactor (TCR) branch of a TCSC, a number of issues are of concern, namely the current rating of both the inductor itself and the thyristors in series with it, the range of delay angles over which TCSC can be controlled, and the likely SSR characteristics of the TCSC [32]. Also, the inductor must be chosen so as to ensure that there is only a single resonant frequency in the TCSC's reactance versus firing angle characteristic [3].

$$\alpha_{res} = \pi (2n - 1) \frac{\pi}{2} \sqrt{\frac{X_{TCR}}{X_C}} \quad \text{.....} \quad \text{.....} \quad \text{.....} \quad (3.1)$$

$$n = 1, 2, 3 \text{.....}$$

Equation 3.1, from [3], was used to ensure that there was only one resonant point in the TCSC firing region. In ensuring that only one resonant point occurs in the firing region, Equation 3.1 was evaluated for several values of n for a chosen ratio of X_{TCR}/X_C, as shown in Table 3.2. The inductive reactance of the

TCR inductor is typically chosen as 0.1 to 0.3 times the TCSC's internal capacitive reactance X_C, although higher ratios have been reported [23]. Briefly, a lowering of the TCR inductance requires increased current rating of the circuit elements in the TCR branch and decreases the range of delay angle over which TCSC can be controlled; a higher TCR inductance reduces current rating of the TCR branch's circuit elements and increases the range of angles over which the TCSC can be controlled.

The TCR inductor values chosen were 2.55, 3.83 and 5.10 mH (0.8, 1.2 and 1.6 Ω at 50 Hz) allowing X_{TCR}/X_C ratios of 0.4, 0.6 and 0.8 to be selected for each TCSC module. Three different sizes of the TCR inductor were chosen to have more flexibility, since this is an experimental TCSC and having different sizes would allow the TCSC to be used for investigating the impact of different X_{TCR}/X_C ratios on TCSC performance in later projects. The X_{TCR}/X_C ratios were chosen to be somewhat higher than the typical range of 0.1 to 0.3 so as to reduce the current ratings of the inductors and thyristors in the TCR branch whilst still maintaining a workable range of delay angles and a single resonant frequency in the TCSC's impedance versus firing angle characteristics.

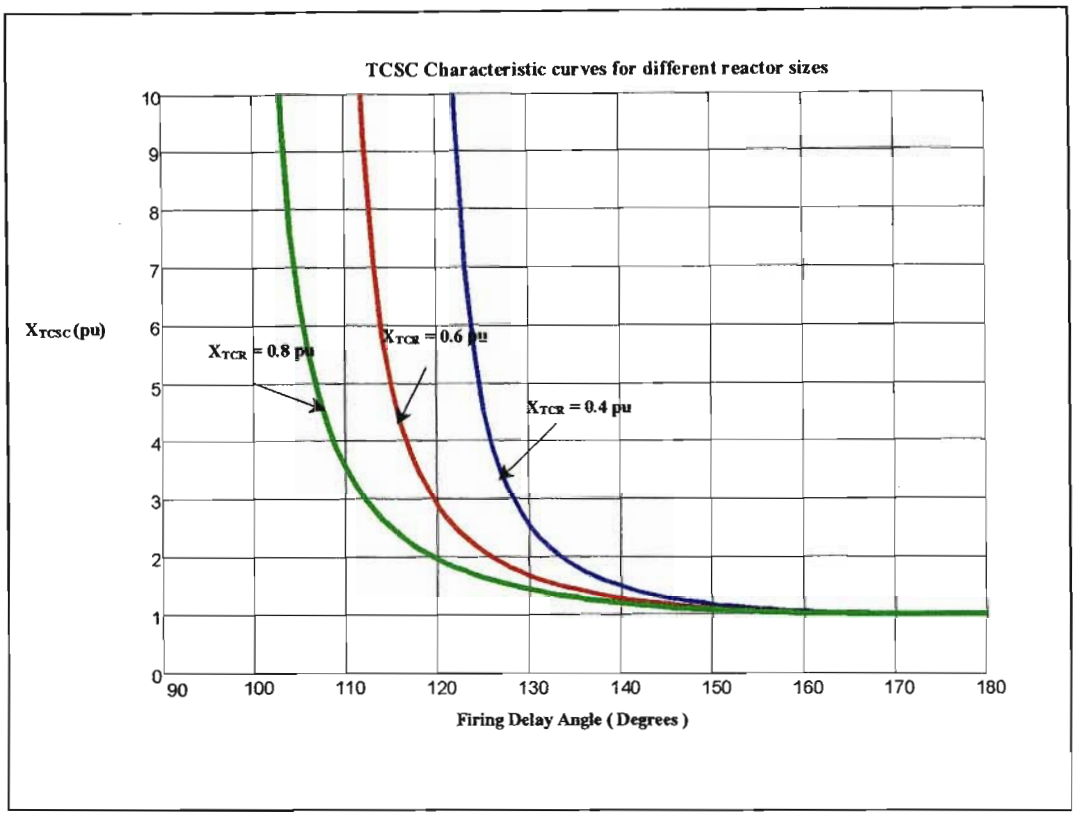

Figure 3.4: TCSC characteristic curves' variations with three sizes of the reactor

Figure 3.4 shows the TCSC characteristic curves for different TCR inductor values. The figure shows that the firing range increases as the reactor size is increased.

TCR Reactance @ 50 Hz	Resonant point (n=1)	Resonant point (n=2)	Resonant point (n=3)	Resonant point (n=4)
0.2 Ω	151.54 °	94.62°	37.70°	-19.22°
0.8 Ω	123.08°	9.24°	-104.61°	-218.45°
1.2 Ω	110.29°	-29.14°	-168.57°	-307.99°
1.6 Ω	99.50°	-61.50°	-222.49°	-383.50°

Table 3.2: The relationship of X_{TCR} size and the resonant point for a given value of n and X_C = -j2 Ω

Table 3.2 shows that, for the chosen values of reactors, only one resonant point exists in the operating range of the firing delay angle (i.e. between firing 90° to 180°). However, if the reactor size were chosen to be 0.2 Ohms (as the table shows), two resonant points would have occurred in the operating range of the firing delay angle.

TCSC Simulation Results

The next step, after deciding on the TCSC's component sizes, in constructing the laboratory-scaled TCSC was to simulate the circuit in order to verify its operation and the effect of changing the reactor size. Another important observation that was made from the simulations, was the response of the circuit when the reactance order is changed.

There are two sets of results that were captured from this simulation study. The first set of simulation results show the circuit response when the reactance order was changed and the second set shows the circuit response when the reactor size was increased.

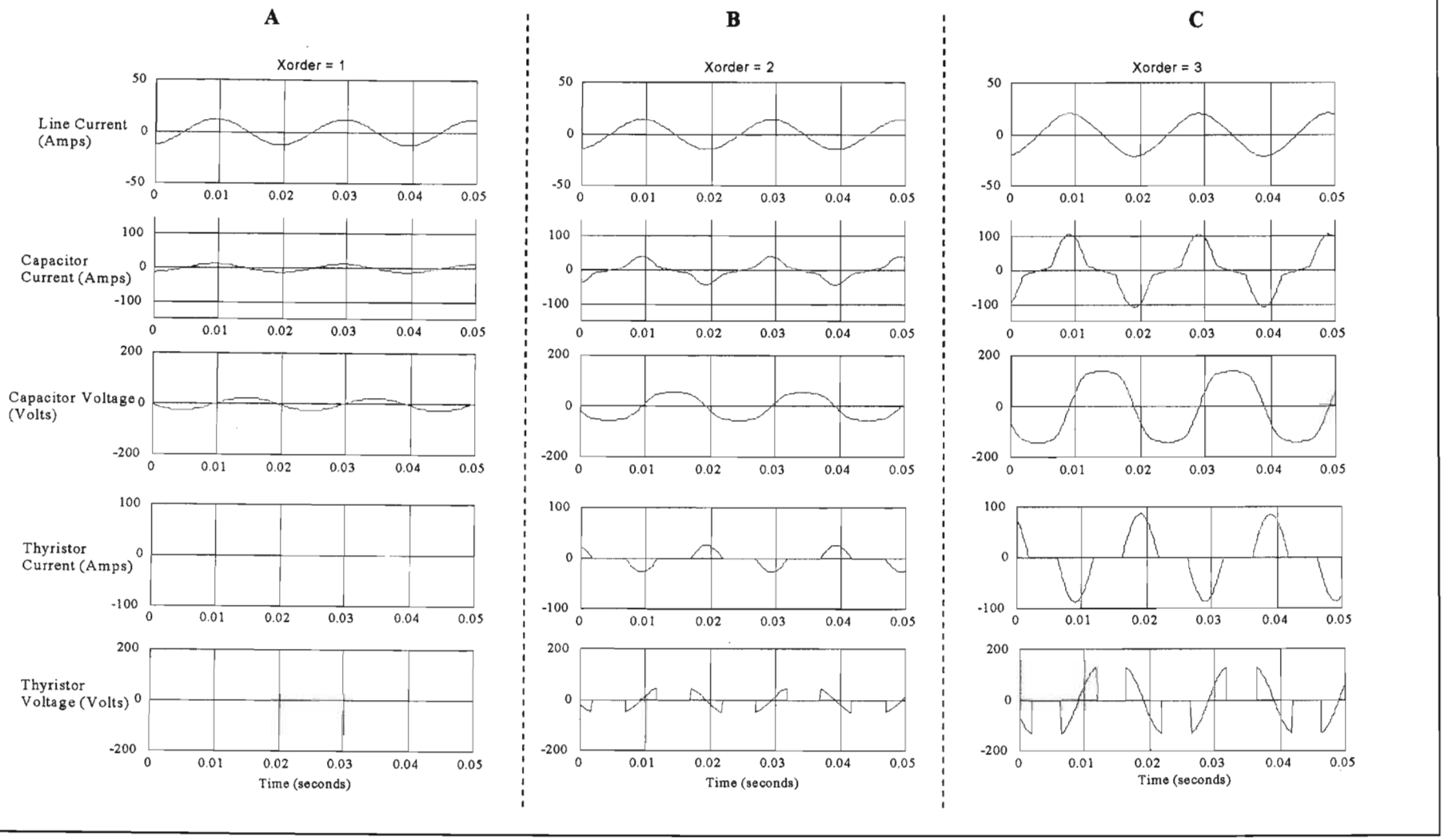

Figure 3.5: EMTDC/PSCAD time-domain simulation results of the TCSC with the X_{TCR} = 0.8 Ω. The simulation was done at X_{ORDER} of 1 (A), X_{ORDER} of 2 (B) and X_{ORDER} of 3 (C).

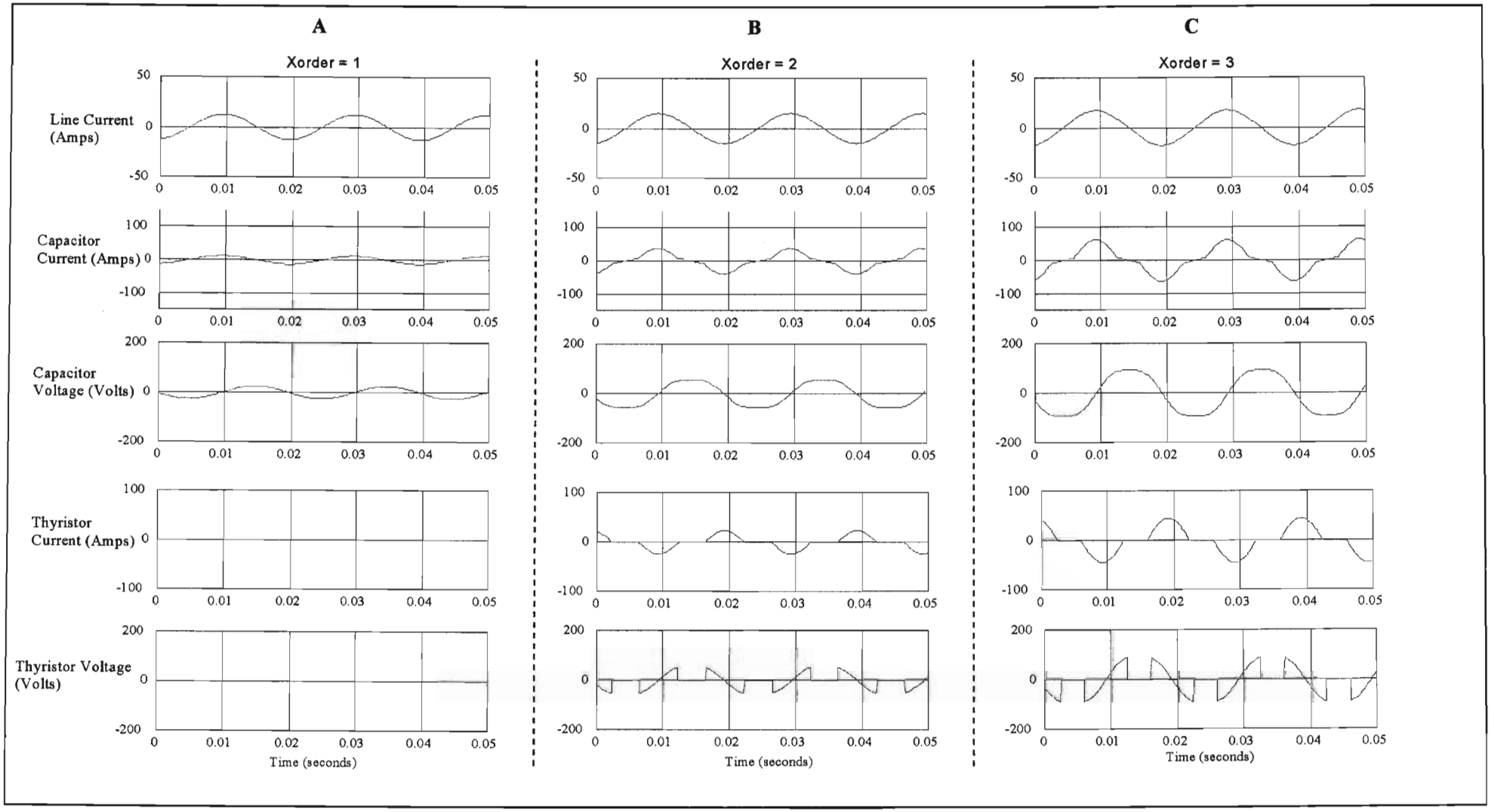

Figure 3.6: EMTDC/PSCAD time-domain simulation results of the TCSC with the X_{TCR} = 1.2 Ω

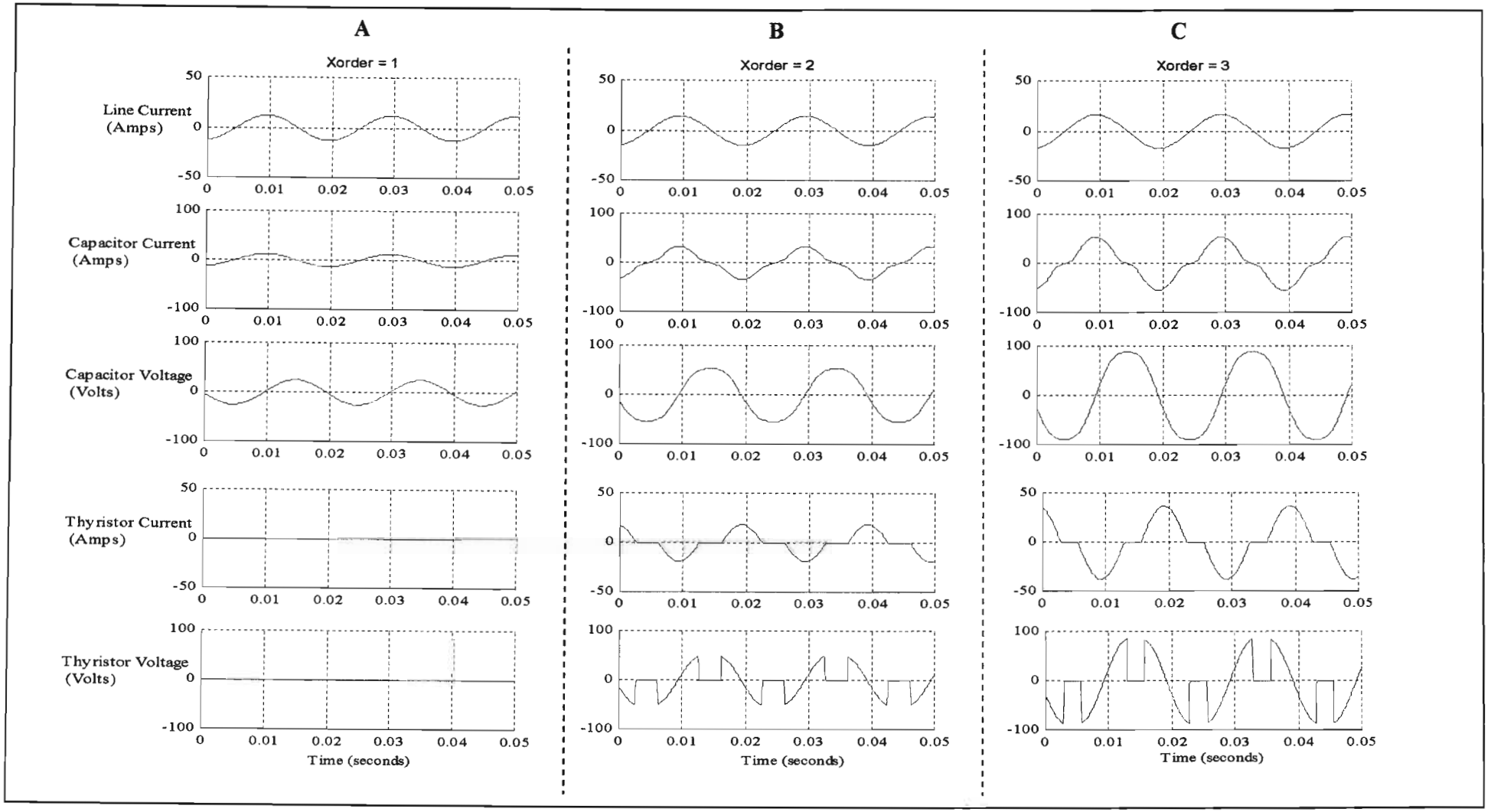

Figure 3.7: EMTDC/PSCAD time-domain simulation results of the TCSC with the X_{TCR} = 1.6 Ω. The simulation was done at X_{ORDER} of 1 (A), X_{ORDER} of 2 (B) and X_{ORDER} of 3 (C).

Observations from the simulation

- Figures 3.5 – 3.7 show that at reactance order of 1, there is no current flowing through reactor and thyristor switches. This is because the thyristors are gated at the angle of 180°.
- The figures also show that both the capacitor voltage and capacitor current increase as the reactance order is changed from the value of 1 to the value of 3.
- The figures also show that during capacitive firing mode, the capacitor current is the sum of the line current and the TCR branch current.

The effect of changing the TCR branch reactor was investigated. Figures 3.8 – 3.10 show the time-domain simulations for different reactor sizes and the following observations were made:

- At the firing delay angle of 180°, the TCR reactor has no effect on the TCSC circuit because the thyristors are blocked (no conduction). Hence, the line current is equal to the capacitor current and both the capacitor current and capacitor voltage do not change with changes of the TCR reactor size.
- Figure 3.9 and 3.10, illustrate that both the magnitude of the TCR current and capacitor current (hence reactor voltage magnitude and capacitor voltage magnitude) decrease as the reactor size increases. This implies that to decrease the current rating of the capacitor, reactor and thyristor valves, a larger reactor should be used

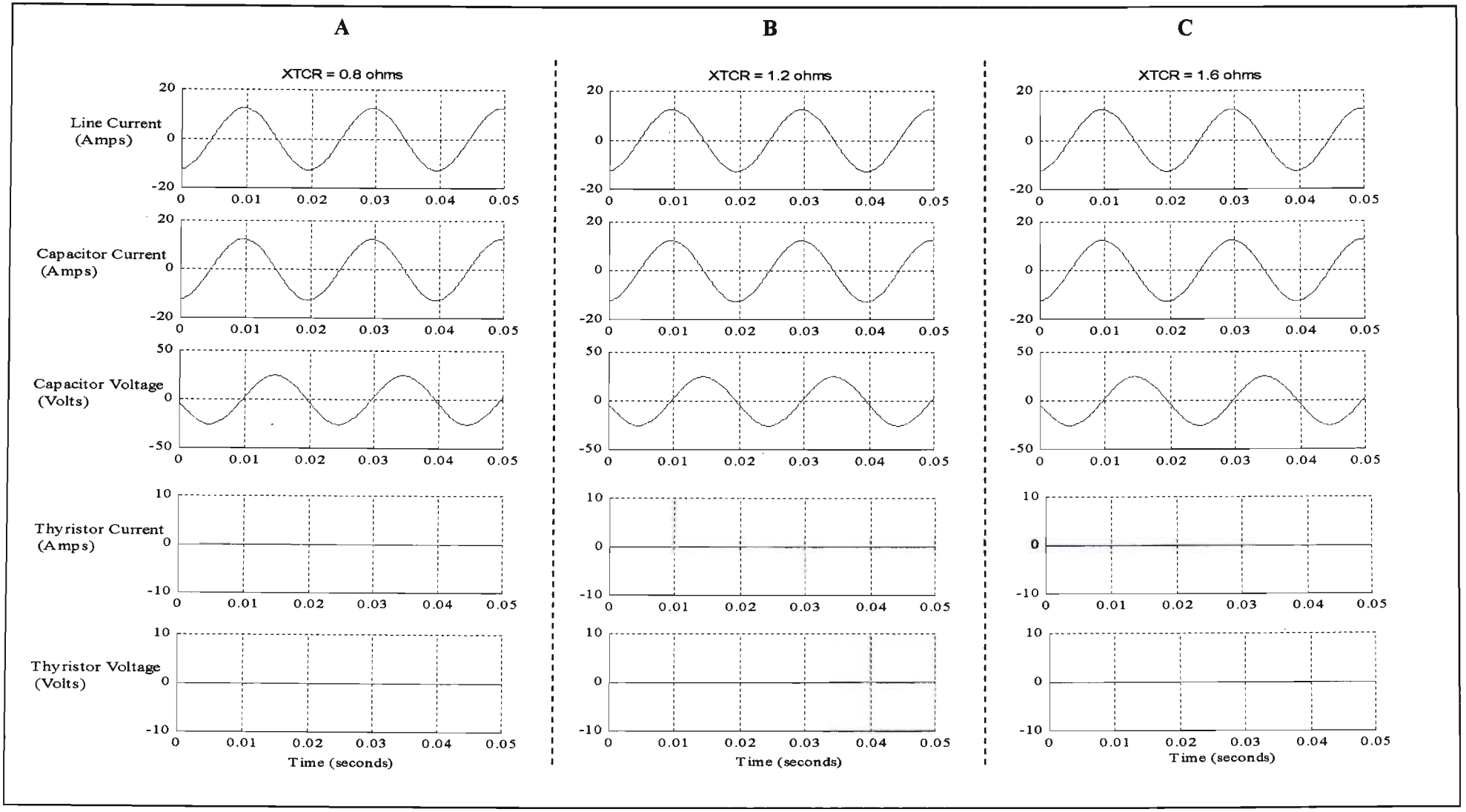

Figure 3.8: EMTDC/PSCAD time-domain simulation results of the TCSC with the X_{TCR} = 0.8 Ω (A), 1.2 Ω (B) and 1.6 Ω (C). The simulation was done at X_{ORDER} of 1.

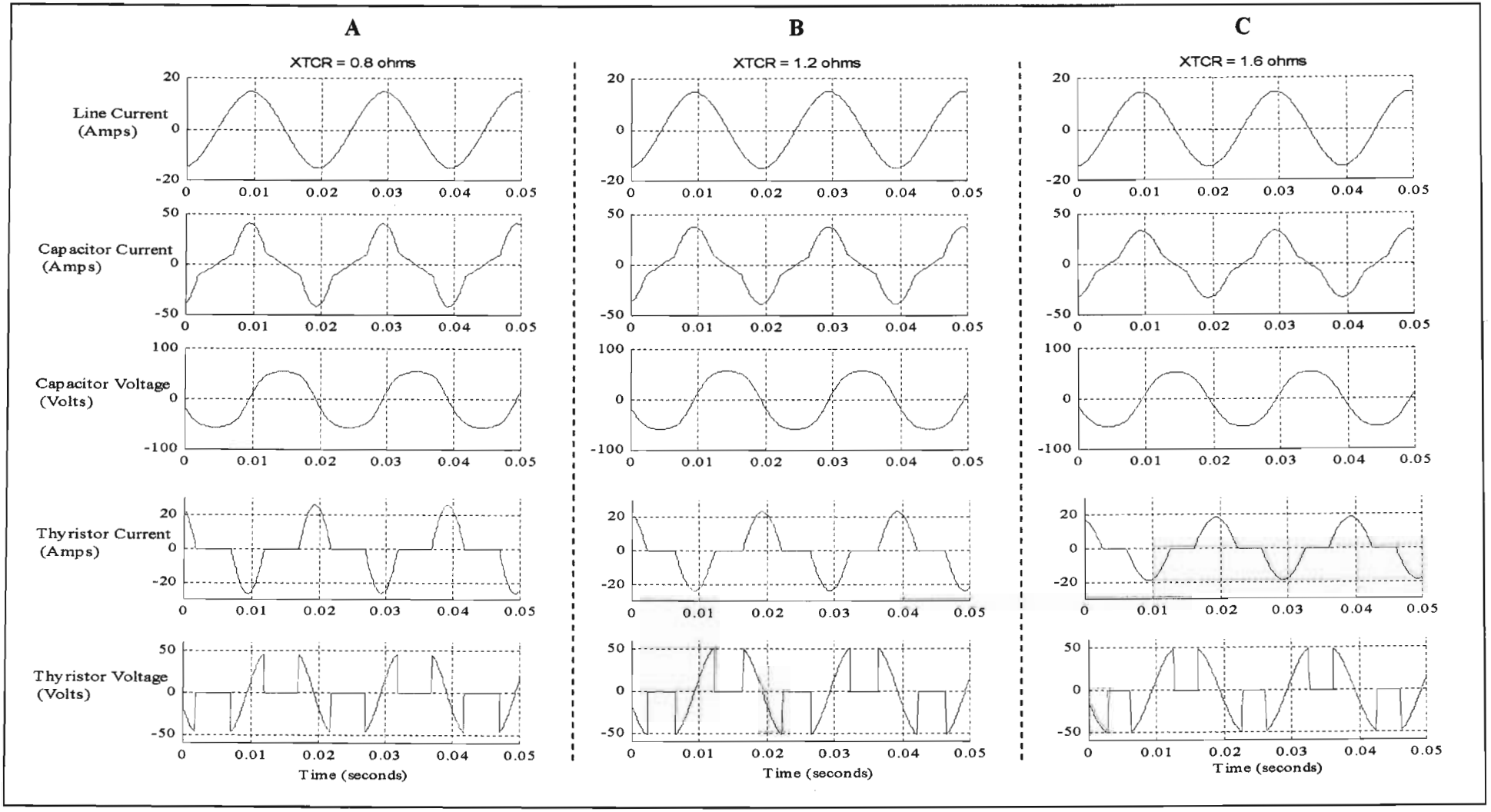

Figure 3.9: EMTDC/PSCAD time-domain simulation results of the TCSC with the X_{TCR} = 0.8 Ω (A), 1.2 Ω (B) and 1.6 Ω (C). The simulation was done at X_{ORDER} of 2

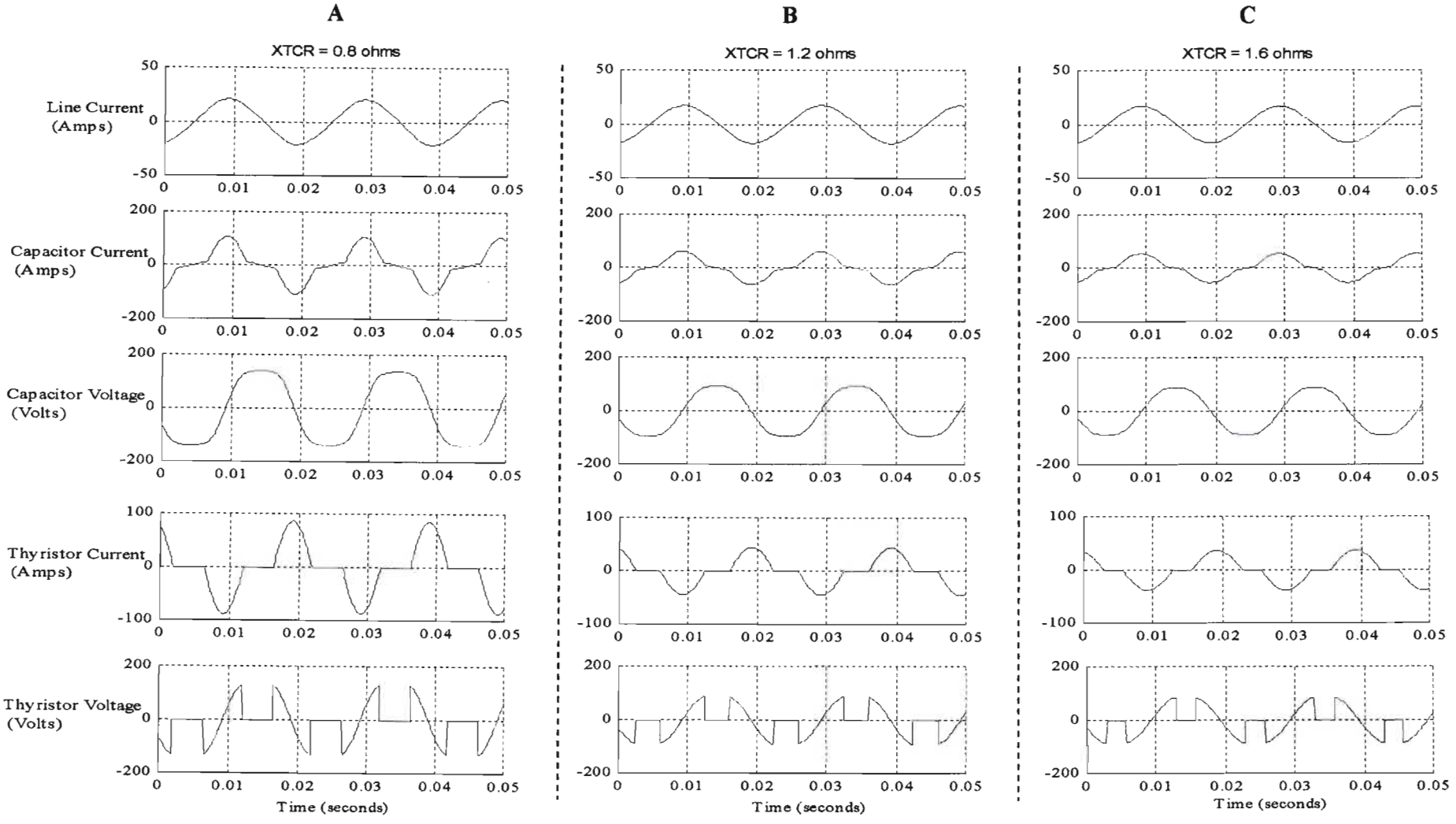

Figure 3.10: EMTDC/PSCAD time-domain simulation results of the TCSC with the X_{TCR} = 0.8 Ω (A), 1.2 Ω (B) and 1.6 Ω (C). The simulation was done at X_{ORDER} of 3

3.4.4 Rating the TCSC's circuit components

The detailed EMTDC simulation model of a TCSC that was developed was used to run a number of additional case studies in order to predict the actual reactance versus firing angle characteristics of the designed TCSC and to decide upon appropriate current and voltage ratings for its circuit components.

Tables 3.3 to 3.5 summarise the rating requirements obtained from the studies done for each value of TCR inductor at two transmission line conditions: rated line current and twice rated line current based on the parameters of the Machine's Research Laboratory. In each case, the study was carried out with the TCSC module providing its maximum capacitive reactance of –j6 Ω, since this is the condition under which its voltages and currents are at a maximum for a given line current. The performance of the TCSC at higher than rated line current is of interest since the device may be required to tolerate temporary overcurrents during transient studies in the laboratory.

X_{TCR} = 0.8 Ω			
Line Current	**Capacitor**		**Reactor**
	kVAr	Voltage (rms)	Current (rms)
1 pu (7.87 A rms)	6.63	53.89	29.69
2 pu (15.74 A rms)	26.69	108.06	82.34

Table 3.3: TCSC component ratings at X_{TCSC} = -j6 Ω with X_{TCR} = j0.8 Ω

X_{TCR} = 1.2 Ω			
Line Current	**Capacitor**		**Reactor**
	kVAr	Voltage (rms)	Current (rms)
1 pu (7.87 A rms)	5.77	53.55	24.68
2 pu (15.74 A rms)	23.31	107.62	49.73

Table 3.4: TCSC component ratings at X_{TCSC} = -j6 Ω with X_{TCR} = j1.2 Ω

$X_{TCR} = 1.6\ \Omega$			
Line Current	**Capacitor**		**Reactor**
	kVAr	Voltage (rms)	Current (rms)
1 pu (7.87 A rms)	4.486	49.213	19.29
2 pu (15.74 A rms)	20.886	106.31	49.10

Table 3.5: TCSC component ratings at $X_{TCSC} = -j6\ \Omega$ with $X_{TCR} = j1.6\ \Omega$

The results of the studies confirmed that the required current rating of the thyristors and the reactor within the TCSC decreases as the TCR inductance is increased. Based on the results in the above Tables, air core inductors were built for the laboratory TCSC using 3.15 mm diameter copper wire, resulting in a worst-case current carrying requirement of 55 Amps.

The same current rating was applied when choosing the thyristors for the TCSC. Finally, six 400V, 777 μF capacitors were purchased. These hardware components were combined to form the first –j2 Ω to –j6 Ω module of the laboratory-scale three-phase TCSC in order that testing and evaluation could be done.

3.5 Harmonic Analysis of the TCSC

The EMTDC model of TCSC was used to investigate the impact of harmonics on the transmission line and on the TCSC's loop current for the laboratory TCSC design carried out in the previous section. The harmonics of the capacitor voltage and their effects on the power system were studied. The component sizes for the mathematical model are the same as those found in Appendix A, however the results presented in this section are only those captured for X_{TCR} = 0.8 Ω.

3.5.1 TCSC Harmonic Voltage

The measured 3rd, 5th and 7th TCSC harmonic voltages versus firing angle are shown in Table 3.6. These results were then plotted in Matlab to graphically illustrate the characteristic of the magnitude of each harmonic voltage as the firing angle was varied. Figure 3.11 shows the characteristics of the harmonic voltages as the firing angle was varied. Each harmonic is expressed as a percentage ratio with respect to the fundamental frequency voltage component.

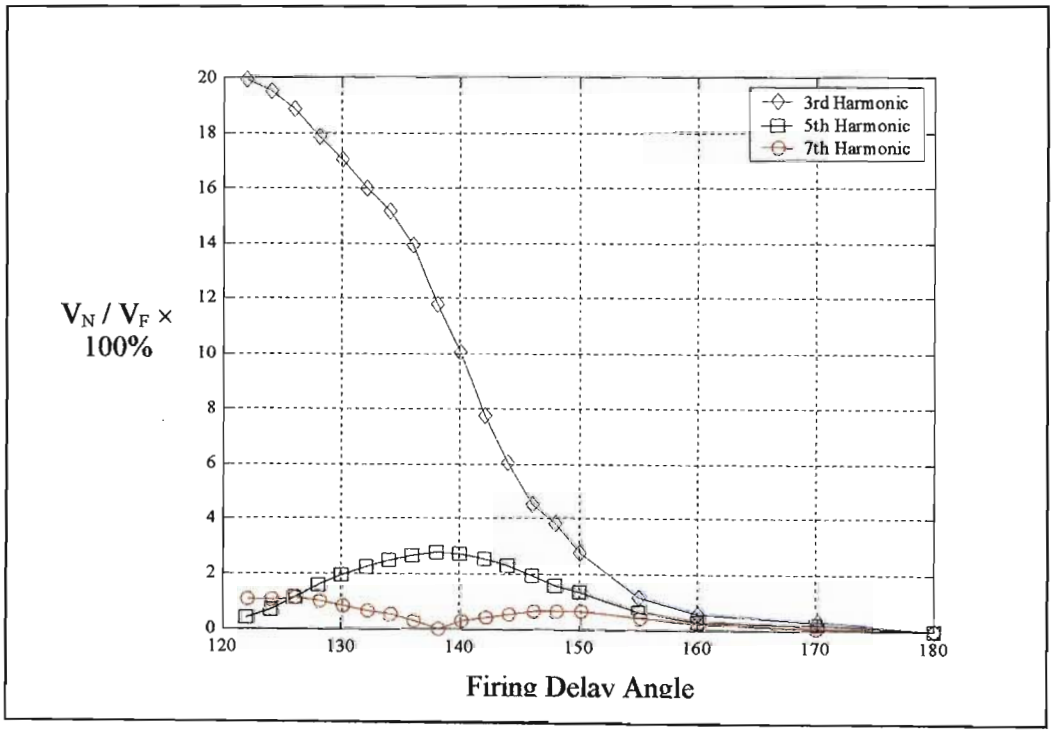

Figure 3.11: Harmonic generated in pu of fundamental as a function of alpha

Firing Delay Angle (Angle)	50 Hz TCSC Voltage (Volts)	3^{RD} Order TCSC Voltage (% of fundamental)	5^{TH} Order TCSC Voltage (% of fundamental)	7^{TH} Order TCSC Voltage (% of fundamental)
180	9.697	0.00	0.00	0.00
170	9.810	0.29	0.16	0.05
160	9.922	0.57	0.31	0.21
155	10.175	1.16	0.67	0.40
150	11.230	2.75	1.36	0.65
148	11.665	3.82	1.61	0.67
146	12.195	4.50	1.93	0.64
144	14.541	6.02	2.28	0.55
142	15.654	7.74	2.51	0.43
140	20.380	10.03	2.67	0.29
138	27.510	11.80	2.77	0.00
136	30.410	13.98	2.65	0.29
134	108.320	15.21	2.49	0.52
132	123.930	16.03	2.20	0.67
130	90.270	17.08	1.94	0.81
128	35.780	17.91	1.60	0.99
126	23.001	18.91	1.10	1.09
124	18.020	19.54	0.69	1.08
122	15.927	19.94	0.43	1.04

Table 3.6: Harmonics of TCSC voltage at $X_{TCR} = 0.8\ \Omega$

3.5.2 Harmonic Analysis of the Line Current

The Table 3.7 shows the results of the harmonic analysis of the line current at $X_{TCR} = 0.8\ \Omega$. The resonant point of the TCSC circuit with reactor of 0.8 ohms is approximately 123°, hence the operation range of the TCSC is [135°, 180°]. It can be seen, from Table 3.7 that the worst-case harmonics are below 5% of the fundamental frequency current. The same trend is found in the case of other reactor values ($X_{TCR} = 1.2\ \Omega$ and $X_{TCR} = 1.6\ \Omega$). It can therefore be seen that the harmonics are indeed largely confined inside the TCSC loop and, moreover, that the effect of the harmonics presents in the TCSC capacitor voltage on the rest of the power system is also slight.

Clearly though, the TCSC capacitor must itself be rated to handle the harmonics present in its voltage under normal operating conditions (Figure 3.11). In the case of the laboratory-scale TCSC, the 777μF capacitors that were purchased were rated to 400 V rms for normal fundamental frequency operation. It was thus assumed that because the peak amplitudes of all the voltages in the harmonic spectrum of the laboratory TCSC would be significantly below 400V, and because the laboratory TCSC would not be in continuous service, the 400 V capacitors would be acceptable for this application.

Firing Delay Angle (Degrees)	Line Current (Amps) (Fundamental)	3^{RD} Harmonic Line Current (Amps)	5^{TH} Harmonic Line Current (Amps)	7^{TH} Harmonic Line Current (Amps)	Sum of the Harmonic currents (Amps)	Harmonic currents as a % of the fundamental component
180	2.424	0	0	0	0	0 %
160	2.437	0.001	0.0004	0.0002	0.0016	0.065654 %
155	2.452	0.002	0.0008	0.0004	0.0032	0.130506 %
150	2.514	0.007	0.0019	0.0006	0.0095	0.377884 %
145	2.570	0.001	0.0028	0.0030	0.0068	0.264591 %
140	3.042	0.030	0.0069	0.0004	0.0373	1.226167 %
135	7.630	0.342	0.0325	0.0068	0.3813	4.997379 %

Table 3.7: Harmonics of the Line Current at $X_{TCR} = 0.8\ \Omega$

3.6 Conclusion

Chapter Three has presented the development of the mathematical model to investigate the characteristics of the TCSC. As an important integral part of the TCSC circuit design, the control circuit that generates the firing pulses for the TCR thyristors was presented and its operation was also explained. The chapter has outlined the methodology that was followed to determine the sizes of both the capacitor and the reactor in the laboratory-scale TCSC to be constructed.

The effect of changing the size of reactor was investigated. Reactors of sizes 0.8 Ω, 1.2 Ω and 1.6 Ω were chosen for the laboratory-scale TCSC. The investigation confirmed that the ratings of the TCSC components are dependent on the size of the TCSC reactor. The current and kVAr ratings of both the capacitor and reactor decrease as the size of the reactor is increased.

This chapter has also discussed the impact of TCSC harmonics on the transmission line currents. Several simulations were conducted to deduce the effect of the TCSC harmonics on the power system. The simulation results showed that:

- The TCSC 3rd harmonic voltage is dominant and other orders of voltage harmonics are negligible in magnitude. The results also show that the magnitude of the harmonic voltages increases as the reactor size is decreased;
- The harmonic currents were found to be largely confined within the TCSC loop. Only a small magnitude of the harmonic currents (5% at most) was found in the line currents.

Chapter Four considers the actual construction of the laboratory-scale TCSC. Chapter Four also presents a comparison of the simulated and measured performance of the laboratory-scale TCSC.

CHAPTER FOUR

DEVELOPMENT OF A LABORATORY PROTOTYPE TCSC

4.1 Introduction

The earlier chapters of this thesis have dealt with the theoretical development of the Thyristor-Controlled Series Capacitor (TCSC) and its associated trigger circuit. Chapter Three has outlined the development of the TCSC's trigger circuit and its capability to vary the capacitive magnitude of the TCSC. Chapter Three has also outlined the methodology that was followed to determine the components' sizes and their voltage / current ratings in the laboratory-scale TCSC model.

The development of the mathematical model of the TCSC was also described in Chapter Three. Time-domain simulations and frequency responses of the TCSC mathematical model were also included in Chapter Three.

Chapter Four describes the development of a laboratory-scale TCSC for the Machines Research Laboratory at Natal University. The purpose of this laboratory-scale TCSC development is to confirm, using practical measurements, those capabilities of the TCSC model, which were demonstrated in the simulation studies of earlier chapters and, in so doing, to demonstrate the practicality of the TCSC. However, the laboratory-scale model is also intended to form the basis for possible future investigations into the use of the TCSC to dynamically control the reactance of the transmission line as a means of enhancing power system stability. Hence, the parameters of the TCSC have been designed specifically for the Machines Research Laboratory system [39].

Finally, this chapter provides measured results of the performance of the laboratory-scale TCSC; these measured results are compared with the performance predicted using the simulation model of the TCSC developed in Chapter Three.

4.2 Practical Implementation

The first section of this chapter begins by providing a description of different equipment, which was used during the development and testing of the laboratory-scale TCSC.

4.2.1 Hardware Description

Figure 4.1 shows the detailed diagram of the circuit used during the testing phase of the TCSC. The measured results from the TCSC, which are presented in this chapter, were captured using a data acquisition card mounted in a personal computer. The hardware TCSC will eventually be fully integrated into the Machines Research Laboratory that already exists at Natal University. However, for the purpose of this project, the hardware TCSC was tested using a combination of the transmission line simulator and AC voltage sources in the Machines Research Laboratory. Although not all the equipment in the laboratory was used in the testing of the hardware TCSC, some of it is included in the following description for completeness, since it is likely to form part of future TCSC studies.

Voltage Source

A three-phase variac (variable voltage transformer) provided the variable voltage supply. The input voltage to the variac was connected to the infinite bus supply in the laboratory (220 V line).

TCSC Hardware

As discussed in earlier chapters, the TCSC is made up of a conventional capacitor connected in parallel with a thyristor-controlled reactor (TCR). Figure 4.1 shows a single-line diagram of the TCSC together with other components of the test circuit. The capacitance in each phase of the circuit in Figure 4.1 is 1554 μF (rated at 400 V per phase) corresponding to 2 Ω at 50 Hz.

As discussed in Chapter Three, three different TCR inductor sizes were chosen for future flexibility. Thus, depending on the tests conducted, the TCR inductors, in each phase in Figure 4.1, were either 2.55 mH, 3.83 mH or 5.10 mH air core devices (either 0.8 Ω, 1.2 Ω or 1.6 Ω at 50 Hz).

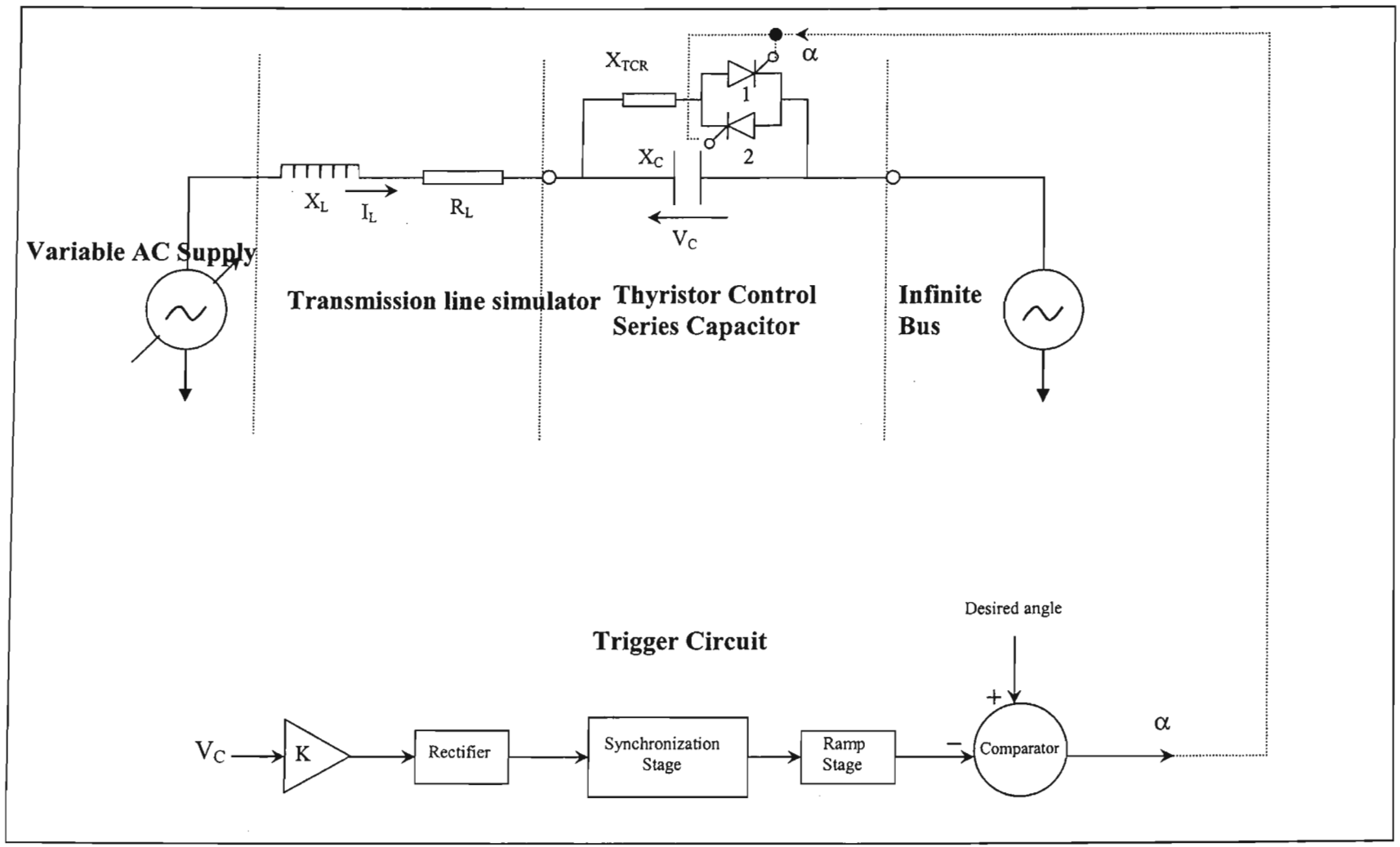

Figure 4.1: Diagram of the laboratory-scale TCSC

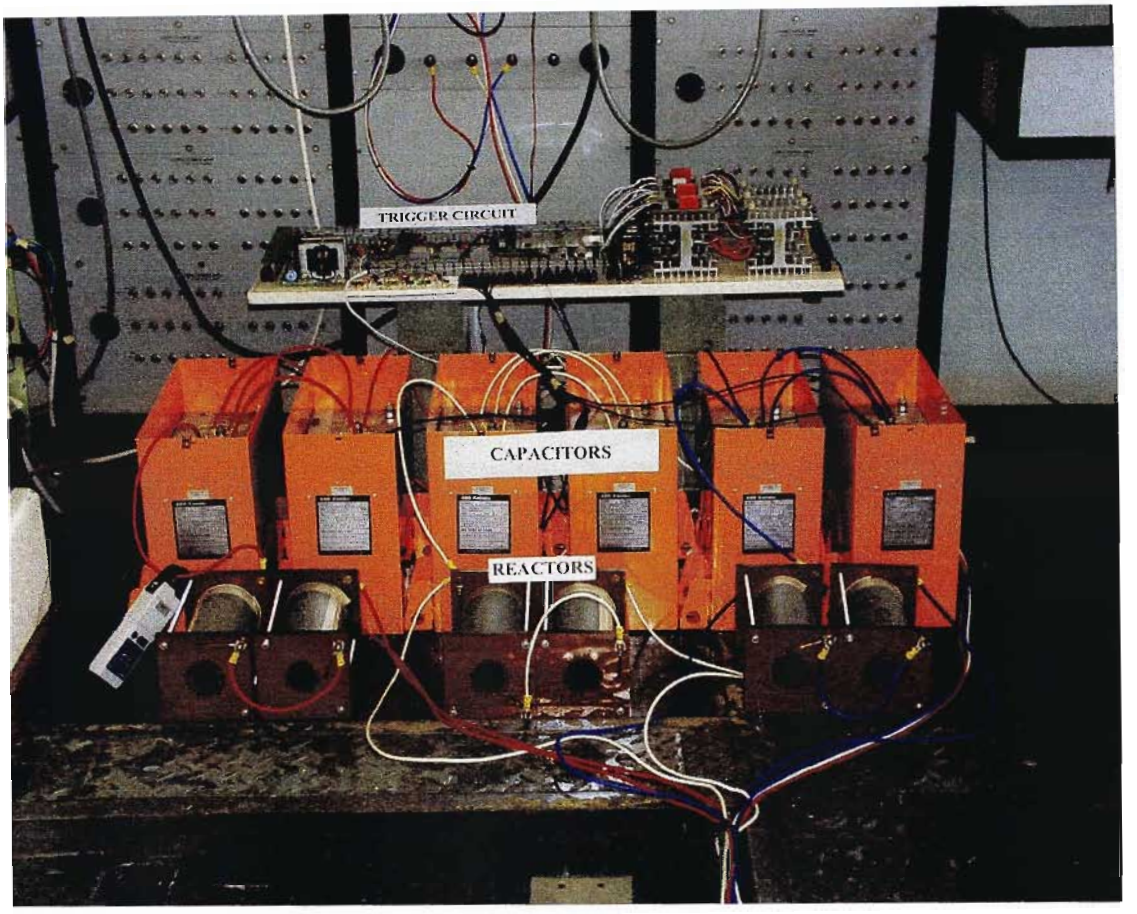

Figure 4.2: The three-phase TCSC circuit

Transmission Line Simulator

The Micro-Machine Research Laboratory contains a transmission line simulator that can model transmission networks of up to 1700 km in length. The transmission line simulator is composed of a bank of lumped inductors and capacitors that may be switched in or out as per requirement [39], [40]. The inductors were specially designed with large air gaps in order to avoid saturation.

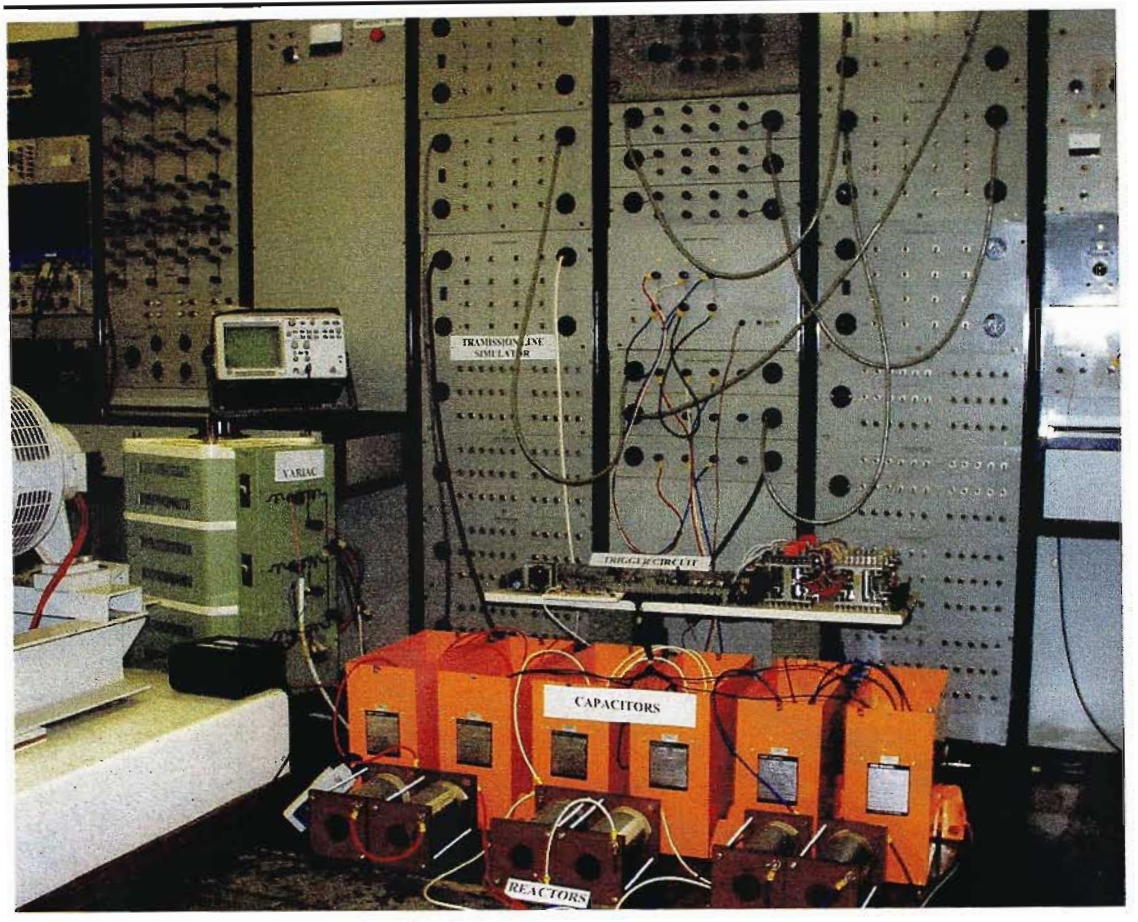

Figure 4.3: The transmission line simulator

Micro-Alternator

Although the measurements carried out in this thesis did not make use of the micro-alternators in the laboratory, it is assumed that the future TCSC investigations will include these machines. Indeed, the ratings and impedance range of the hardware TCSC that has been designed are ultimately related to the parameters and ratings of the laboratory micro-alternators. The laboratory micro-alternators are three-phase machines with a rated line-to-line voltage of 220 V and a rated per-phase current of 7.87 A, resulting in an overall three-phase power rating of 3 kVA.

Trigger Circuit

For the laboratory testing, an existing three-phase trigger channel circuit was adapted for the TCSC application. The need to adapt this trigger channel circuitry arose because firing of the TCSC's thyristors is synchronized to the TCSC capacitor voltage. The capacitor voltage in a TCSC application varies significantly in amplitude as the transmission line current (and TCSC firing condition) varies. As a result, the conventional synchronizing stage of the existing analogue trigger channel was found to give inaccurate and inconsistent performance when used to determine the required turn on pulses for the TCSC's thyristors.

These inaccuracies are due to following reasons:

a). In the analogue synchronizing stage (zero crossing detector), the width of the zero crossing pulses depends on the magnitude of AC voltage, as shown in Appendix B. The amplitude of the TCSC capacitor voltage is expected to vary by a significant amount (2-3 times) under normal operating conditions.

b). The ramp stage of the analogue trigger channel can only be set up to provide accurate generation of firing pulses for one amplitude of TCSC capacitor voltage. At other values of TCSC capacitor voltage, the turn on pulse occurs at incorrect points on the waveform, as clearly seen in Appendix B.

To minimize the impact of variations in the amplitude of the capacitor voltage, two design changes were made in the trigger channel. Extra gain was added in the synchronization stage, as shown by Figure 4.5. This extra gain reduces (but does not completely get rid of) the variation in width of the zero crossing pulses as the capacitor voltage amplitude changes. Secondly, the value of resistor **R** (Figure 4.5) was carefully chosen such that the trigger channel has its best accuracy at a TCSC capacitor voltage in the middle of the expected operating

range. Clearly, these measures do not remove the errors, but there were found to significantly reduce their impact on the overall operation of the trigger channel. A set of diagrams that illustrates the impact of variations in the TCSC capacitor voltage amplitude on the accuracy of the firing pulses is found in Appendix B.

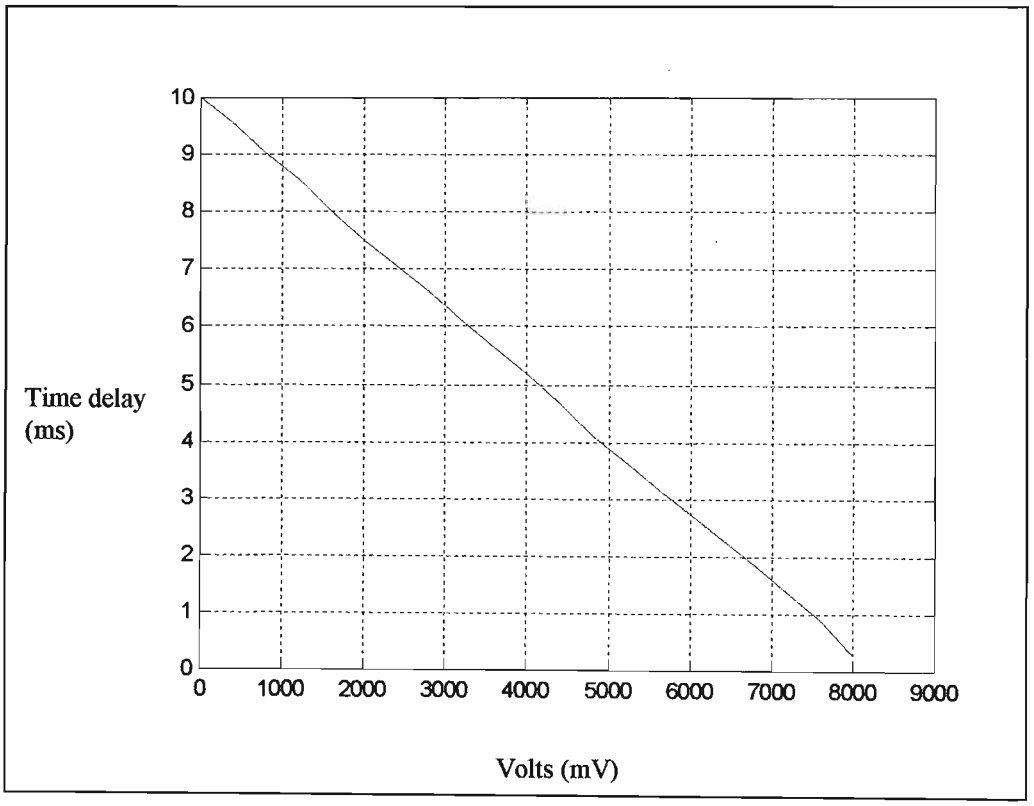

Figure 4.4: Relationship between the variable pot resistance and the firing angle

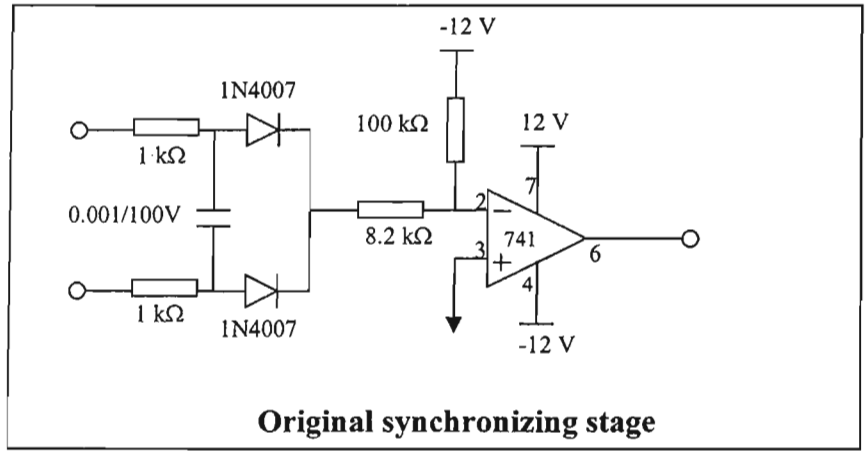

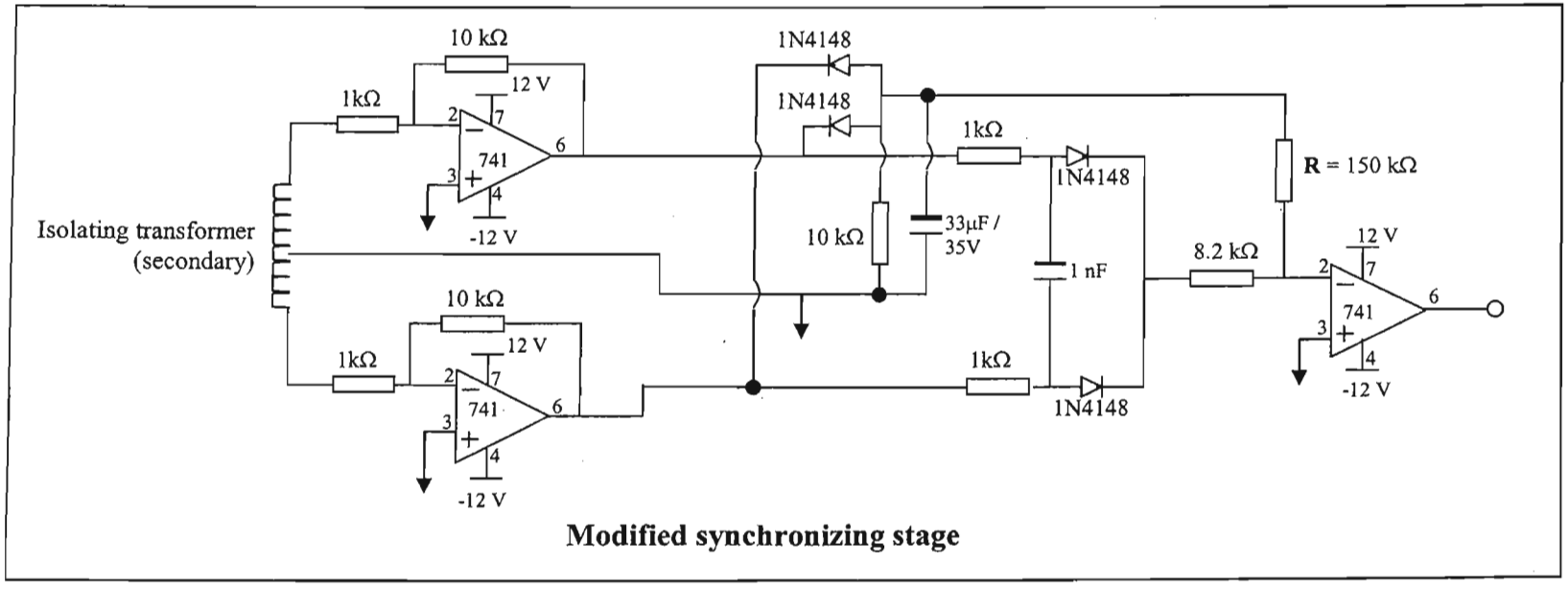

Figure 4.5: Original and modified synchronizing stage circuit

4.3 Practical Results

This section of the thesis presents and discusses the measured results that were obtained from the laboratory-scale TCSC. The measured results are also compared to the results of the mathematical model developed and simulated on EMTDC. The laboratory-scale TCSC has three phases (A, B, and C), however only phase A results are shown in this chapter. The rest of the results can be found in Appendix C.

4.3.1 Practical TCSC Characteristics

Figure 4.6 to Figure 4.8 show that for each value of TCR inductor used, the TCSC's capacitive reactance increases with decreasing thyristor delay angle as expected. Hence, the TCSC that was designed and constructed is in fact capable of acting as a controllable series capacitive reactance in the expected manner.

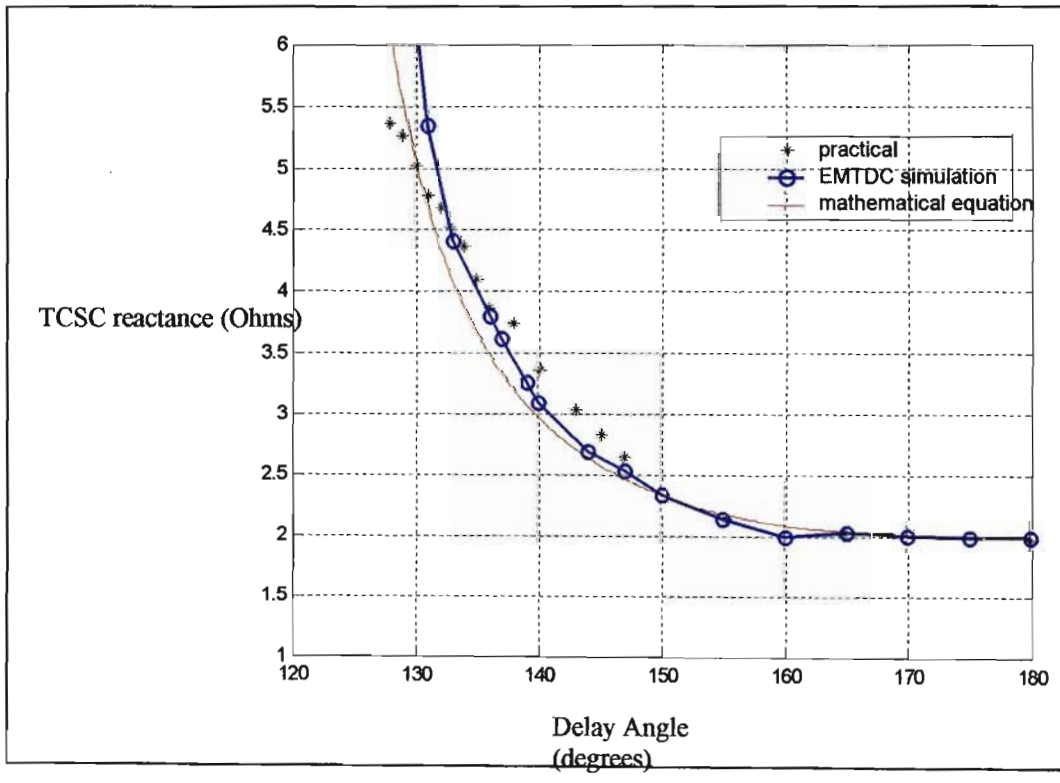

Figure 4.6:TCSC characteristic curve for a TCR = 0.8 ohms

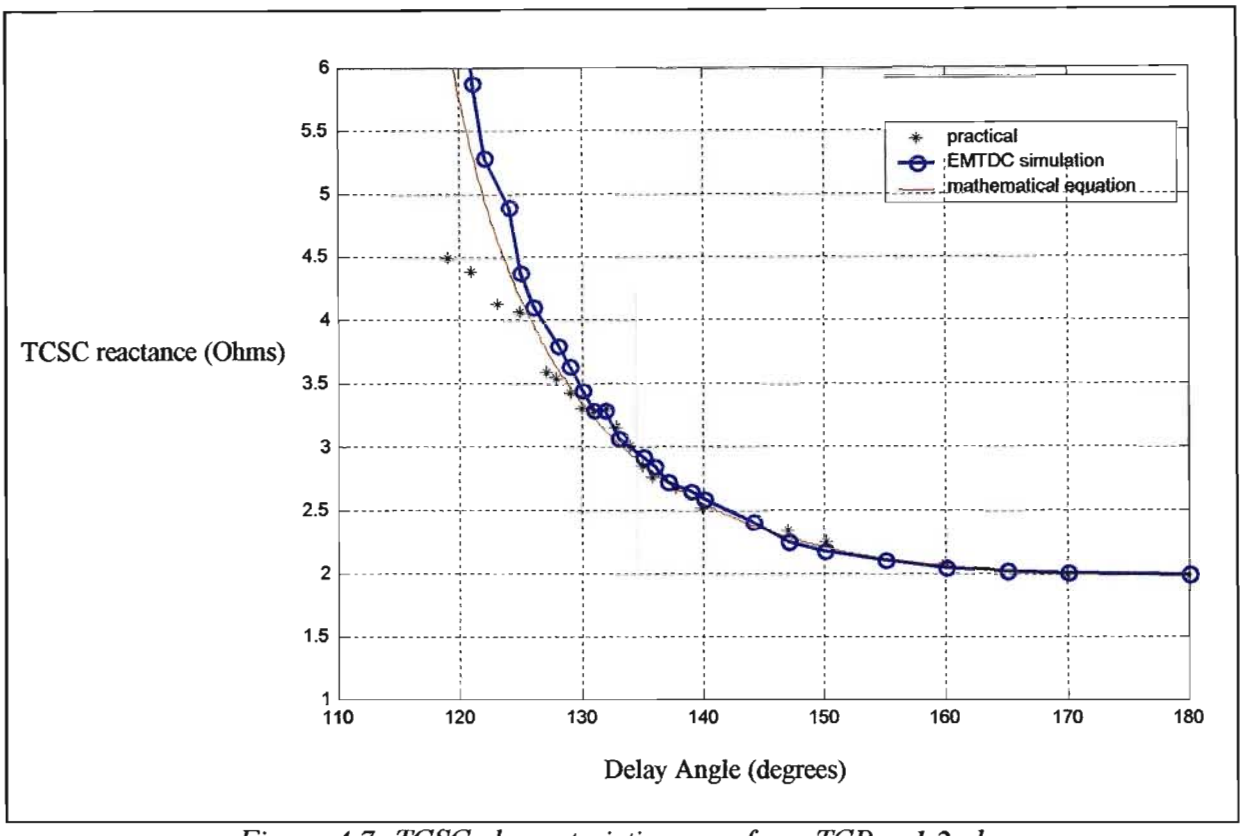

Figure 4.7: TCSC characteristic curve for a TCR = 1.2 ohms

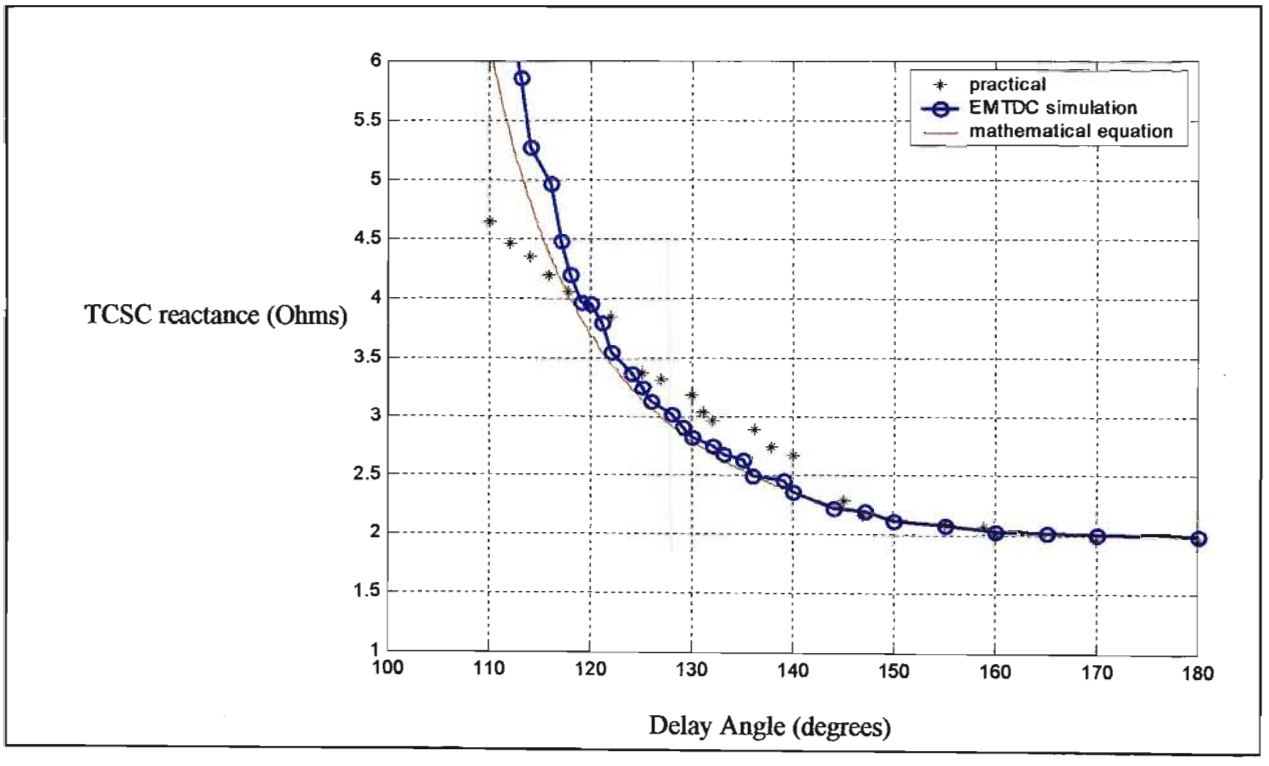

Figure 4.8: TCSC characteristic curve for a TCR = 1.6 ohms

Figure 4.6 to 4.8 illustrate that there are some discrepancies between the simulated results, measured results and the behavior predicted using the equation 2.1 found in Chapter Two. The approximate equation cited in Chapter Two is known to understate the actual capacitive reactance obtained from a TCSC at delay angles near the TCSC's resonant point. However, Figures 4.6 to 4.8 show that in each case the measured TCSC reactance near the resonant point is not only lower than that predicted by the accurate simulation model but also lower than that predicted by the approximate equation.

It was also noted that the discrepancy between the curves increases with increasing TCR inductor size; furthermore a number of studies that show significantly better agreement, used a TCSC with a smaller TCR inductor than in any of three cases shown in this section [3], [22] and [23].

4.3.2 Comparison of Simulated and Measured Results

Figures 4.6 to 4.8 have illustrated the operating range, in the capacitive-reactance region, of the laboratory-scale TCSC that is obtained from the design procedure described in the previous chapters. This section focuses on time-domain results that were measured from the laboratory-scale TCSC. These results are compared to those generated from the EMTDC mathematical model included in Appendix C.

Figures 4.9 to 4.11 show the time-domain response of laboratory-scale TCSC compared to simulated results. Only phase-A results are presented in this chapter; the rest of the results are found in Appendix C. The tests results presented in this section were conducted for all TCR inductors (0.8Ω, 1.2Ω and 1.6Ω).

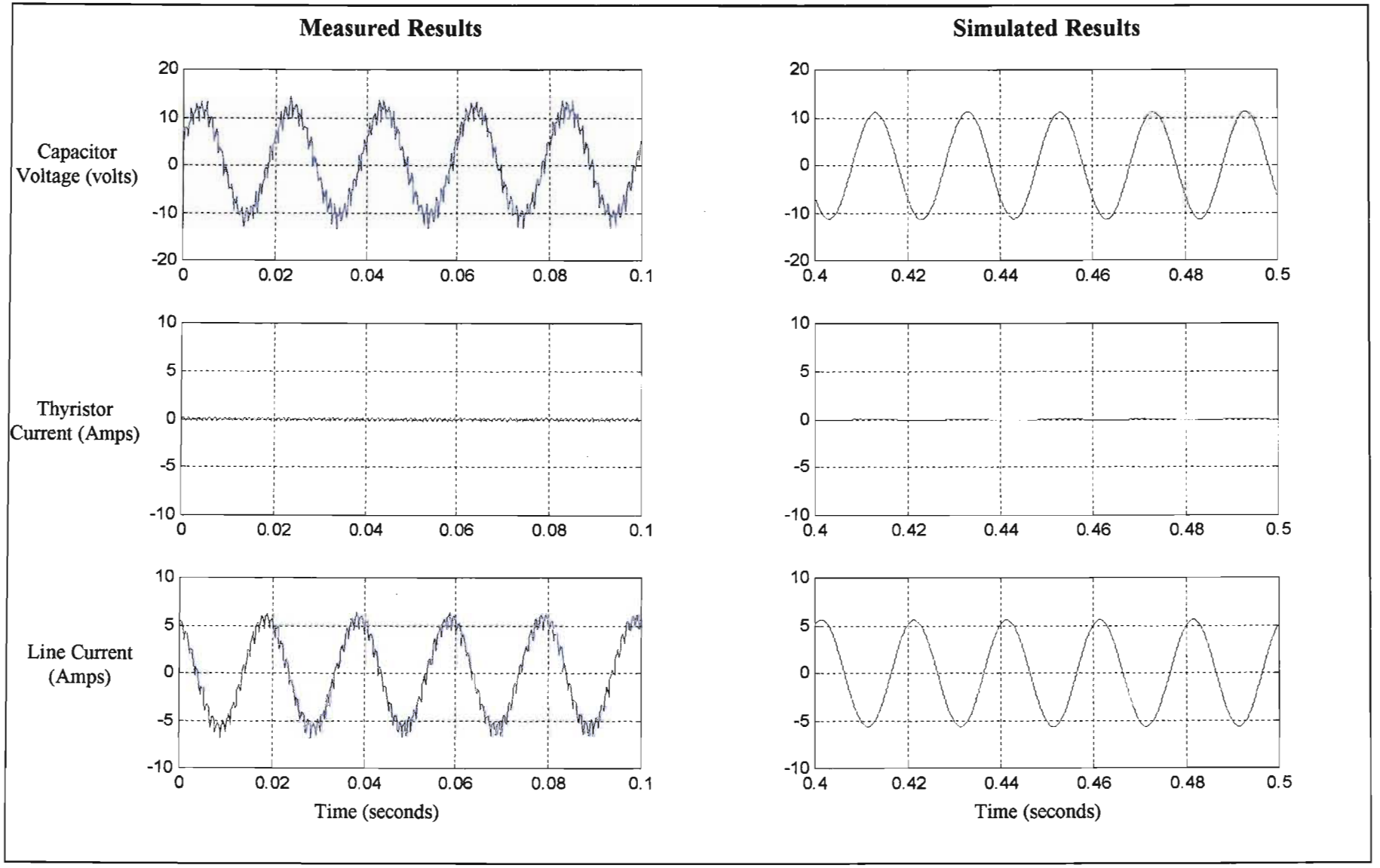

Figure 4.9: Comparison of phase A time-domain results at reactance order of 1: Xtcr = 0.8Ω.

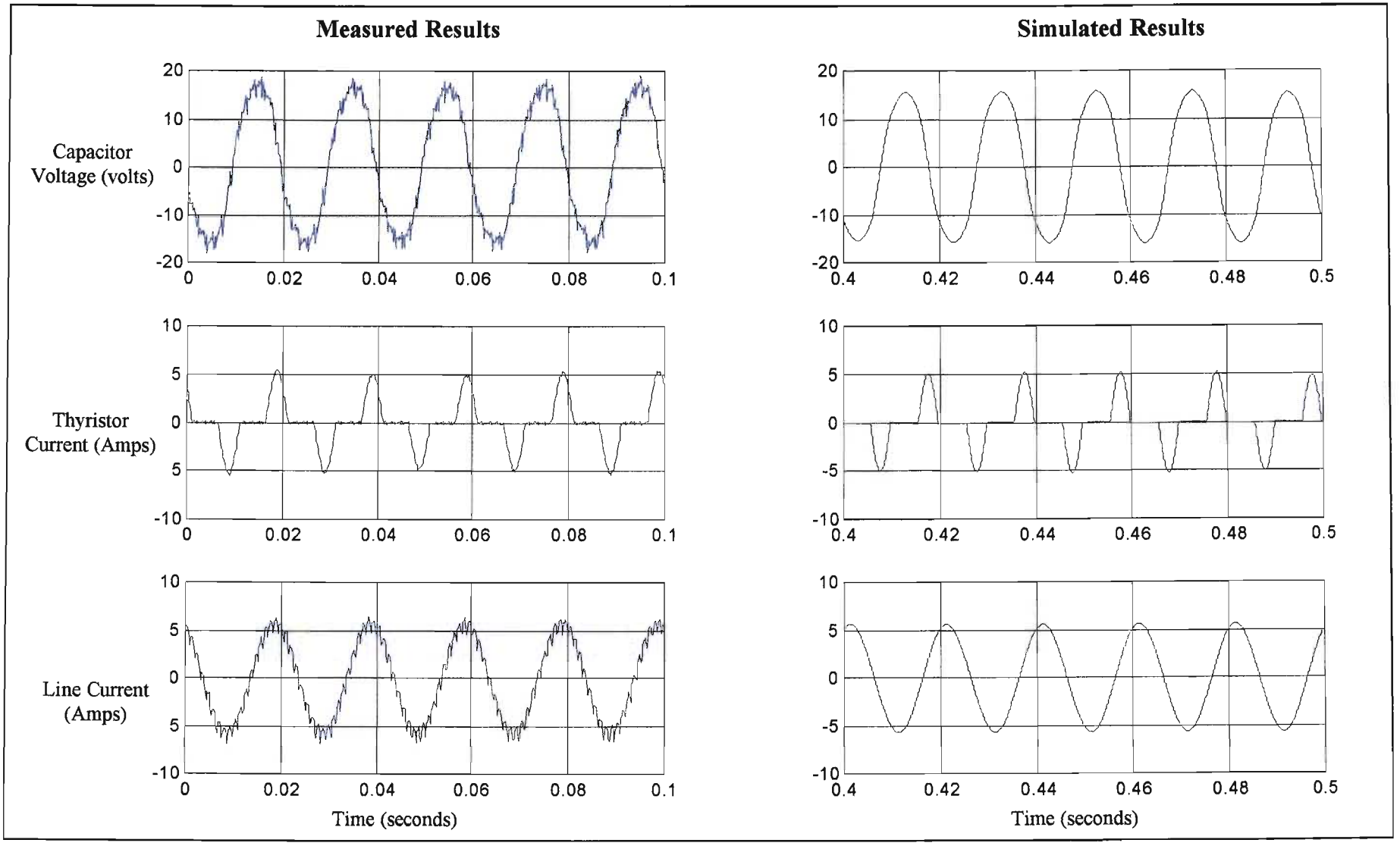

Figure 4.10: Comparison of phase A time-domain results at reactance order of 1.5: Xtcr =0.8Ω.

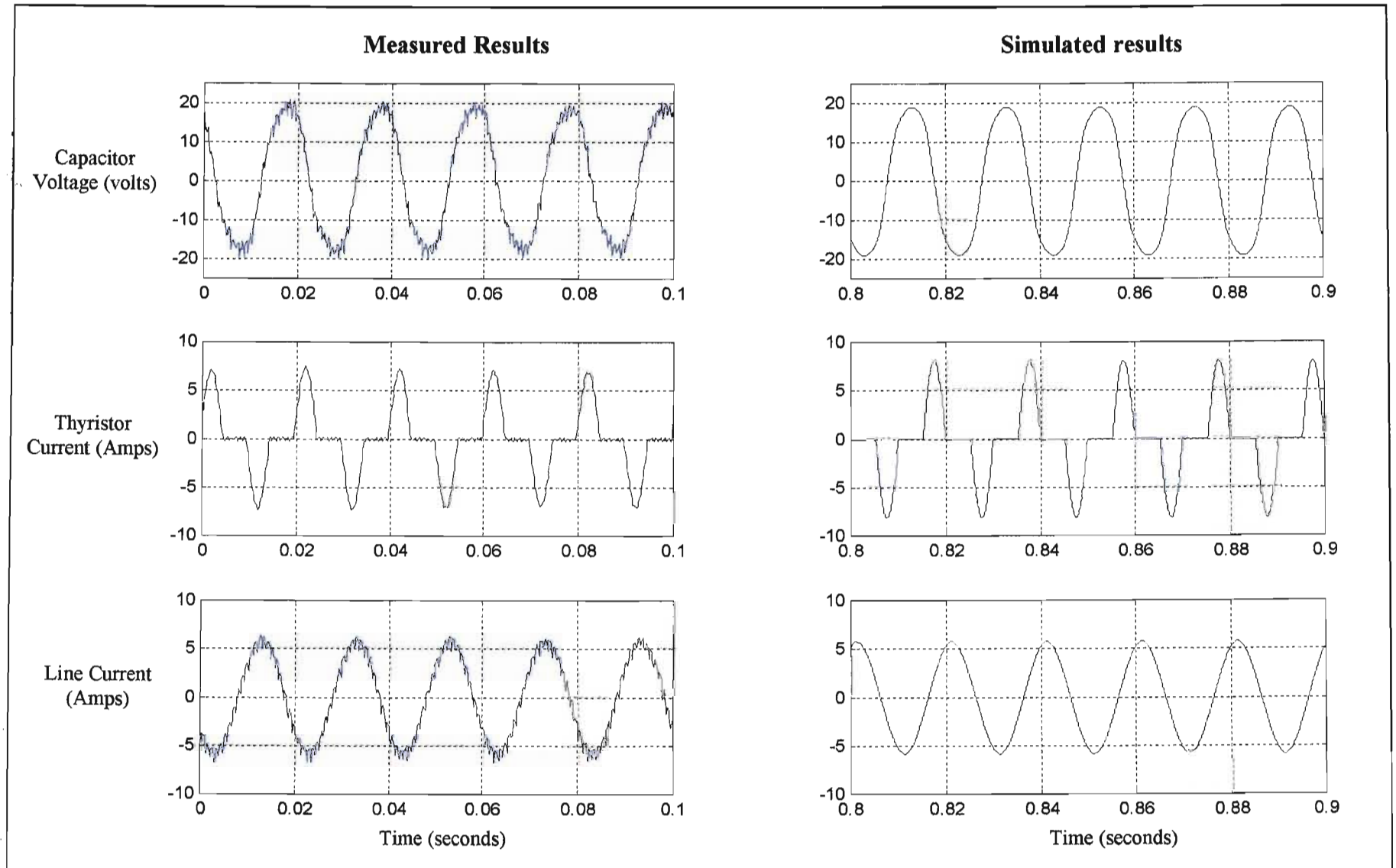

Figure 4.11: Comparison of phase A time-domain results at reactance order of 2: Xtcr = 0.8Ω.

The results from the laboratory-scale TCSC, Figure 4.9 to Figure 4.11, demonstrate that the TCSC is capable of producing a variable capacitive reactance. The practical results presented are only for the TCSC operated at approximately 50% of rated transmission line current. However, the results obtained are sufficient to conclude whether the TCSC functions correctly or not.

As shown by Figure 4.9, virtually zero current was flowing through the TCR branch when the firing angle was set to 180°. The TCSC is effectively acting as a conventional capacitor. However, as the firing angle was decreased, the current flowing through the TCR branch increased. As it was explained in Chapter Two, under capacitive mode, the current that flows through the series capacitor is a sum of the line current and the TCR branch current. Hence, as the figures show, the decrease of the firing angle causes the increase of the capacitor voltage.

Figure 4.11 shows the discrepancy (mentioned in the previous section) between the simulated results and the practical results that occurs at low firing angles. In particular, Figure 4.11 shows that the amplitude of the TCR current pulses is lower in the measured results than the simulated results.

Transient Response

The simulation results of the mathematical model of the TCSC, developed in Chapter Three, demonstrated that the TCSC could be used to modulate reactance when required. This characteristic was also investigated using the laboratory-scale TCSC, as shown by Figures 4.12 to 4.15. This was achieved by continuously varying the firing angle and observing the response of other TCSC variables. Only results for the TCR reactor of 0.8 ohms are shown in this chapter, the complete set of results is found in Appendix C.

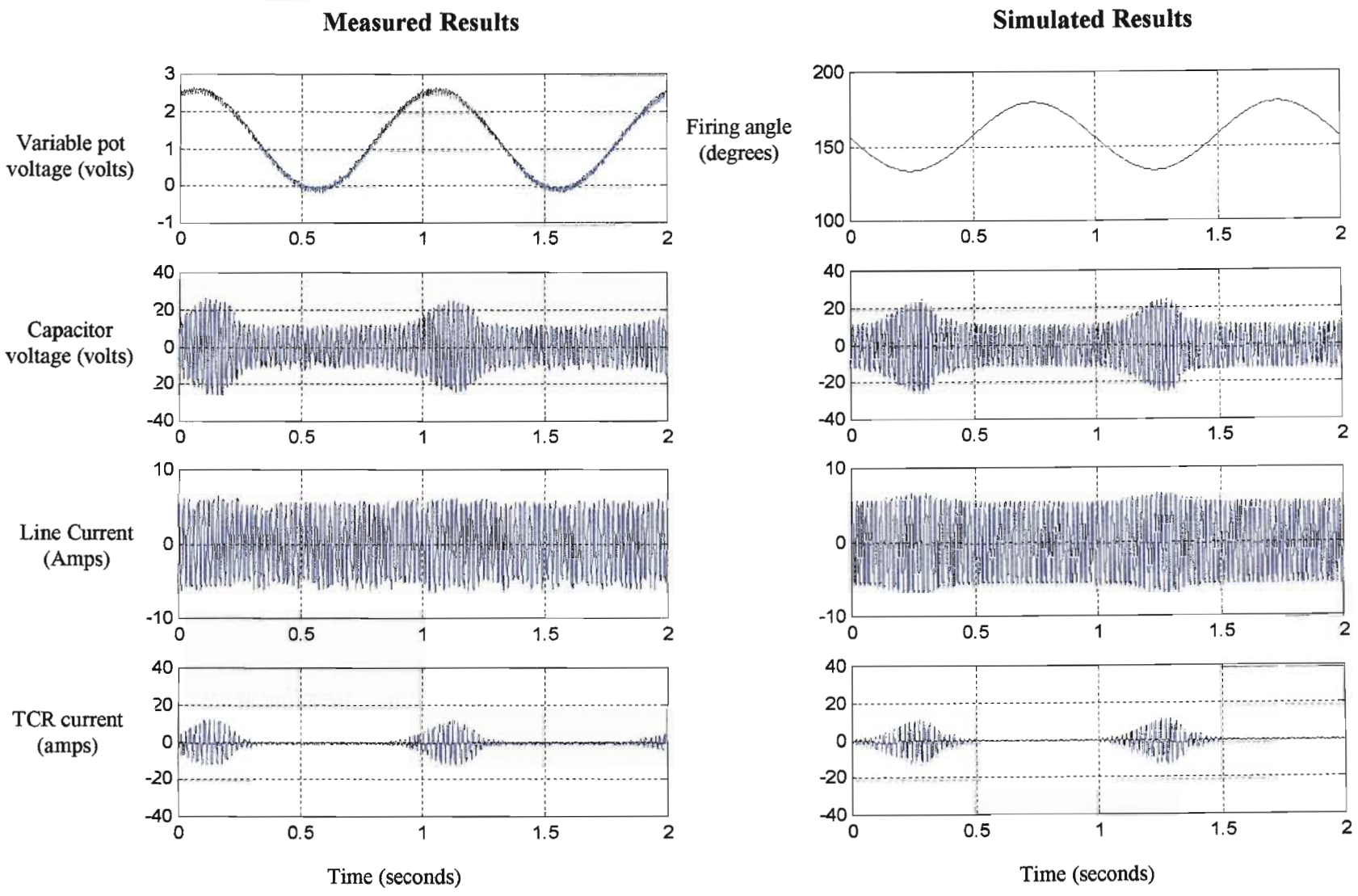

Figure 4.12: TCSC response to a 1 Hz modulation of reactance order between 1 and 2. Xtcr = 0.8 Ω.

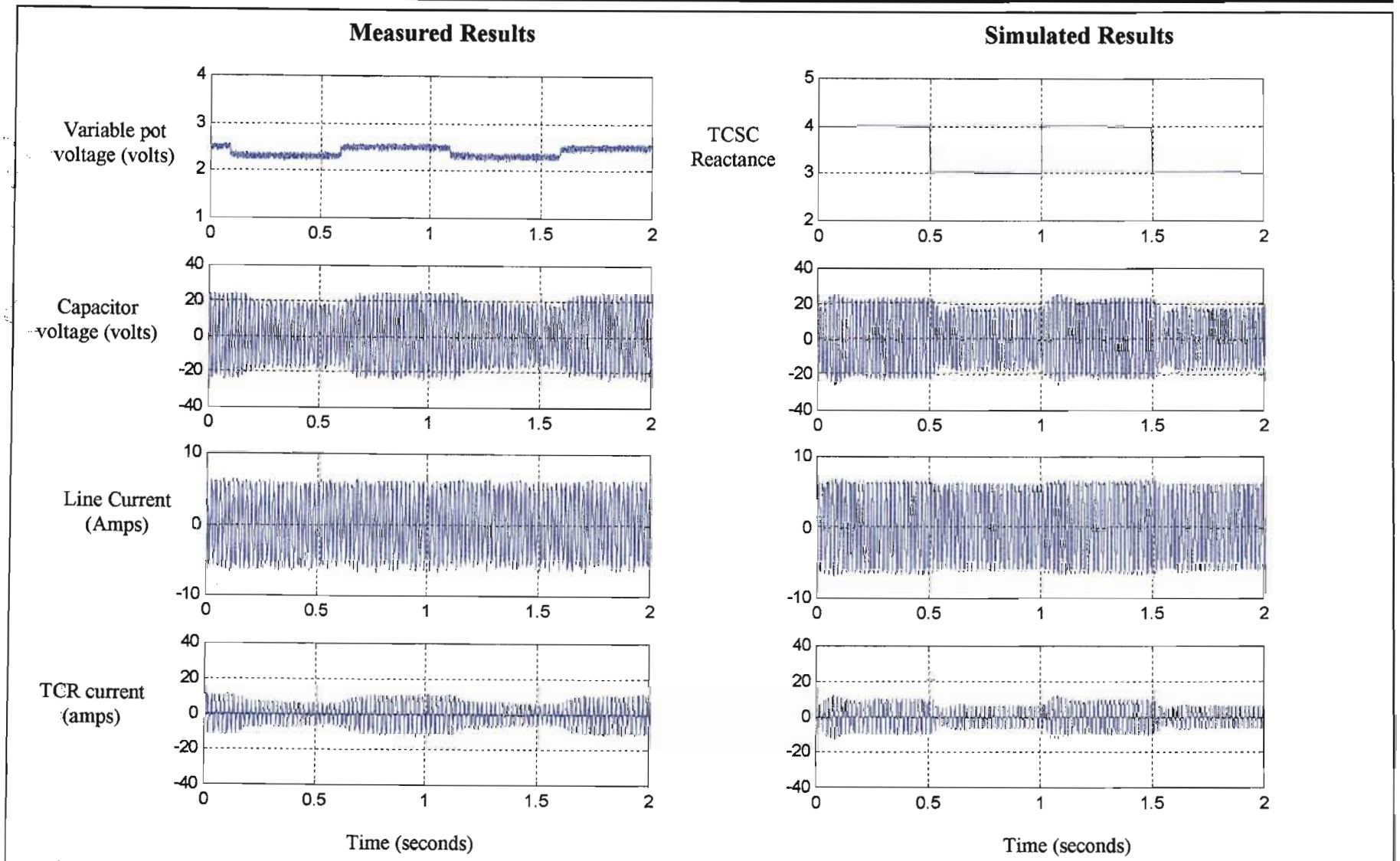

Figure 4.13: TCSC response to a two level modulation of reactance order between 1.5 and 2. Xtcr = 0.8 Ω.

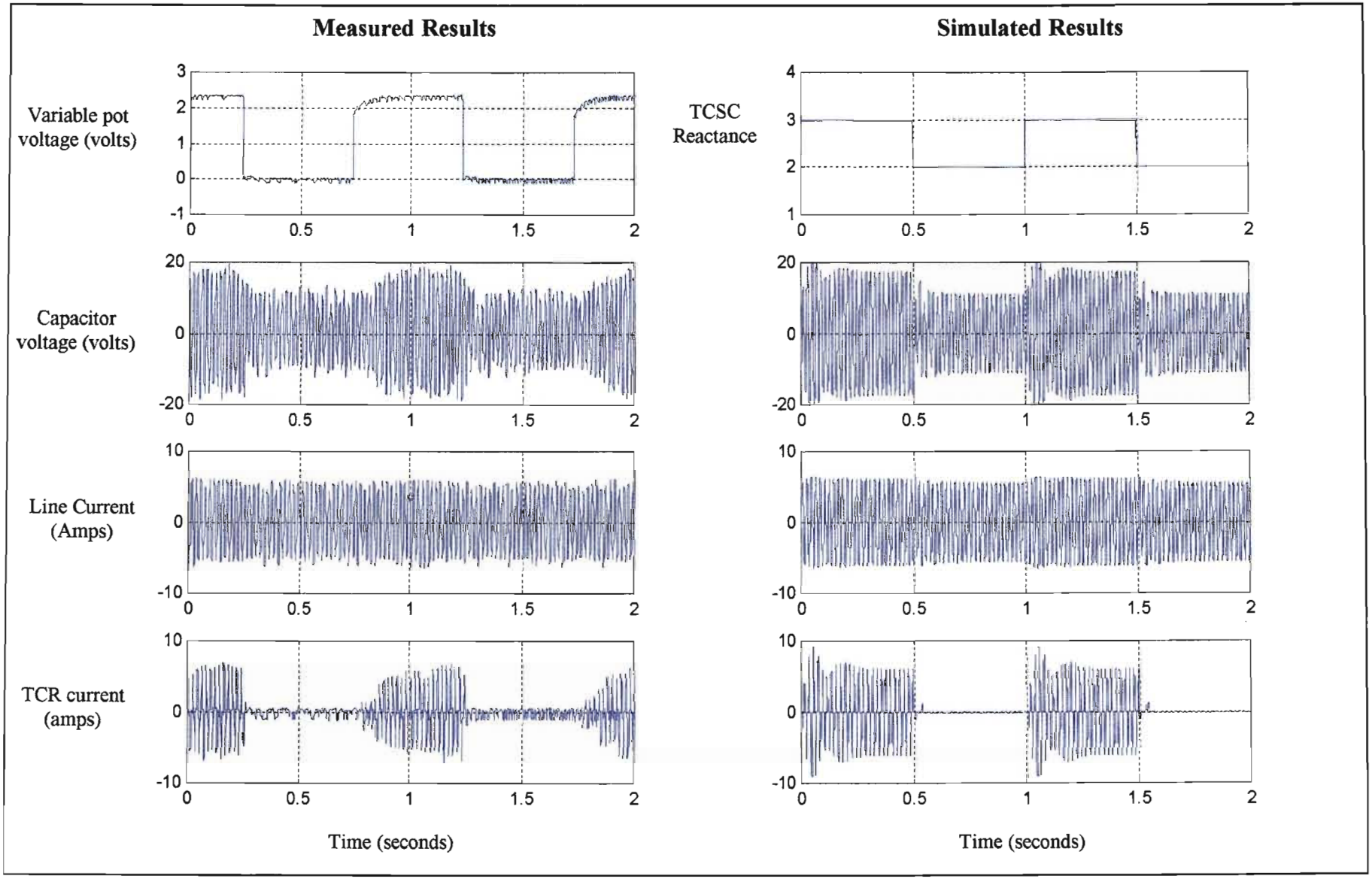

Figure 4.14: TCSC response to a two level modulation of reactance order between 1 and 1.5. Xtcr = 0.8 Ω.

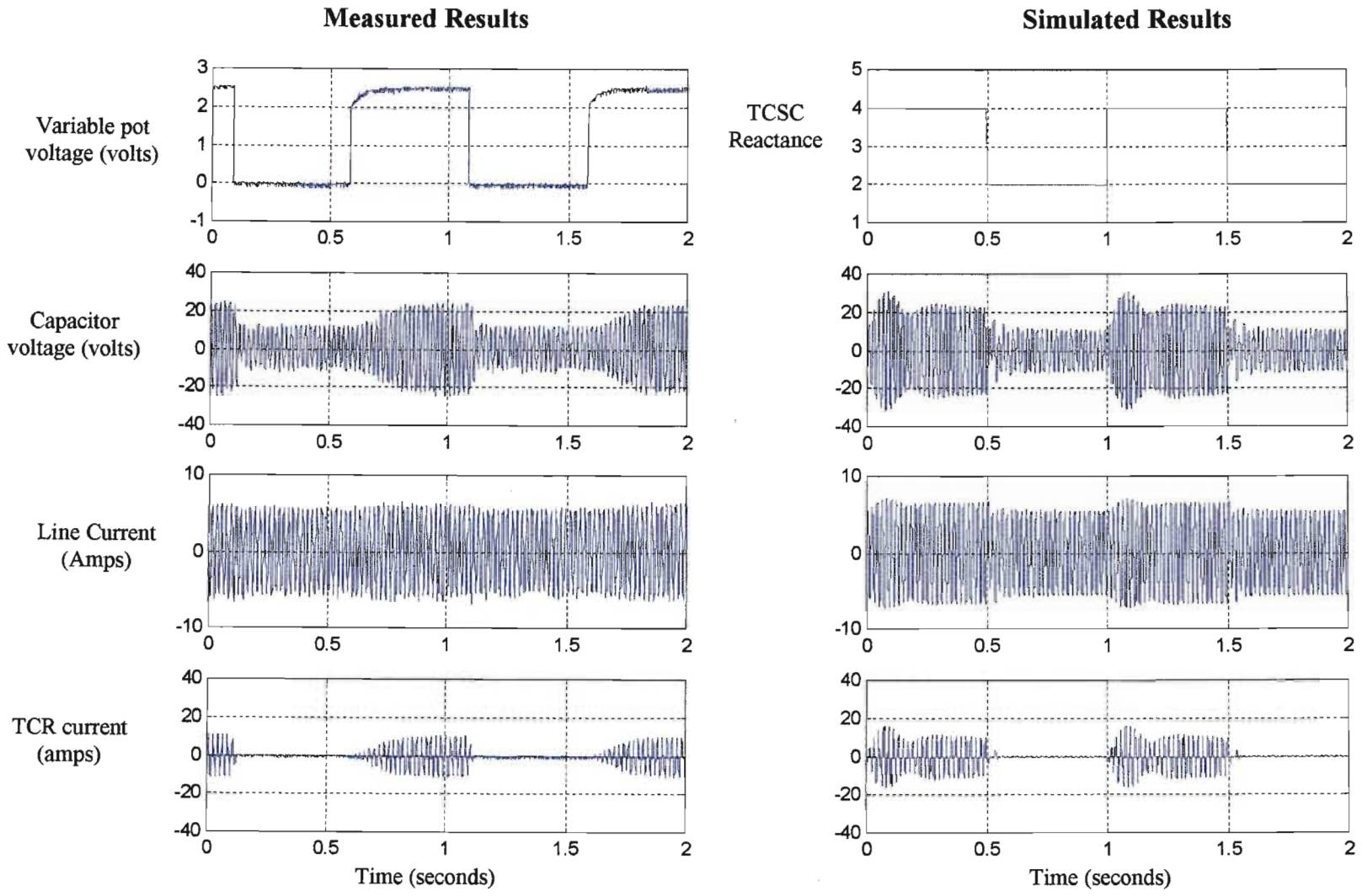

Figure 4.15: TCSC response to a two level modulation of reactance order between 1 and 2. Xtcr = 0.8 Ω.

Figures 4.12 to 4.15 continue with the comparison between the measured results and those generated in EMTDC using the mathematical model of the TCSC. As the figures demonstrate, the reactance of the TCSC can be modulated by changing the control input signal (firing angle). The analysis of the simulated results and other similar cases [24] suggest that the TCSC responds to reactance orders with a simple time constant of from 10ms to 15ms, quite satisfactory for aiding power system stability. This claim was proved to be correct by performing the tests and obtaining the results in Figures 4.16 to 4.18.

The results of Figures 4.16 to 4.18 show the transient response of the TCSC voltage when the firing angle is suddenly changed from one state to another. These results agree with the findings made in Chapter Two that the TCSC responds faster when a step-up change is made in the firing angle (Xorder decreased) compared to the step-down change (Xorder increased). The results of this study demonstrate the capability of the laboratory scale TCSC for rapid dynamic response.

A comparison of the responses in Figures 4.18 to 4.20 shows that the practical TCSC exhibits a damped response whereas the simulated TCSC shows a slightly underdamped response to step changes in Xorder. This discrepancy is probably due to the non-idealities in the practical TCSC system (resistance in the TCR inductors, forward volt drops of the thyristors and the limitations of the thyristor firing circuitry previously discussed).

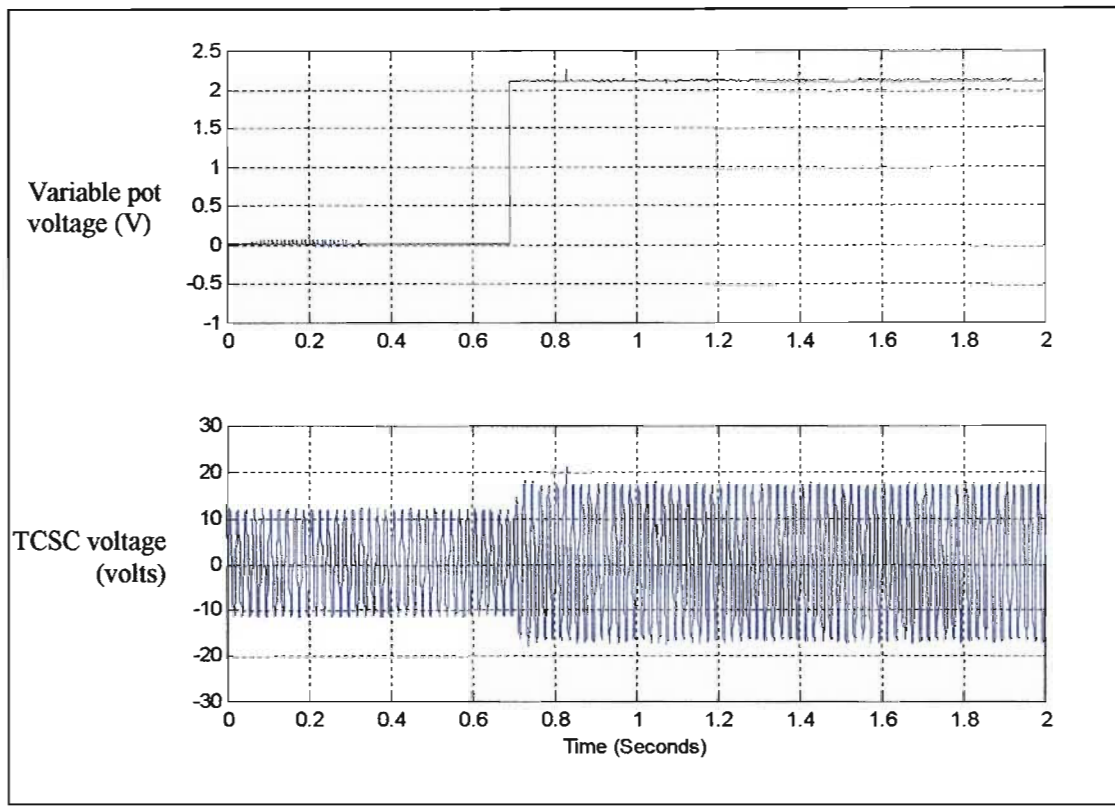

Figure 4.16: TCSC measured transient response as the reactance order is changed from 1 to 3.

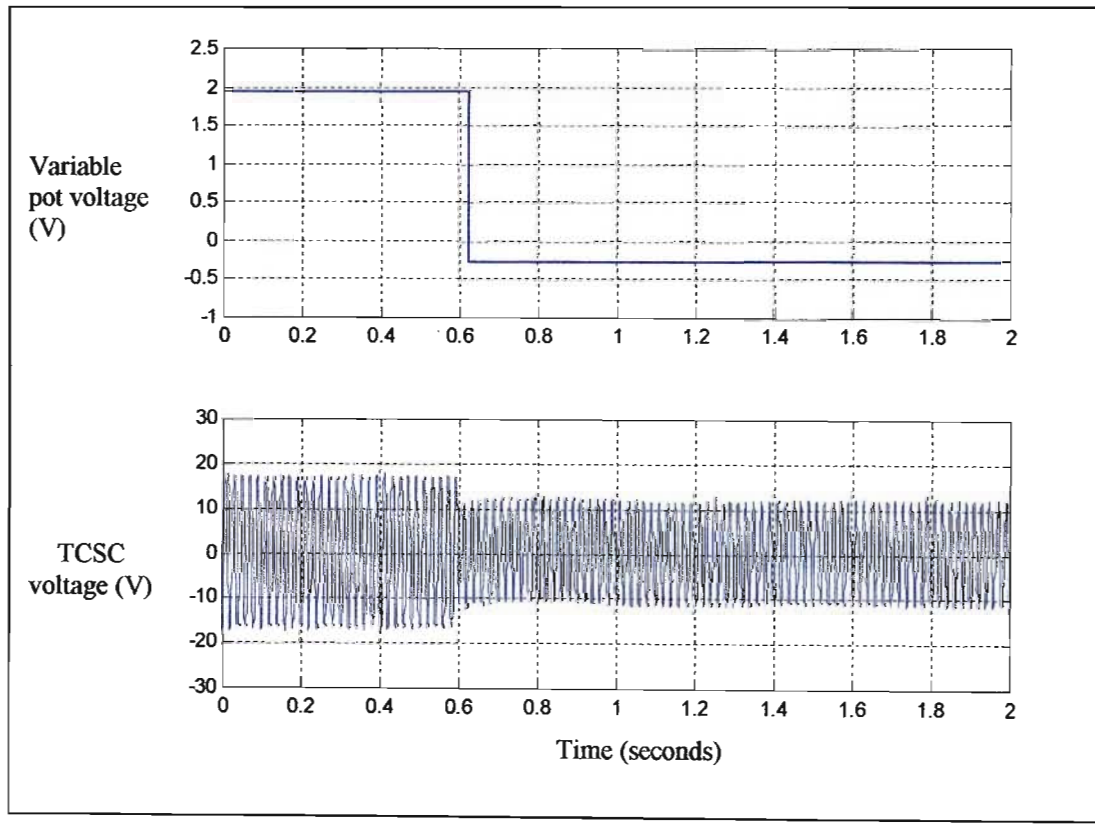

Figure 4.17: TCSC measured transient response as the reactance order is changed from 3 to1.

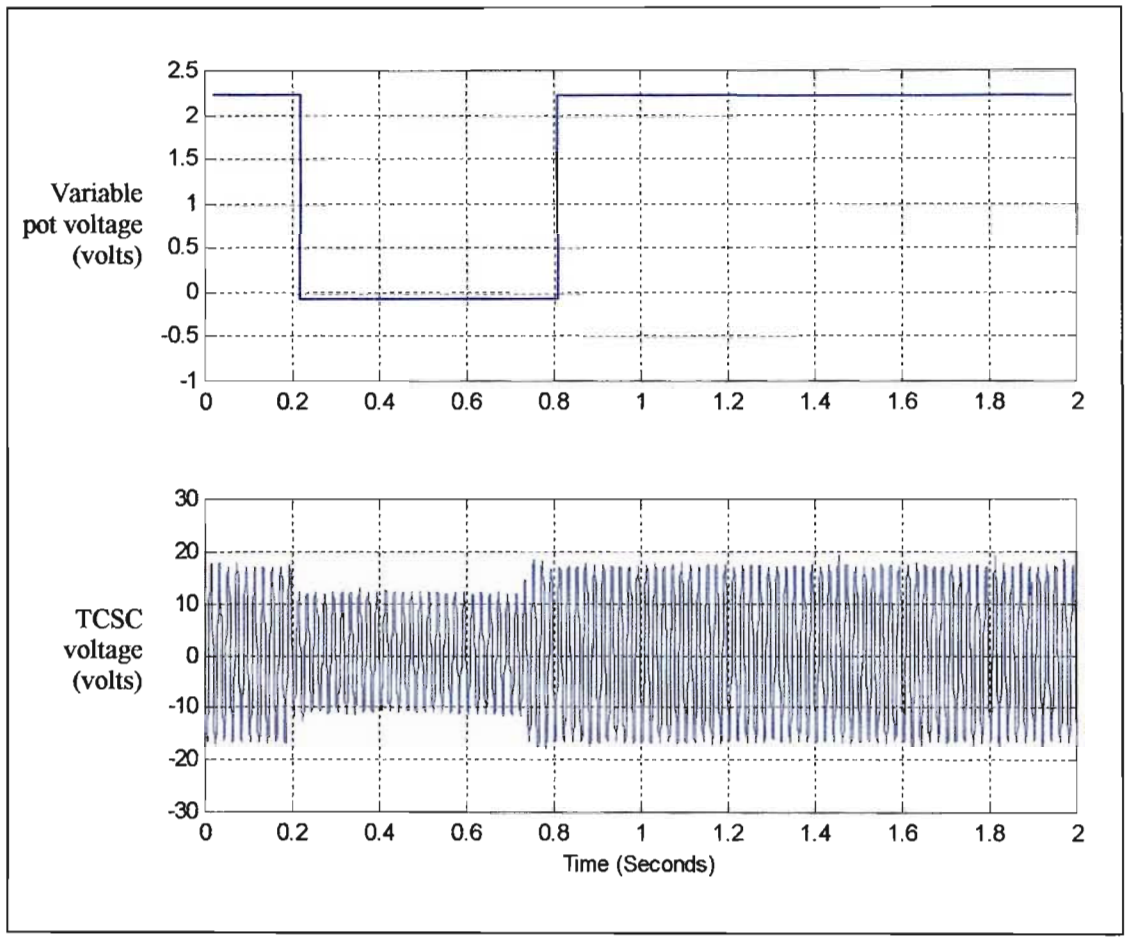

Figure 4.18: TCSC measured transient response as the reactance order is changed from 3 to1 back to 3.

4.4 Conclusion

Chapter Four has described the development and testing of the laboratory-scale TCSC for Natal University's Machines Research Laboratory. The chapter began by presenting the original trigger channel circuit that was eventually modified to better suit the requirements of the TCSC circuit. The circuit diagrams that illustrate changes from the original circuit are included and explained in this chapter

A comparison of the predicted response of the TCSC simulation model, the approximate TCSC reactance versus delay angle equation, and the actual laboratory-scale TCSC's performance was made. As discussed in the previous section, the comparison of the results has shown some discrepancies between the measured results and the simulation results, more visibly at lower firing angles. This is mainly due to non-idealities in the practical system that are not in the simulation model, in particular the thyristor volt-drops and the non-ideal performance of the practical trigger circuit.

Time-domain simulation results were compared to the practical results measured from the TCSC. These results proved that the laboratory-scale TCSC could be used to vary its capacitive reactance by changing the firing angle.

Transient response of the laboratory-scale TCSC was also investigated in this chapter. This was achieved by modulating the firing angle of the trigger circuit and observing the response of different TCSC variables, such as TCSC voltage and TCR current. It was then concluded that the laboratory-scale TCSC could potentially be used for applications such as power swing damping.

The last investigation of this thesis work was to demonstrate that the TCSC circuit could in practice be used to damp a generator power swing caused by a system disturbance. Chapter Five considers the development of an EMTDC simulation of a system similar to the one found in the Machines Research Laboratory. A model of the TCSC developed in this thesis would then be utilized to damp a power swing on that system.

CHAPTER FIVE

APPLICATION OF THE TCSC TO DAMP POWER SYSTEM OSCILLATIONS ON A SMIB SYSTEM

5.1 Introduction

Chapter Four has described the development and testing of the laboratory-scale TCSC model for the Machines Research Laboratory at Natal University. Different components of the TCSC hardware were described in Chapter Four. Chapter Four has also described the modifications that needed to be made to the trigger channel circuit of the TCSC.

The test results of the laboratory-scale TCSC circuit are also included in Chapter Four. The results in Chapter Four showed that the TCSC circuit is indeed capable of providing a variable capacitive reactance. Time-domain simulation results also demonstrated that the laboratory-scale TCSC could be used to rapidly modulate capacitive reactance; this characteristic of the TCSC can be put to use in power oscillation damping applications. Chapter Five presents a simulation study to demonstrate the application of a TCSC to power oscillation damping. The single machine infinite bus system considered in the simulation study is based on the parameters of the Machine Research Laboratory, and the parameters of the TCSC are those of the laboratory-scale device designed in this thesis.

5.2 Application of the TCSC in Power System Oscillation Damping

Damping of power system oscillations has been recognised as an important issue in electric power system operation. Numerous techniques of damping power swings have been studied and applied. Application of power system stabilisers has been one of the first measures employed to improve damping of the power swings. However, with increasing transmission line loading over long distances, the use of conventional power system stabilisers is limited by its slow control of power flow and its inability in providing sufficient damping for inter-area power swings [5].

Previous chapters have shown that, in principle, a TCSC can be used to damp power swings because of its characteristic ability to rapidly vary its capacitive reactance.

A question of great importance is the selection of the input signal to the trigger circuit for the TCSC in order to damp power oscillations in an effective manner. From control design and practical consideration, a desirable input signal should have the following characteristics [41], [7]:

- The swing modes should be observable in the trigger circuit input signal.
- A desirable level of damping should be achieved.
- The input signal should preferably be local.
- The damping effect should be robust with respect to different system operating conditions.

The machine's speed deviation is usually used as an input signal to the trigger circuit. However, not all the above characteristics could be achieved. As an example, the TCSC could be stationed hundreds of kilometers away from the

alternator. This situation will result in difficulties in having the machine's speed deviation as an input to the trigger circuit. However, studies in this subject have shown that the input signal to the trigger circuit can be synthesized from locally measured variables such as capacitor voltage and line current [7], [9] and [41].

5.3 Results of the Power Oscillation Damping Study

Previous chapters have shown that the TCSC circuit is capable of providing variable capacitive reactance by simply varying its trigger circuit's firing angle. The last stage of this thesis research work was to develop a detailed EMTDC model of a SMIB system in the Machines Research Laboratory, and then use the designed TCSC to damp its power oscillations. The power oscillations were initiated by opening the circuit breaker, as shown in the system diagram in Figure 5.1.

The EMTDC model of the SMIB system in the Machines Research Laboratory consists of the individual turbine stages, the synchronous machine with its control circuits, two parallel transmission lines and the infinite bus-bar. One branch of the transmission line is fitted with a circuit breaker and the other branch has a three-phase TCSC. The complete EMTDC circuit can be found in Appendix D.

5.3.1 Trigger Circuit Control Strategy

As Figure 5.1 shows, a bang-bang controller was used in this investigation to generate the firing pulses for the thyristors of the TCSC. The idea of producing the firing pulses using a bang-bang controller is based on either inserting or bypassing the series capacitive reactance at appropriate instants in the transmission line during transient power swings.

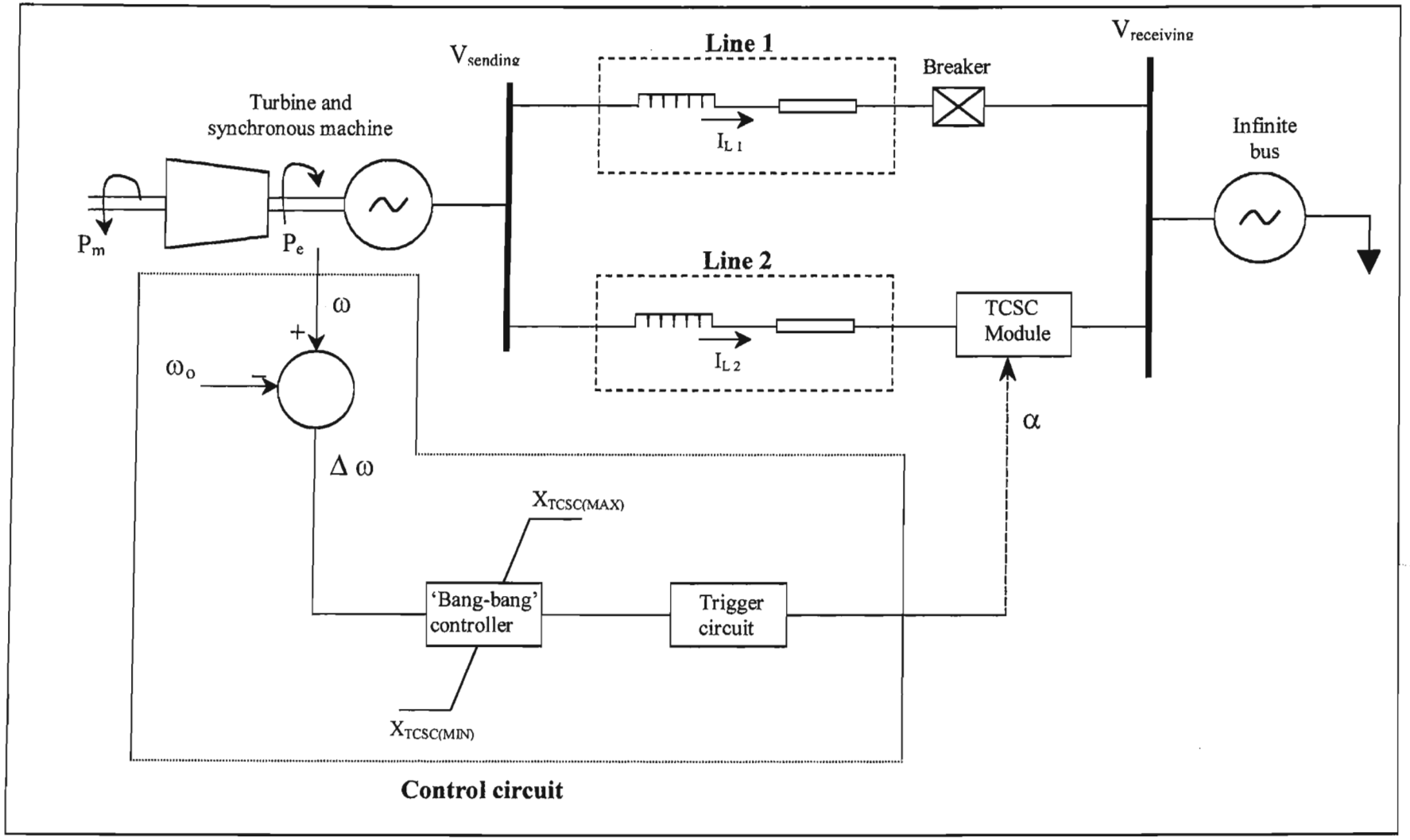

Figure 5.1: SMIB Transmission system with TCSC module used to investigate power oscillation damping

The bang-bang control strategy adopted was to insert and remove additional series compensation based on the speed deviation (ω - ω_o) between generator shaft speed and synchronous speed. The bang-bang control algorithm can be expressed as follows:

Increase X_{TCSC} if ω - ω_o > deadband

Reduce X_{TCSC} if ω - ω_o < deadband (5.1)

The deadband was introduced to prevent the controller from reacting to small variations in shaft speed from the desired synchronous speed. Appendix D contains the EMTDC model and the design values, which were used in simulating the circuit of Figure 5.1.

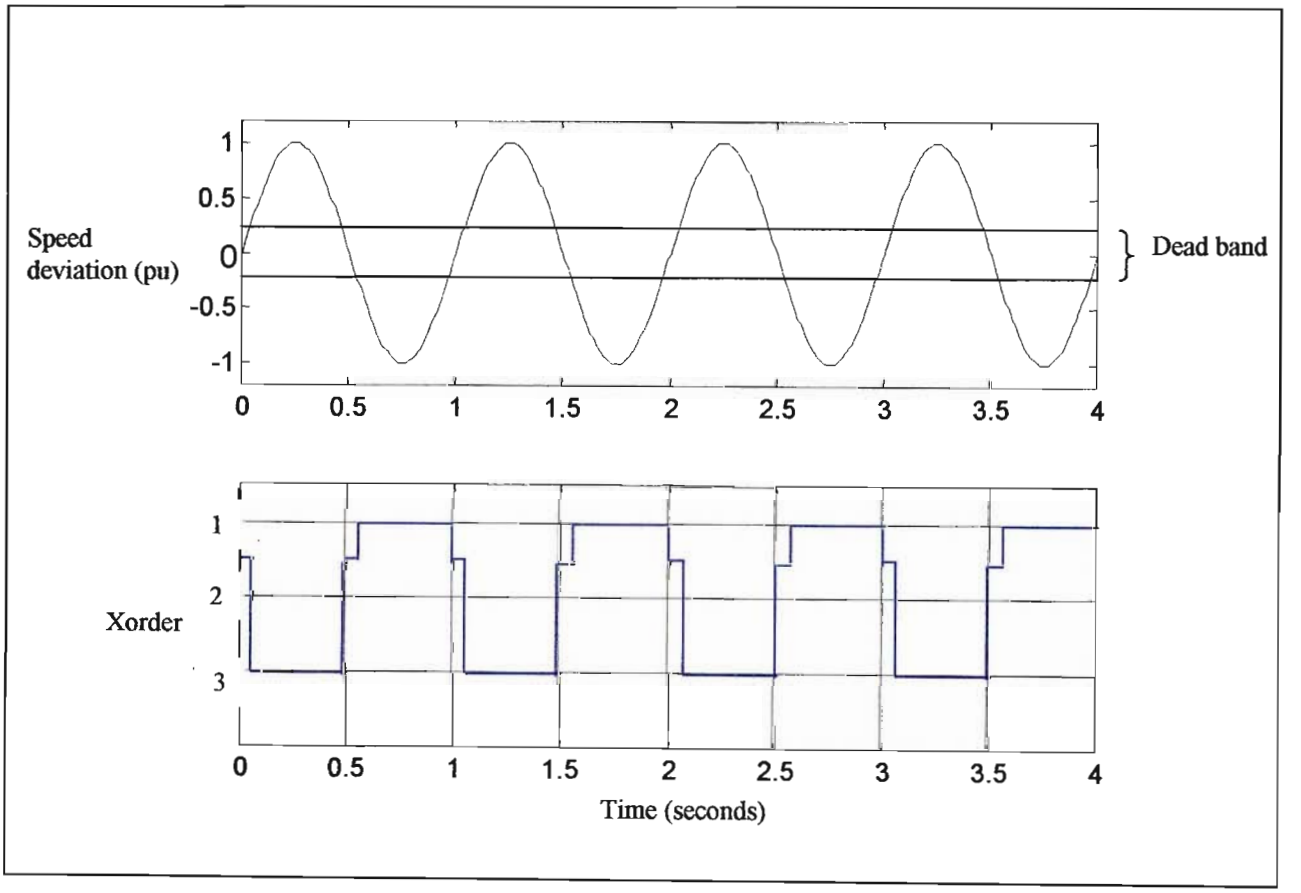

Figure 5.2: Relationship between the input to the controller and the firing angle

It is important to note that research in this subject has shown that bang-bang controller is more effective mainly to damp large-signal power swings; subsequent small-signal damping requires a more continuous controller [9] and [41]. However, the objective of Chapter Five is to demonstrate, using an EMTDC model of the Machines Research Laboratory system that the TCSC is capable, in principle, of damping power oscillations.

EMTDC Simulation Results

The power system network of Figure 5.1 was modeled in EMTDC to demonstrate TCSC's capability to damp power system oscillations. The actual EMTDC model and its parameters can be found in Appendix D. The EMTDC graphical representation of the system comprises, at the sending end, a synchronous generator coupled to a multi-mass turbine unit. The transmission network consists of two parallel lines (Line 1 and Line 2) of lumped impedance $R_L + jX_L$. The TCSC is inserted into one of the lines, while the circuit breaker is inserted to the second line.

The theory of operation of the TCSC control scheme, to ensure that the inserted reactance to the transmission line is providing positive damping torque, has been covered in previous sections of this chapter.

The power oscillation damping controller was designed and the following are its operation parameters:

$X_{ORDER} = 3$ if $\omega - \omega_o >$ deadband

$X_{ORDER} = 1$ if $\omega - \omega_o <$ deadband

$X_{ORDER} = 1.5$ if $\omega - \omega_o$ is within the deadband

Where deadband = [-0.15 , 0.15].

Figure 5.3 compares the time-domain simulation results of the system with no TCSC control to the results of the system with TCSC control. Both results clearly demonstrate the capability of the TCSC to provide positive damping torque. The fault was induced by opening the breaker, as shown in Figure 5.1, at t = 1 second.

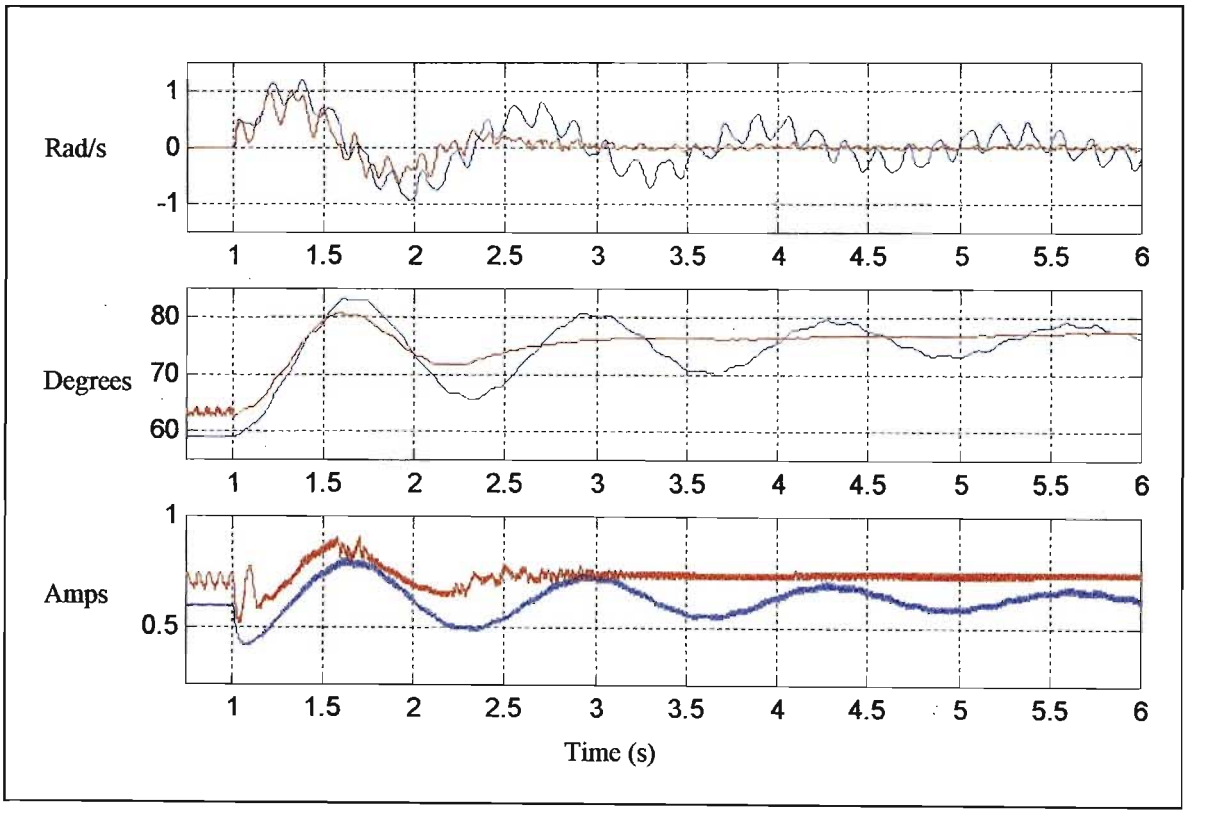

Figure 5.3: Time-domain simulation results of the SMIB system in Figure 5.1 with and without the TCSC.

The rest of the time-domain simulation results are shown in Figure 5.4. As the figure shows, the results are divided into two columns, left column consists of the results of the system with TCSC control and the right column illustrates the results of the system with no TCSC control.

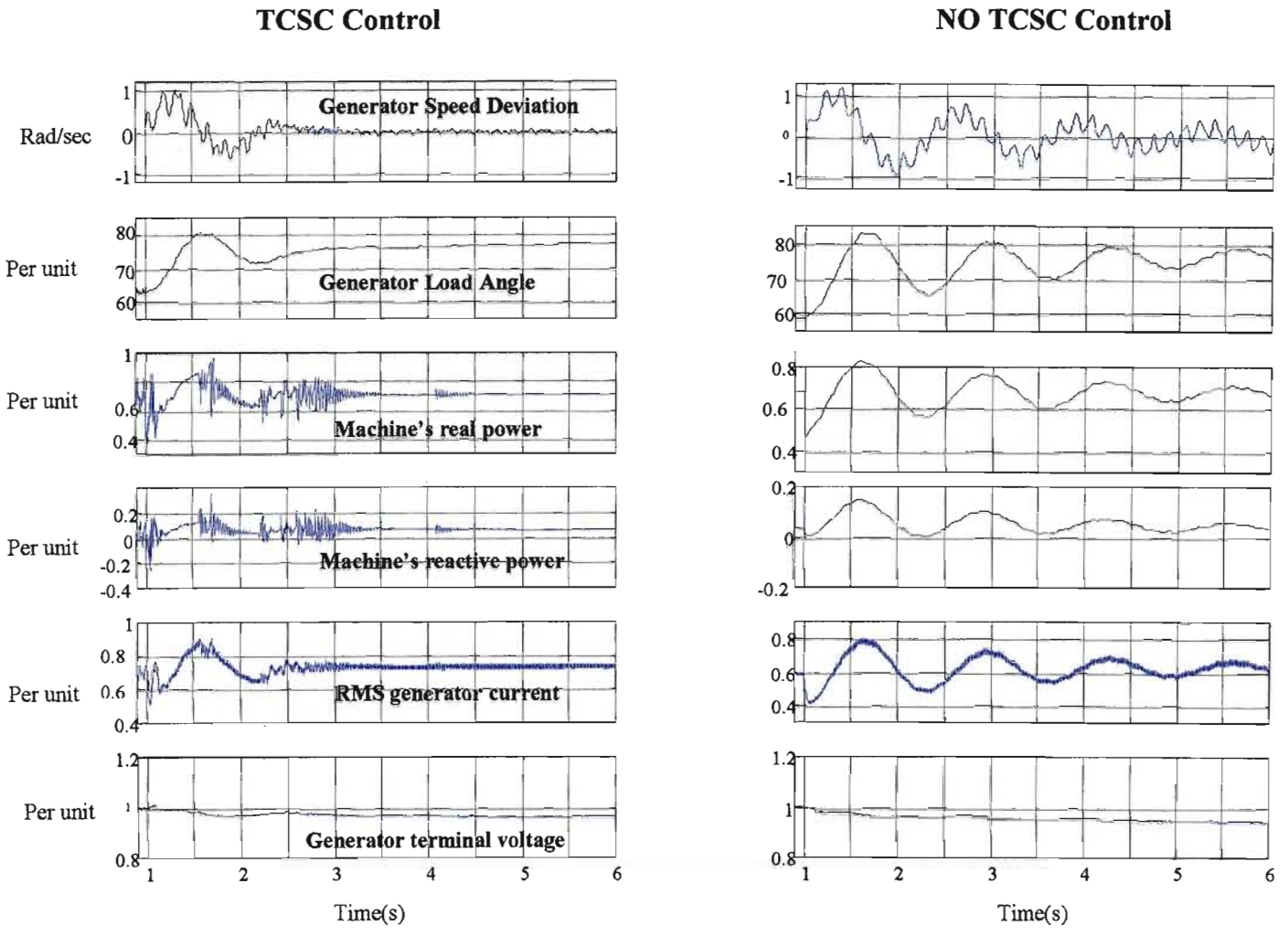

Figure 5.4: Complete Time-domain simulation results of the SMIB system in Figure 5.1 with and without the TCSC

5.4 Conclusion

Previous chapters of this thesis have demonstrated that the TCSC is capable of providing variable capacitive reactance by varying the firing signal of the thyristors. In concluding this research work, the thyristor controlled series capacitor was applied to a simple single machine infinite bus system, similar to the Machines Research Laboratory system, to demonstrate its capability to damp power system oscillations. A detailed EMTDC model of the system was developed and is found in Appendix D.

The trigger circuit, discussed in Chapter Four, was modified to suit the TCSC's application of power swing damping: a bang-bang controller was chosen because of its simplicity and ease to implement. While the results of this chapter have shown that the bang-bang controller can be used to produce the firing signals for the thyristors, it was highlighted that some other form of controller may be more effective, especially to damp small-signal power swings. The synchronous machine's speed deviation was used as the input to the control circuit. It was also noted that it is not always practical to use the speed deviation as the input signal to the controller mainly because the TCSC might be located long distances away from a generator. Hence, some research work in this field has shown that the controller's input signal can be synthesized from the locally measured variables at the TCSC installation [41].

Although the power oscillation damping study presented in this chapter is limited to simulations, the measured results in the previous chapter have shown that the hardware TCSC that has been designed in this thesis could be used in such a scheme. The measured results of the laboratory-scale TCSC have shown that the device is capable of varying its capacitive reactance at a frequency of 1 Hz, as required in a typical power oscillation damping application. Furthermore, the results of Chapter Four confirmed that the laboratory-scale TCSC can provide this variable capacitive reactance in response to both sinusoidal or bang-bang type control input. Thus, on the basis of the measured results in Chapter Four, and the simulation results in this chapter, it can be concluded that the laboratory-scale TCSC designed in this thesis

could potentially be used for practical power oscillation damping studies in the Machines Research Laboratory.

Much advancement, in the field of TCSC design, has happened since the start of this research work. These advancements include the impact of the voltage across the thyristor valves to the accuracy of the firing delay angle, and in this area there is certainly scope of further work as will be discussed in the concluding chapter of the thesis which now follows.

CHAPTER SIX

CONCLUSION

6.1 Introduction

This thesis has examined the specific issue of designing and implementing a thyristor controlled series capacitor with parameters suitable for application studies in the Machines Research Laboratory at Natal University. The investigations have shown that the TCSC is capable of rapidly varying its capacitive reactance when operated in vernier capacitive mode. The investigation has also shown that the TCSC can be used, not only to increase the power transfer capability of a transmission line, but it is also capable of being used as another tool to damp power system oscillations due to system disturbances. This chapter summarises and reviews the principal findings of this thesis, chapter by chapter, and finally suggests further research work that could be undertaken in this area.

6.2 Factors that Influence the Design of the TCSC

Chapter Two has shown that designing a TCSC could prove to be a complicated task, unless all issues involved are clearly defined and addressed. Chapter Two outlined these design issues in detail and discussed the design limits associated with them. The review, of Chapter Two, has shown that the choice of reactor and capacitor sizes of the TCSC not only determines the operating region of the device, but also its operating performance. Rating of the TCSC components and harmonics contributions are a major issues when designing a TCSC. The dominance of the 3^{rd} harmonic voltages was shown.

Chapter Two also discussed both the steady state and transient response of the TCSC. Under steady state conditions, it was shown that when the TCSC (instead of a conventional series capacitor) is fitted in a transmission line a similar resonant condition occurs to a conventionally compensated line. However, the additional resistance introduced by the TCSC at the resonant frequency helps to produce positive damping to suppress power swing oscillations as well as to mitigate SSR. Typical transient response curves for the TCSC were also shown. The literature review also discussed the asymmetric nature of the TCSC's response to a step change in the firing delay angle.

The literature review in Chapter Two also discussed different applications of the TCSC, namely, damping power swings and mitigation of SSR. A typical response of the TCSC, controlled by a bang-bang controller, was shown and different control strategies were also mentioned. The phenomenon of SSR was also mentioned and the benefit of the TCSC to suppress it was also outlined.

6.3 Mathematical Models to Study the Performance of the TCSC

Chapter Three has presented the development of a mathematical model to investigate the characteristics of the TCSC. As an important integral part of the TCSC circuit design, the control circuit that generates the firing pulses for the TCR thyristors was presented and its operation was explained. The chapter also outlined the methodology that was followed to determine the sizes of both the capacitor and the reactor in the laboratory-scale TCSC.

The effect of changing the size of reactor was investigated. Reactors of sizes 0.8 Ω, 1.2 Ω and 1.6 Ω were chosen for the laboratory-scale TCSC. The investigation confirmed that the ratings of the TCSC components are dependent on the size of the TCSC reactor. It was found that the current and kVAr ratings of both the capacitor and reactor decrease as the size of the reactor is increased.

Chapter Three also discussed the impact of TCSC harmonics on the transmission line currents. Several simulations were conducted to deduce the effect of the TCSC harmonics on the power system. The simulation results showed that:

- The TCSC 3rd harmonic voltage is dominant and other orders of voltage harmonics are negligible in magnitude. The results also show that the magnitude of the harmonic voltages increases as the reactor size is decreased;
- The harmonic currents were found to be largely confined within the TCSC loop. Only a small magnitude of the harmonic currents (5% at most) was found in the line currents.

6.4 Development of the Laboratory-Scale TCSC

The main objective of Chapter Four was to outline all major steps that were followed when constructing and eventually testing the laboratory-scale TCSC.

The chapter covers the design and testing of the trigger circuit. Its shortcomings were also discussed. The measured results taken from the laboratory-scale TCSC have shown reasonable agreement with the predictions made using various simulation models of the system. The measured results have thus

i. Confirmed the validity of the mathematical models which have been used during analysis and design of the laboratory-scale TCSC, with its control scheme, in this thesis;

ii. Provided confirmation of the theoretical principles of operation;

iii. Demonstrated the ability of the TCSC to rapidly vary its capacitive reactance.

6.5 Power Oscillation Damping using the TCSC

A number of papers reviewed in the literature survey of Chapter Two have suggested that one of the important applications of the TCSC is to damp power swings. To determine whether the laboratory-scale TCSC could be used to study this application in future, a detailed mathematical model of a single machine infinite bus system was developed in EMTDC, based on the parameters of the Machines Research Laboratory. The simulation model of the laboratory-scale TCSC was inserted in the transmission line of this study system. The results of this theoretical study, together with the laboratory-scale TCSC designed in this thesis could be used for practical investigations of power oscillation damping.

6.6 Suggestions for Further Work

This thesis has presented the first practical implementation of a laboratory-scale TCSC designed for the Machines Research Laboratory at the University of Natal. The work that was undertaken, during the design and implementation stages of this thesis, gave a good insight into issues that need to be considered to produce a functional TCSC. However, as is often the case in such research, the investigations that have been done have addressed some issues and uncovered further questions. Therefore, the author suggests that scope exists for further work in this area as outlined below.

(a) To test the hardware TCSC design of this thesis, an existing analogue thyristor trigger channel was adapted to the TCSC application. As discussed in the main body of the thesis, using an analogue trigger channel synchronized to the TCSC capacitor voltages is not ideal and leads to inaccurate generation of the thyristor turn on signals under some conditions. In practice, transmission line TCSCs use thyristor

firing circuits that are synchronized to the transmission line currents; however this approach requires digital phase-locked loop hardware to be designed, and lay outside the scope of this investigation. It is suggested that the next phase of this project consider the implementation of a digital trigger channel for the laboratory-scale TCSC, synchronized to the transmission line current.

(b) Another area that can benefit from further work is the design of TCSC components, particularly the size of the reactors. This thesis has shown that the size of the reactor determines the kVAr rating of the whole TCSC circuit. In the literature review conducted in the thesis, it was discussed that the TCSC's reactor should fall within recommended range of sizes; for the laboratory-scale TCSC a decision was taken to use reactor sizes of the highest possible values within this range, in order to reduce the required rating of the thyristors and the reactors themselves. However, later research work has shown that this design methodology could lead to under-performance of the TCSC, especially in the lower firing angle range. Hence, the author recommends that in the next phase of the project, the laboratory-scale TCSC's performance should be examined with smaller reactor sizes.

(c) The results of Chapter Four and Five have shown that the laboratory-scale TCSC could be used for practical studies of power oscillation damping. It is recommended that future work consider the use of the laboratory-scale TCSC for damping the power oscillations of the micro-alternators in the Machines Research Laboratory, both using the bang-bang and continuos control approaches.

APPENDIX A

PARAMETERS OF A SIMPLE EMTDC CIRCUIT USED DURING THE TCSC DESIGN STAGE

This section covers the list of parameters used during the design phase of the project. These parameters were also used during the harmonic investigation.

A.1 Parameters of a Simple Circuit with a TCSC device

A.1.1 Voltage Source and Infinite bus

Source Voltage	= 127 V
System Frequency	= 50 Hz
Initial Phase	= 0° / 30°
Ramp up Time	= 0.05 s
Source Resistance	= 1 Ohm

A.1.2 Transmission Line Impedance

L_{LINE}	= 0.0513434 H
R	= 2.0 Ohms

A.1.3 TCSC Device

C	= 1591.55 μF
L	= 0.00255, 0.00383 and 0.0510 H
Thyristor ON resistance	= 0.01 Ohms
Thyristor OFF resistance	= 1.0E6 Ohms
Forward Volt Drop	= 0.1 V
Forward Break Over Voltage	= 1.0E5 V
Reverse Withstand Voltage	= 1.0E5 V
Minimum Extinction Time	= 0 s

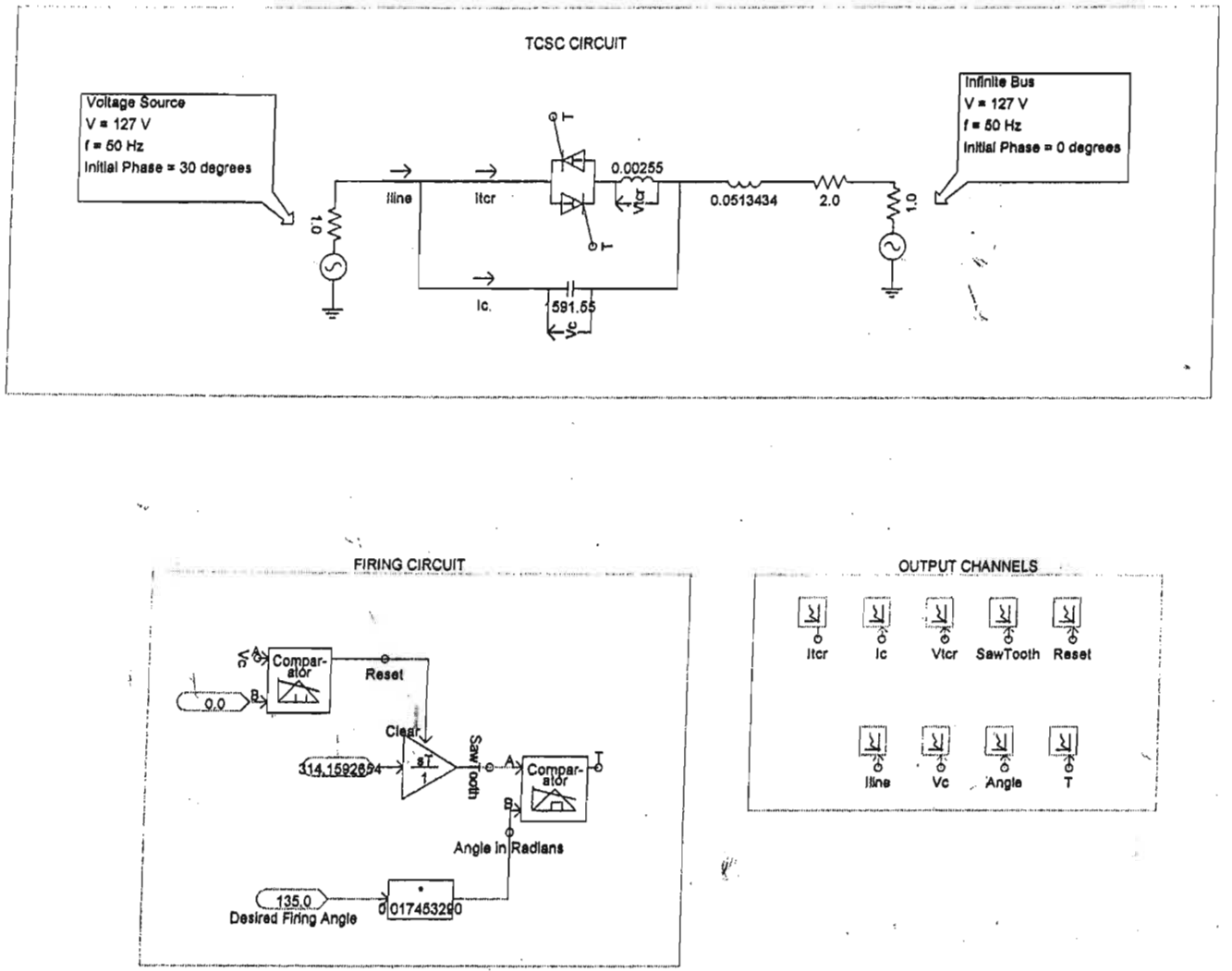

Figure A1: A simple EMTDC TCSC circuit

APPENDIX B

MODIFIED TRIGGER CIRCUIT FOR THE CONTROL OF A THYRISTOR CONTROLED SERIES CAPACITOR

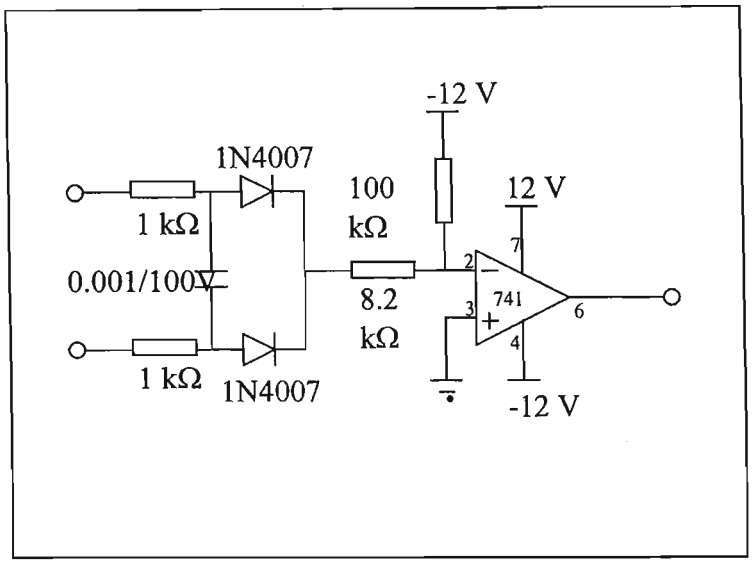

Figure B.1: Original Synchronizing stage of the trigger circuit

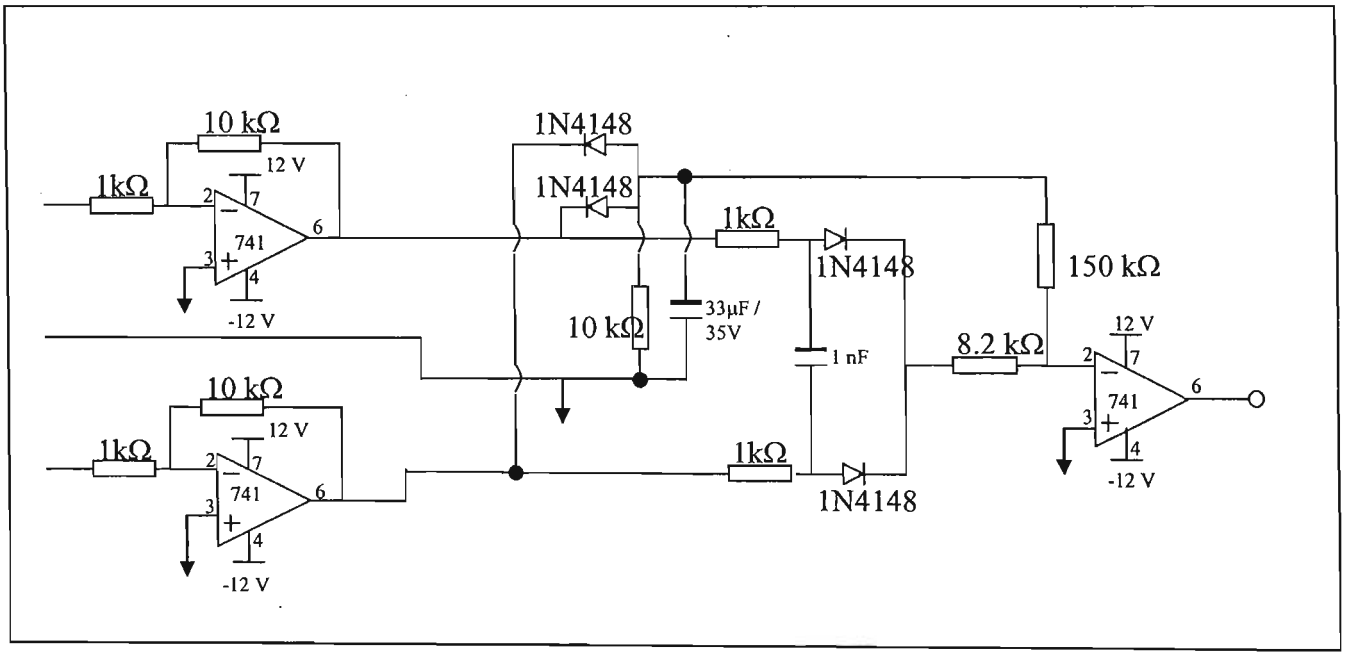

Figure B.2: Modified Synchronizing stage of the trigger circuit

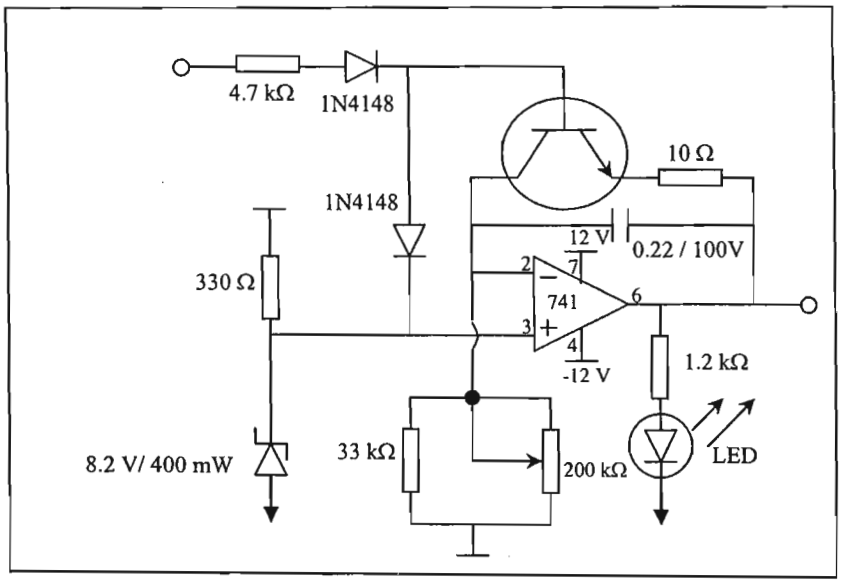

Figure B.3: The Ramp stage

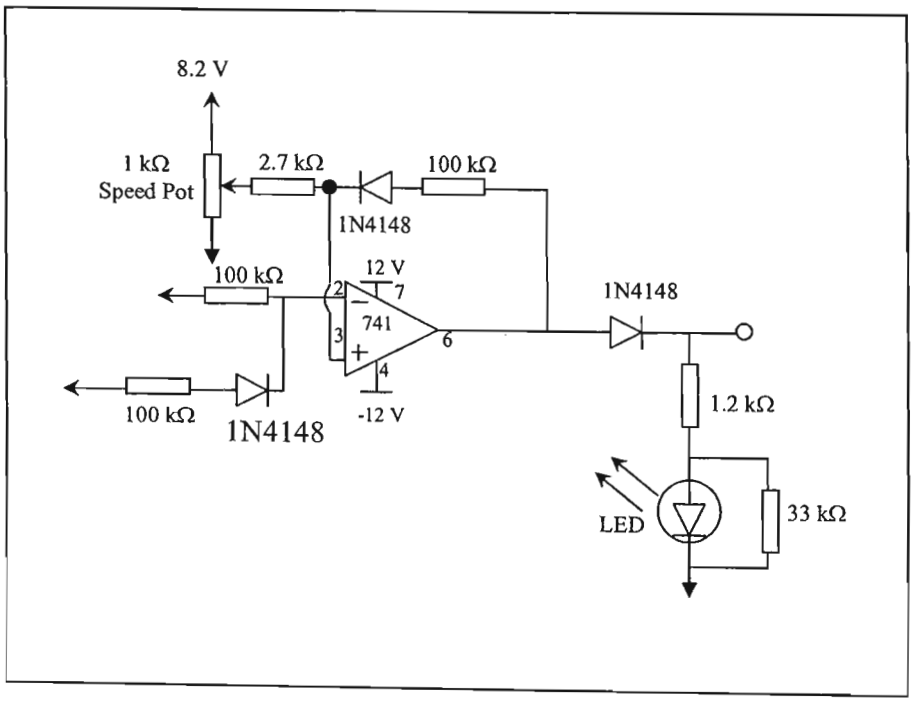

Figure B.4: The Comparator stage

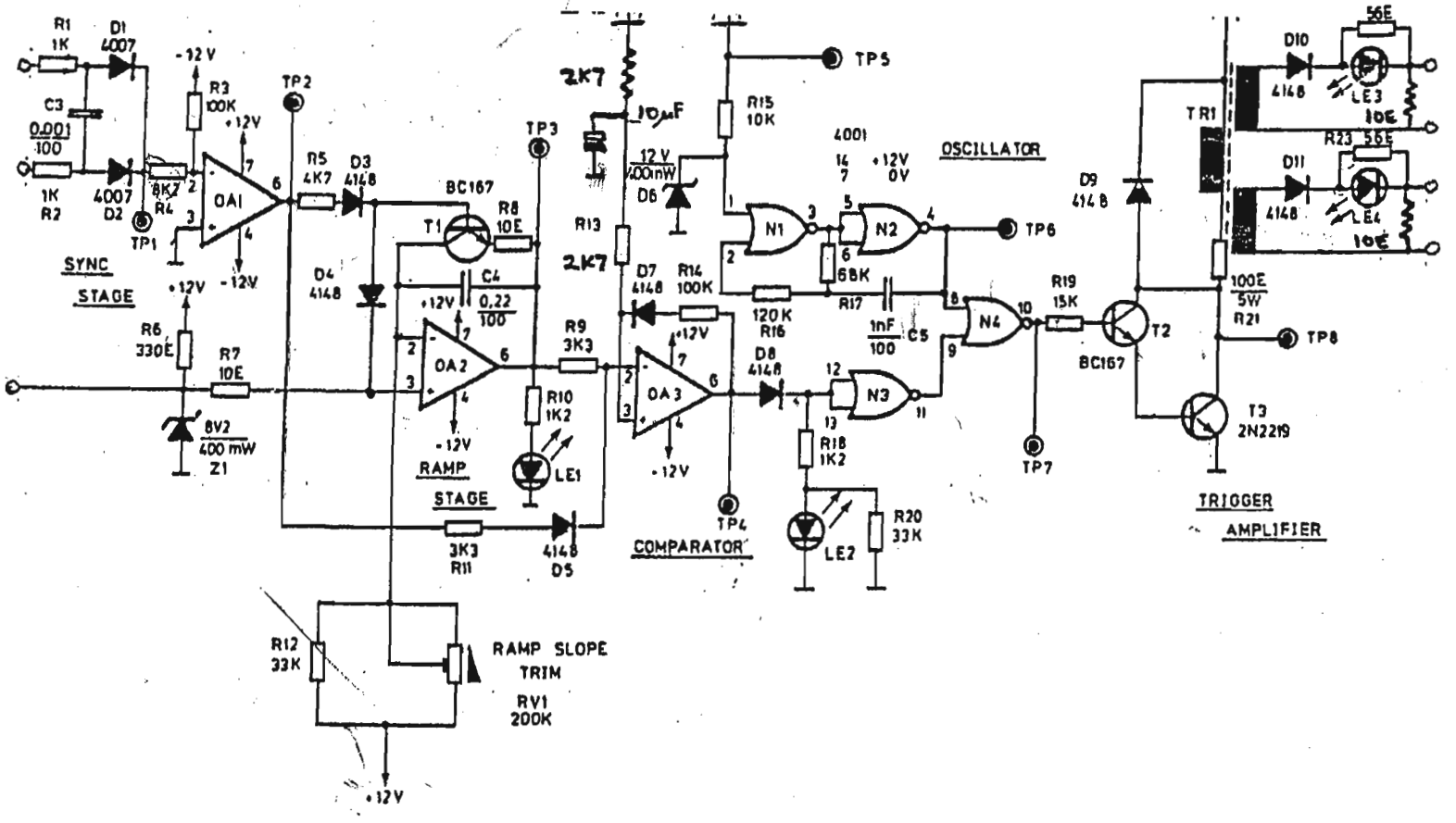

Figure B.5: The initial trigger circuit for each phase of the hardware TCSC

B.2 The Impact of the Changing Capacitor Voltage to the Thyristor Firing Pulses

Chapter Four has discussed the impact of variations in the magnitude of capacitor voltage to the thyristor firing pulses. The objective of this section is to expand the discussion developed in Chapter Four by including graphical results. The problem that is discussed in Chapter Four (and subsequently, in this section) was resolved by modifications in the conventional synchronizing stage (as outlined in Chapter Four). However, it is important to note that the graphical results presented in this section are those of the unmodified trigger channel.

Figure B.5 shows the rated capacitor voltage that was used as the input to the trigger channel. The zero-crossing detector was then used to output the reset pulse (for the ramp signal) each time capacitor voltage becomes zero. The capacitor voltage was then decreased to a value just below 10 volts, as shown by Figure B.6. The figure clearly shows the error in the reset pulses and the ramp signal. This is undesired behavior and it leads to incorrect turn on pulses.

This problem is more visible by the results of Figure B.7, where the capacitor voltage was reduced further. The ramp pulses have now been transformed to a level shape.

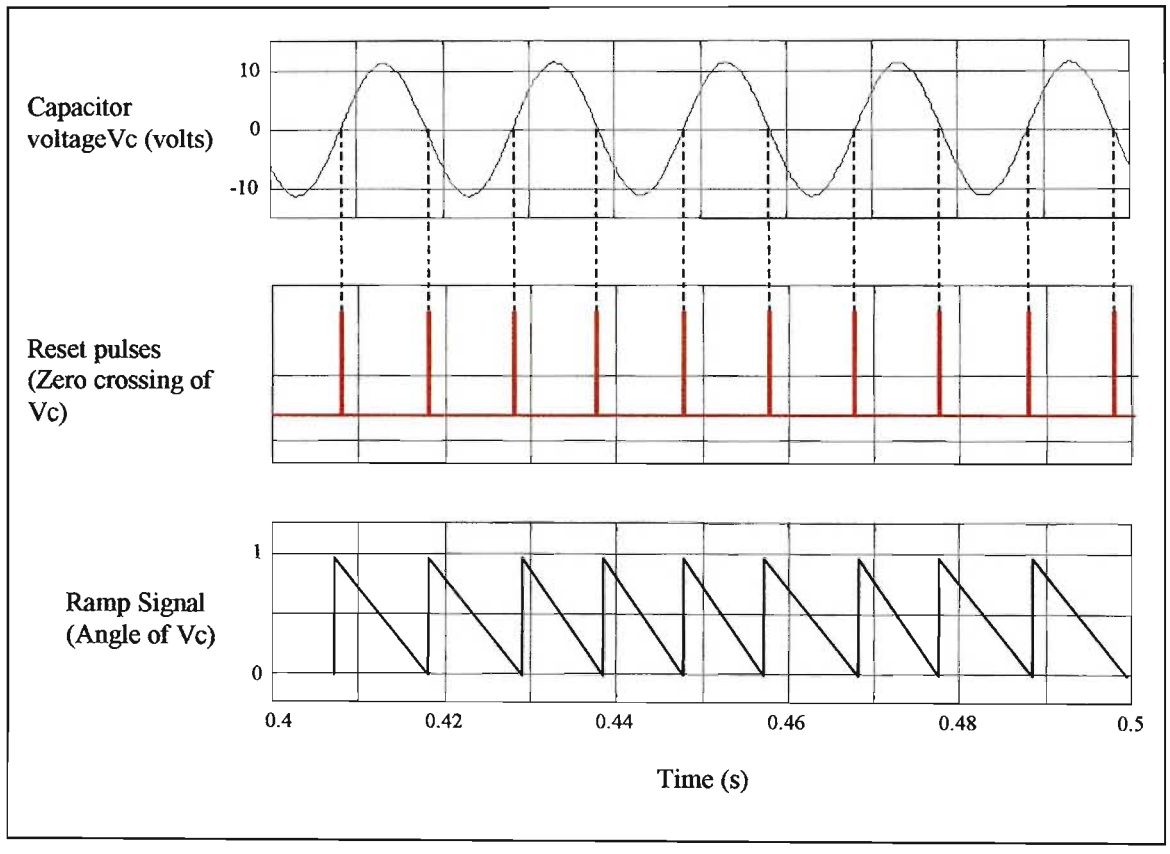

Figure B.5: Ideal capacitor voltage as an input to the zero crossing detector

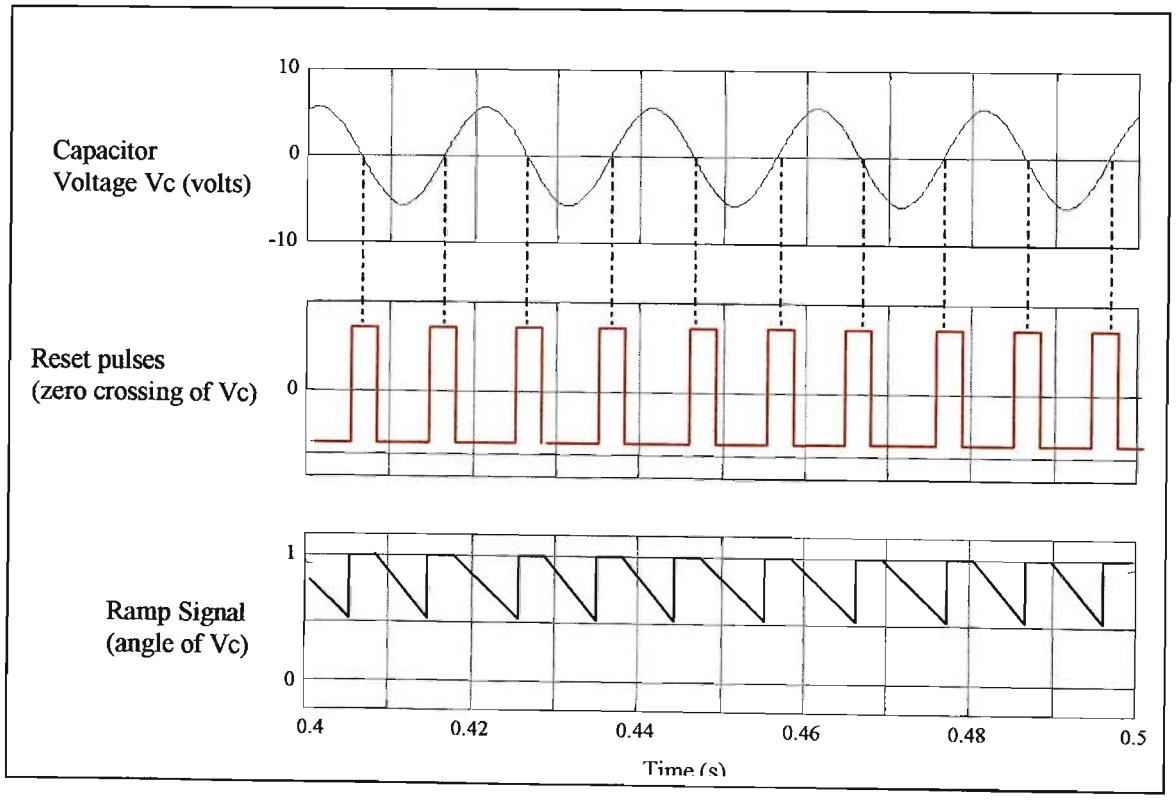

Figure B.6: A small error introduced by the decreased in capacitor voltage

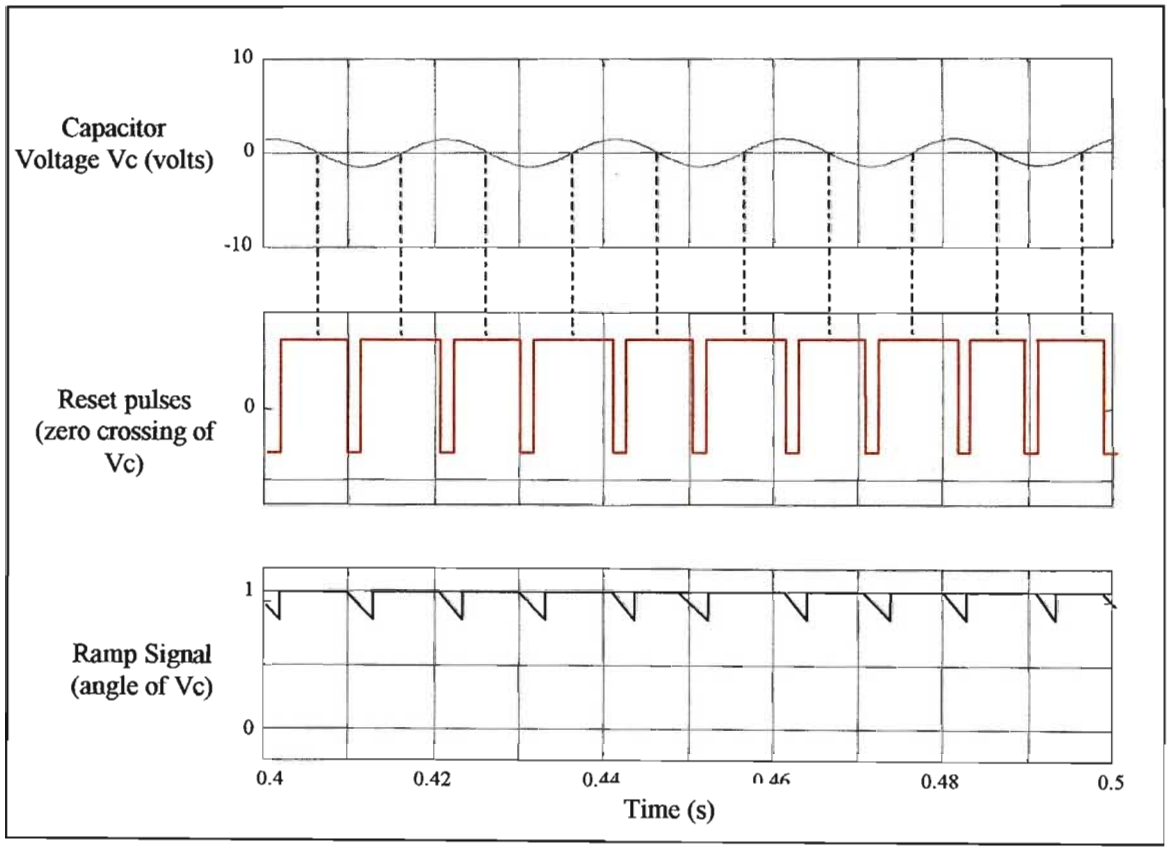

Figure B.7: A larger error introduced by the decreased in capacitor voltage to below 5 volts.

APPENDIX C

ADDITIONAL SIMULATION DETAILS AND RESULTS FROM CHAPTER FOUR

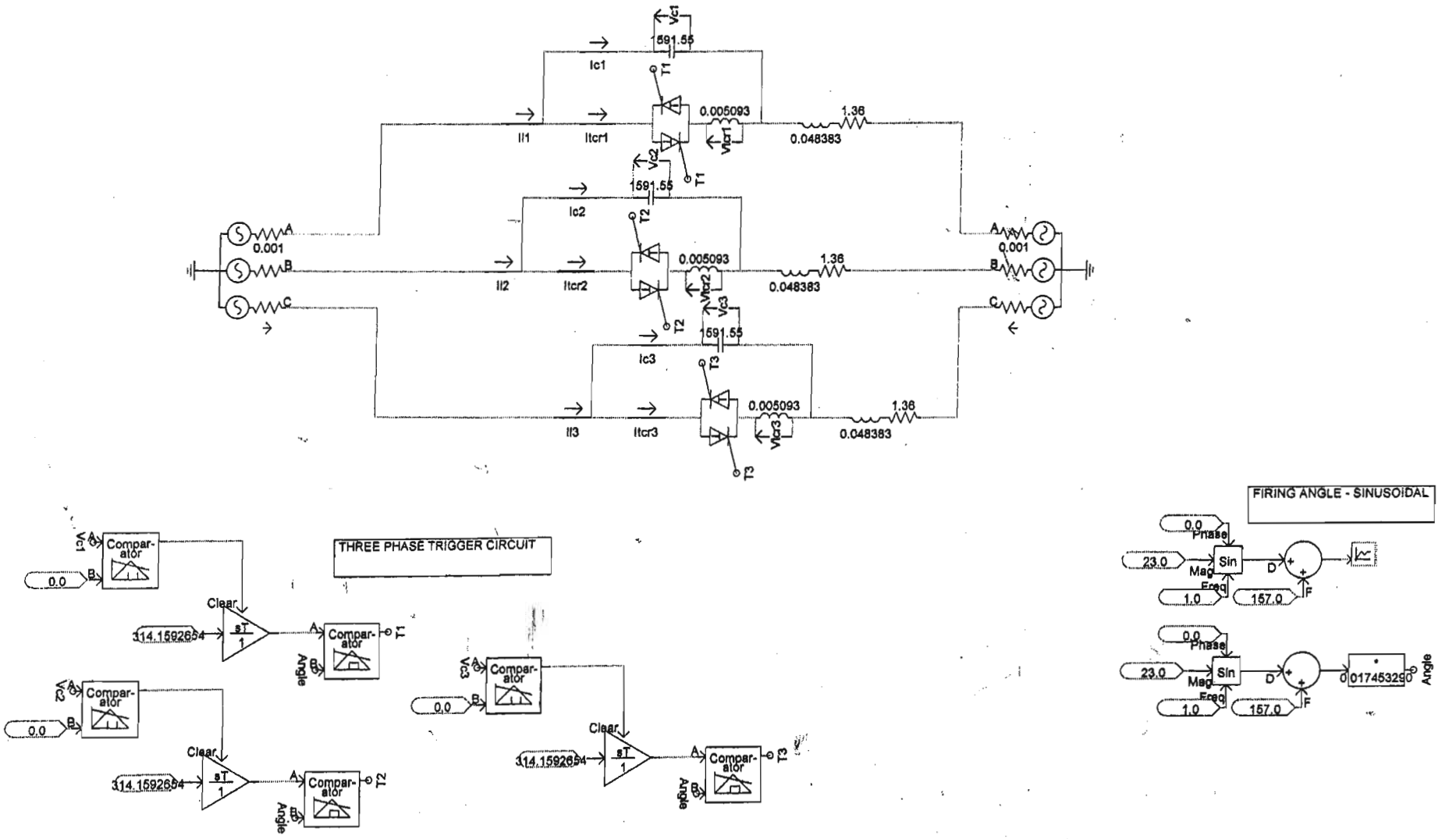

Figure C.1: The EMTDC circuit diagram of the TCSC with sinusoidal modulation of the firing angle

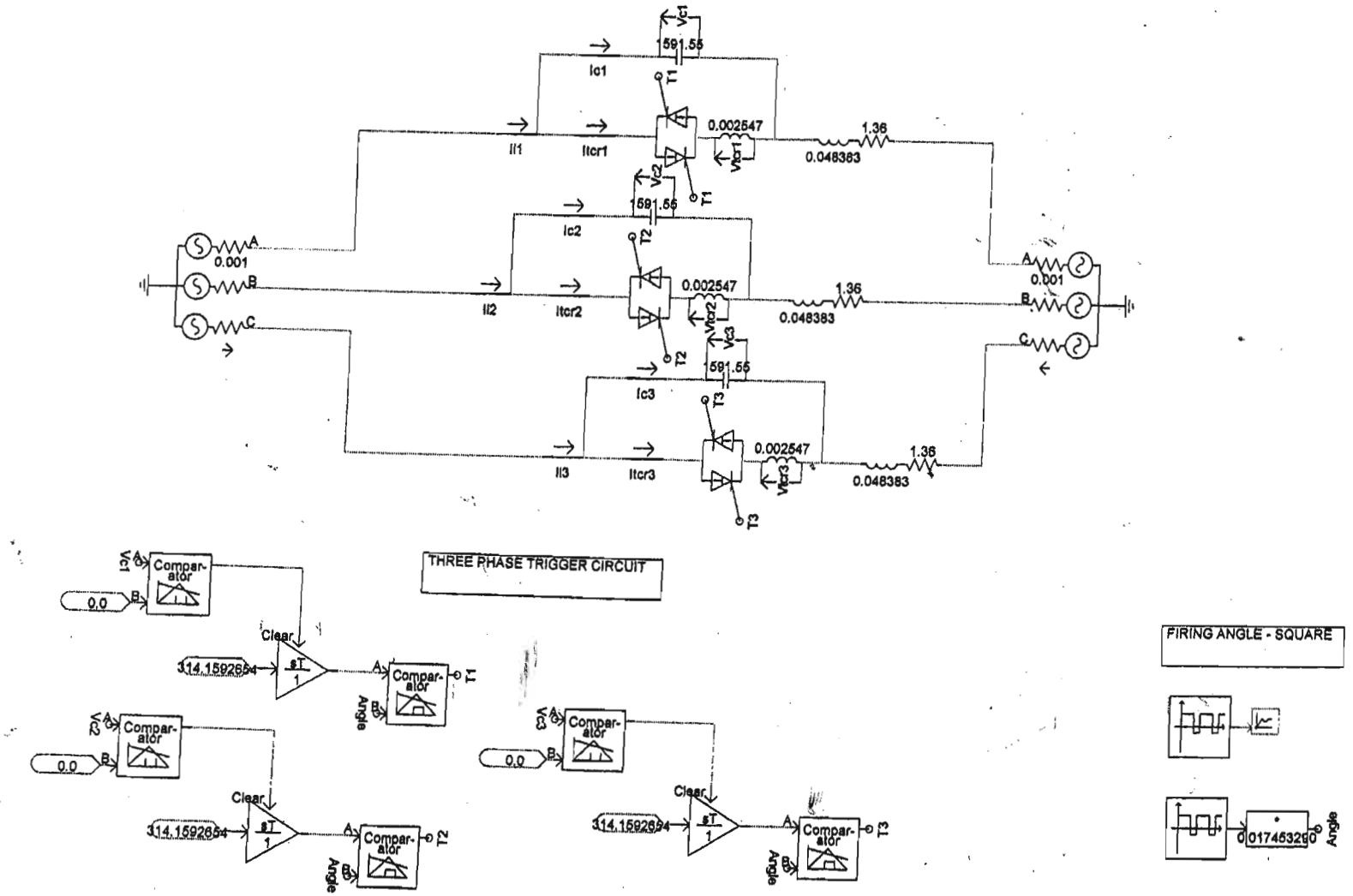

Figure C.2: The EMTDC circuit diagram of the TCSC with square modulation of the firing angle

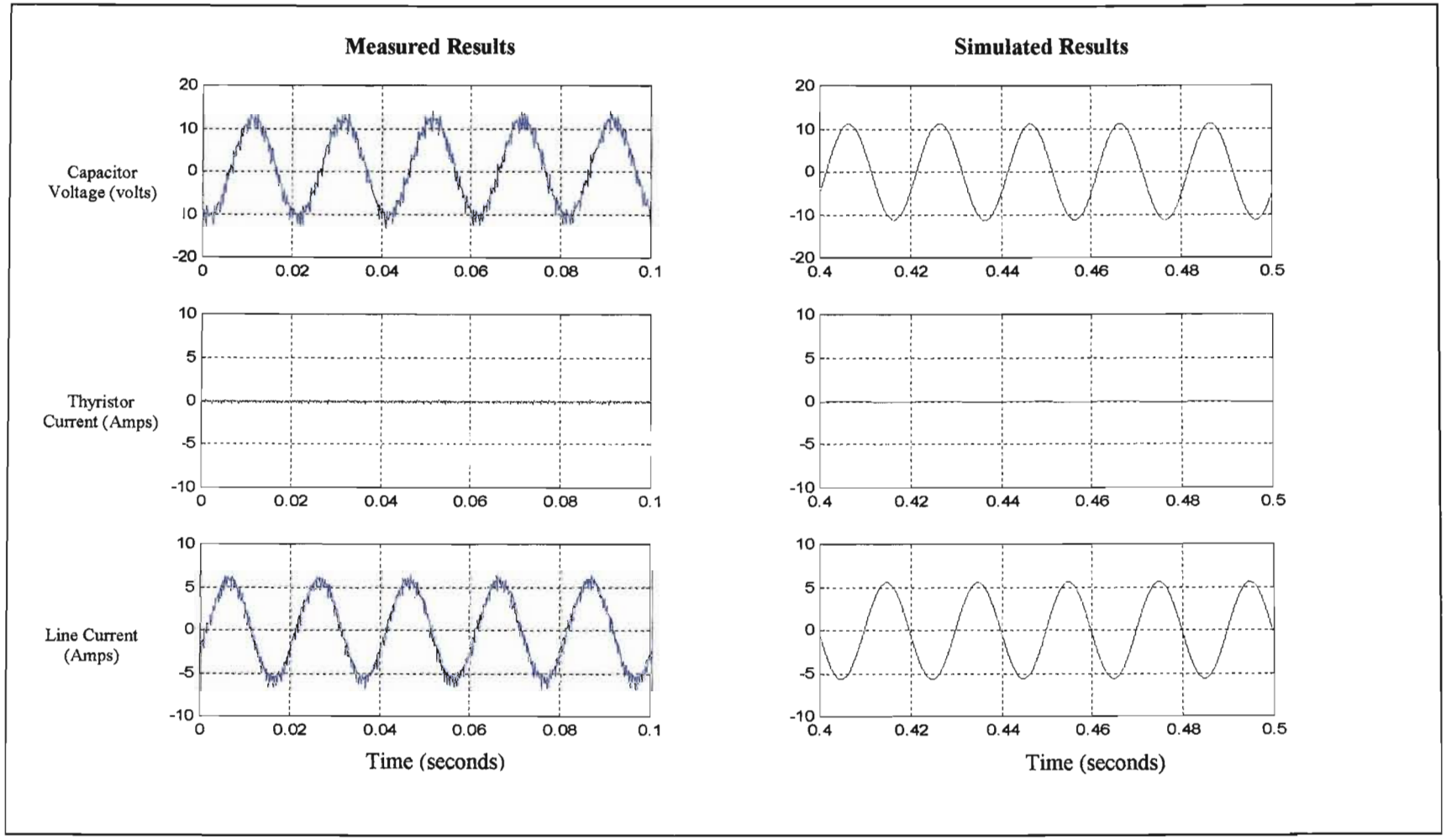

Figure C.3: Comparison of phase B time-domain results at reactance order of 1

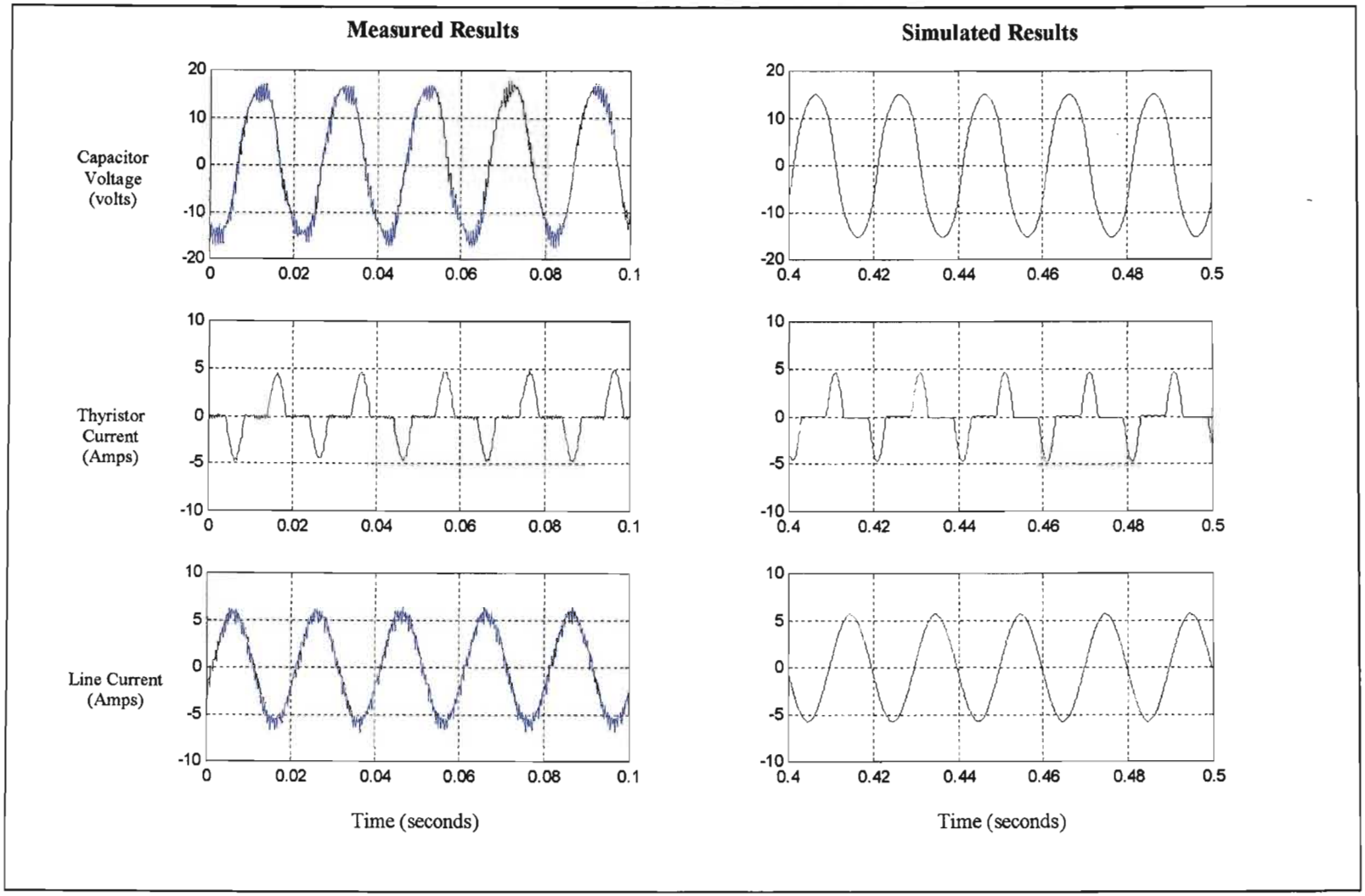

Figure C.4: Comparison of phase B time-domain results at reactance order of 1.5

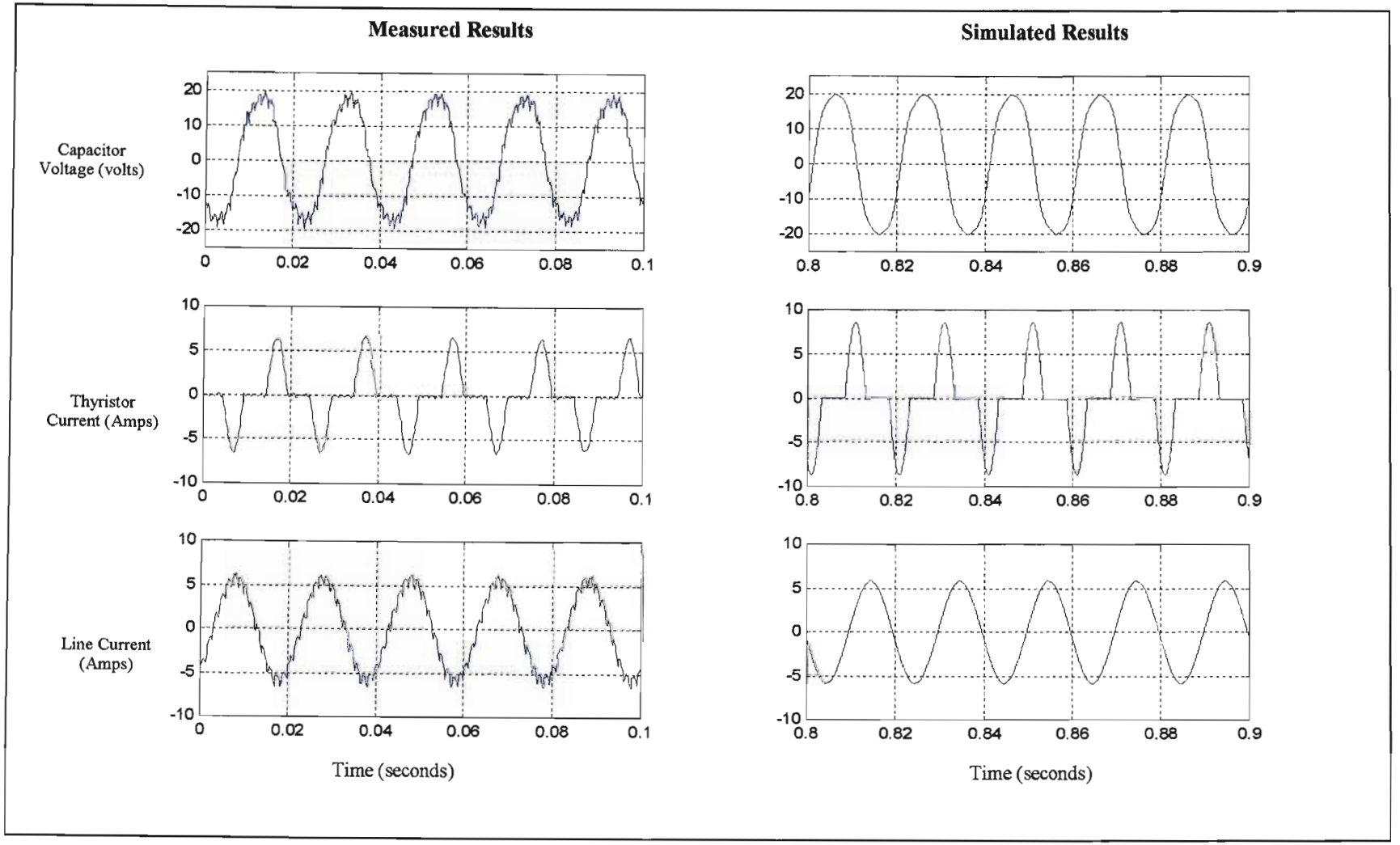

Figure C.5: Comparison of phase B time-domain results at reactance order of 2

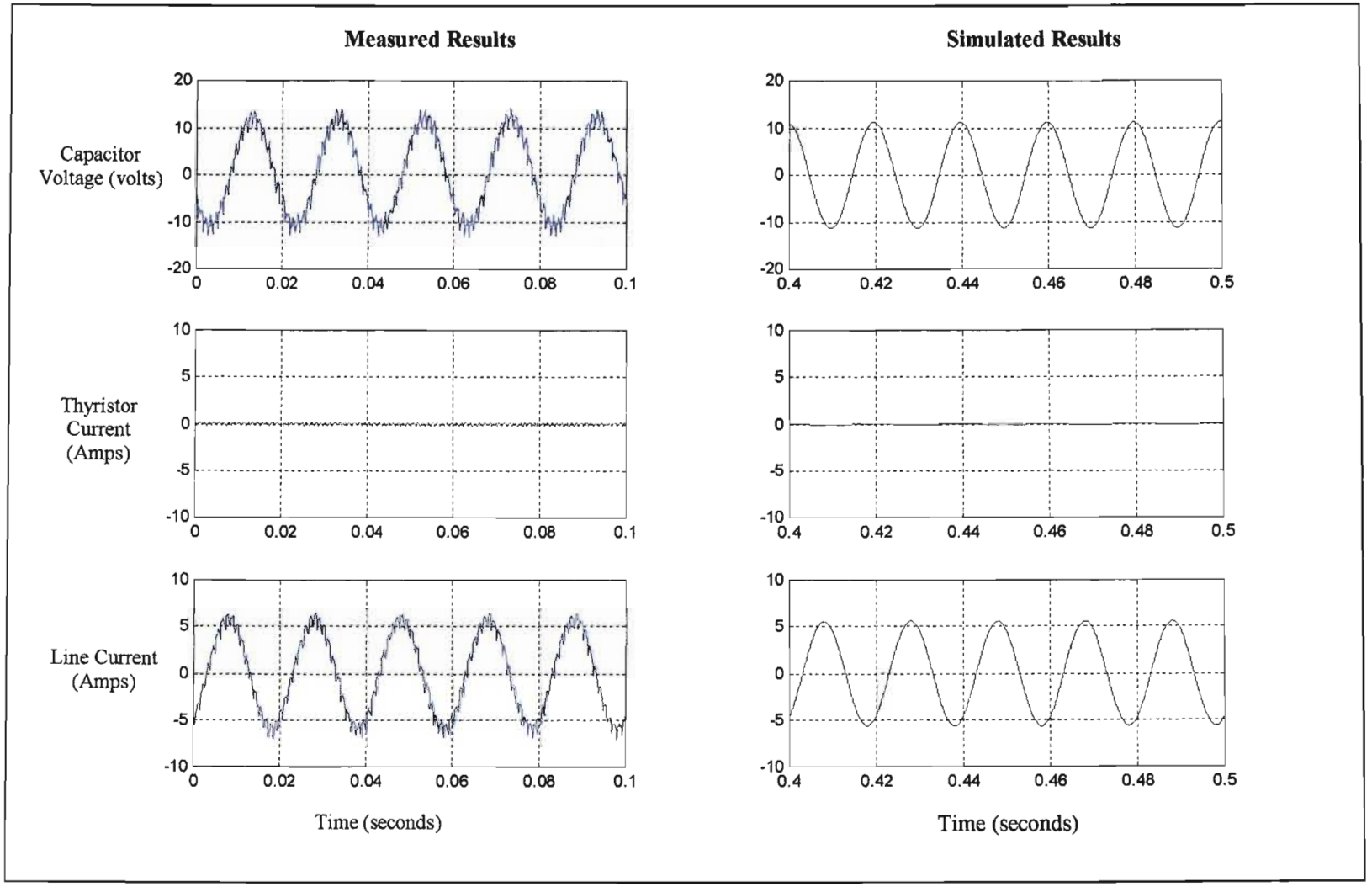

Figure C.6: Comparison of phase C time-domain results at reactance order of 1

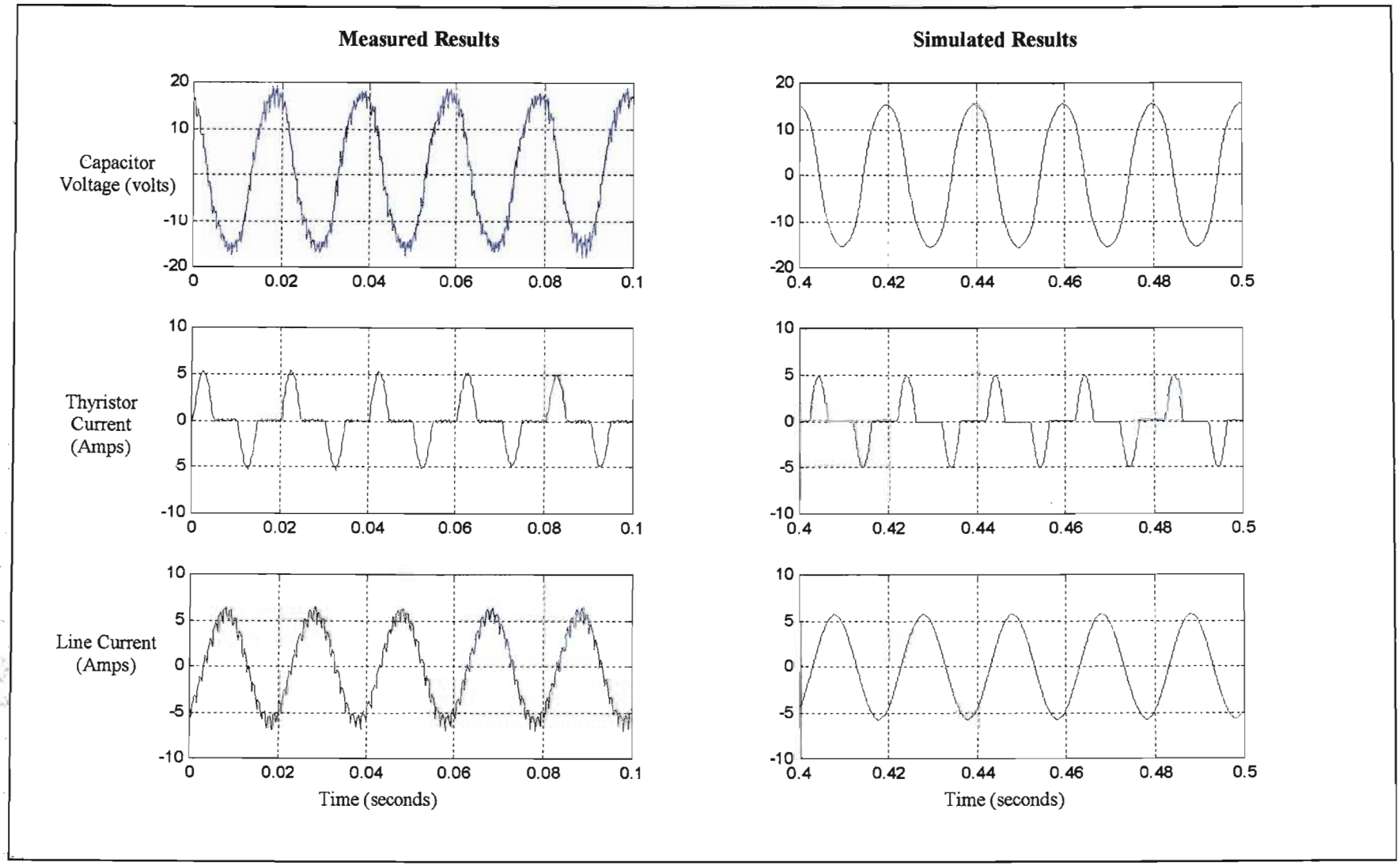

Figure C.7: Comparison of phase C time-domain results at reactance order of 1.5

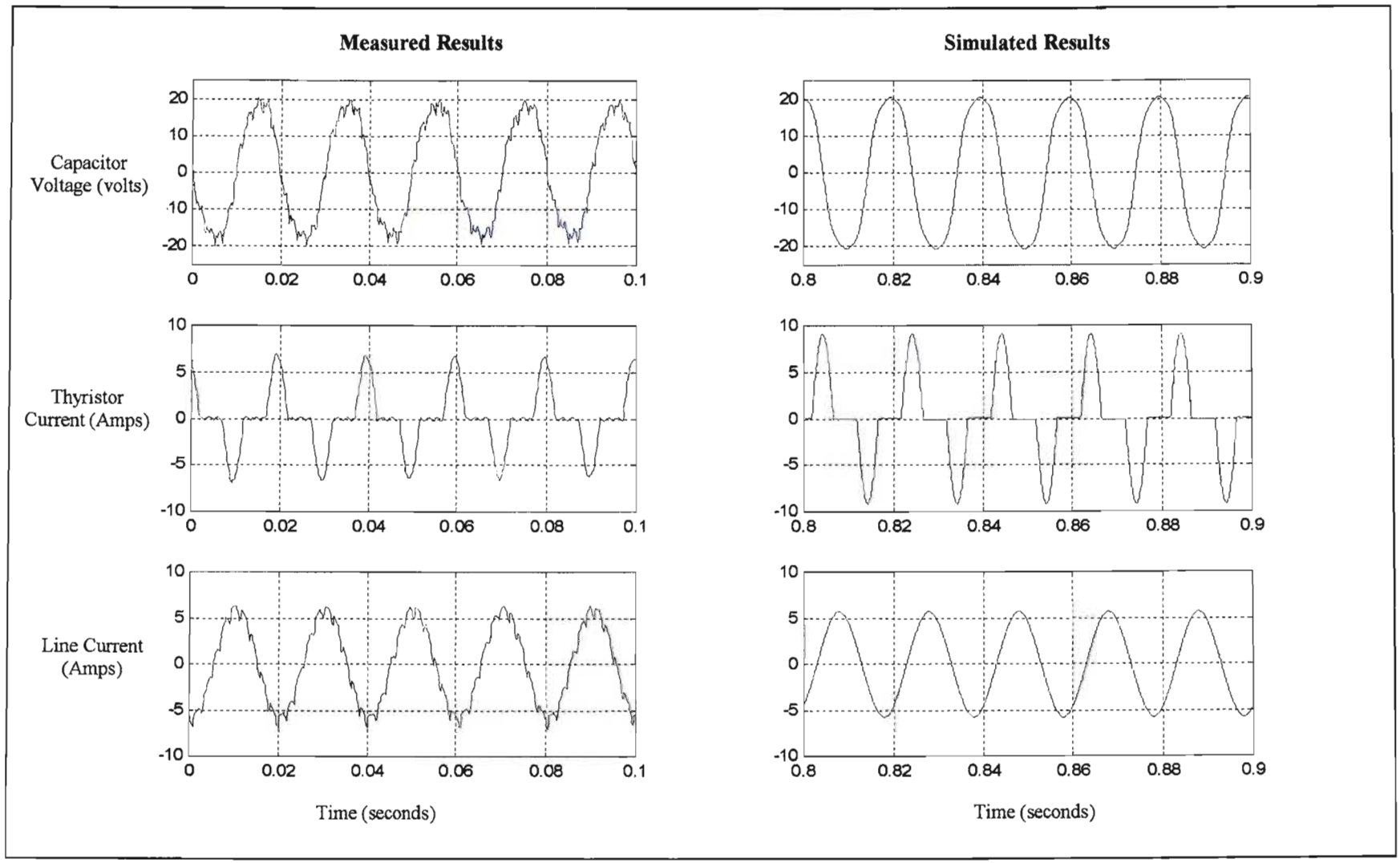

Figure C.8: Comparison of phase C time-domain results at reactance order of 2

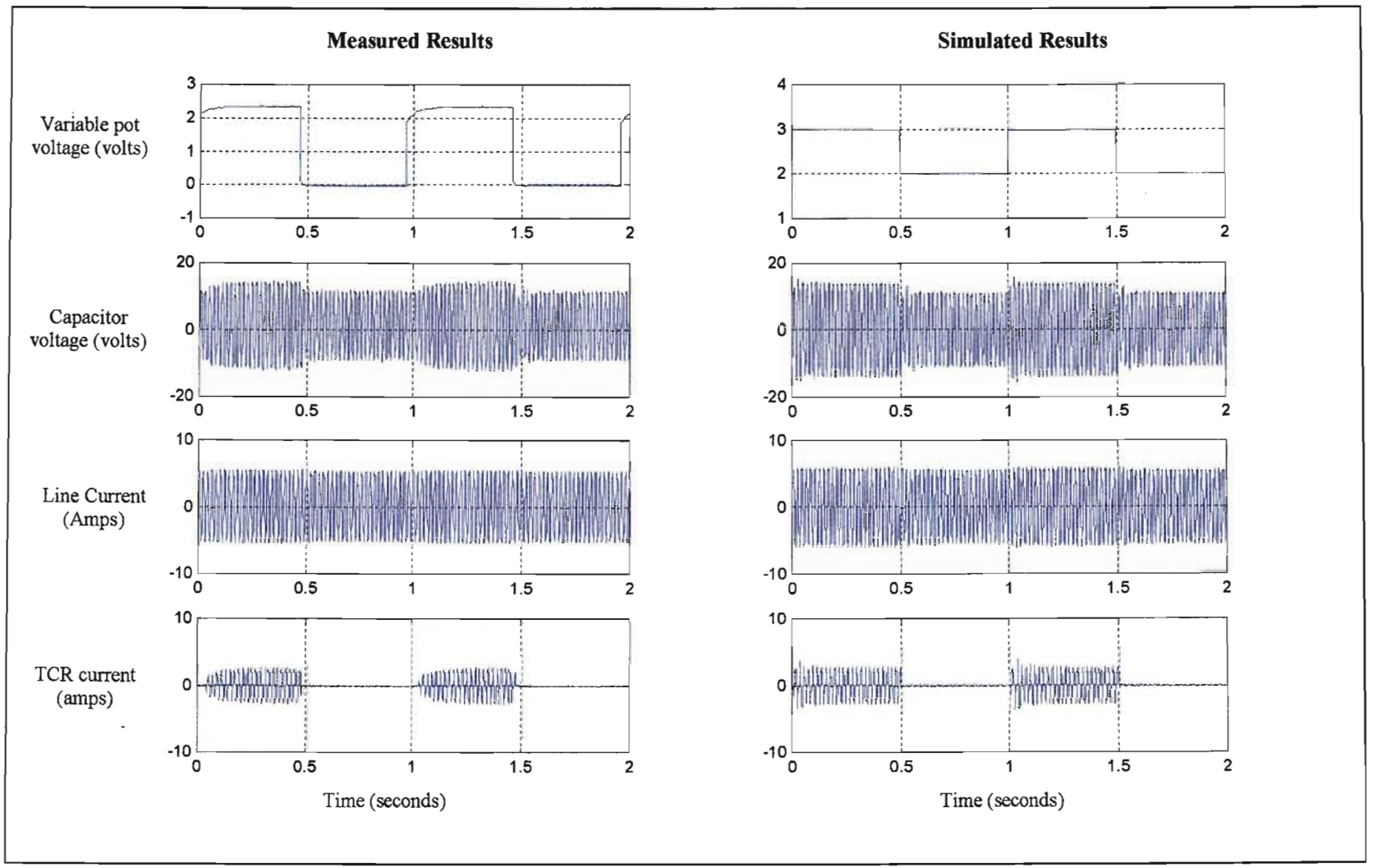

Figure C.9: TCSC response to a two level modulation of reactance order between 1 and 1.5; Xtcr = 1.2 Ω.

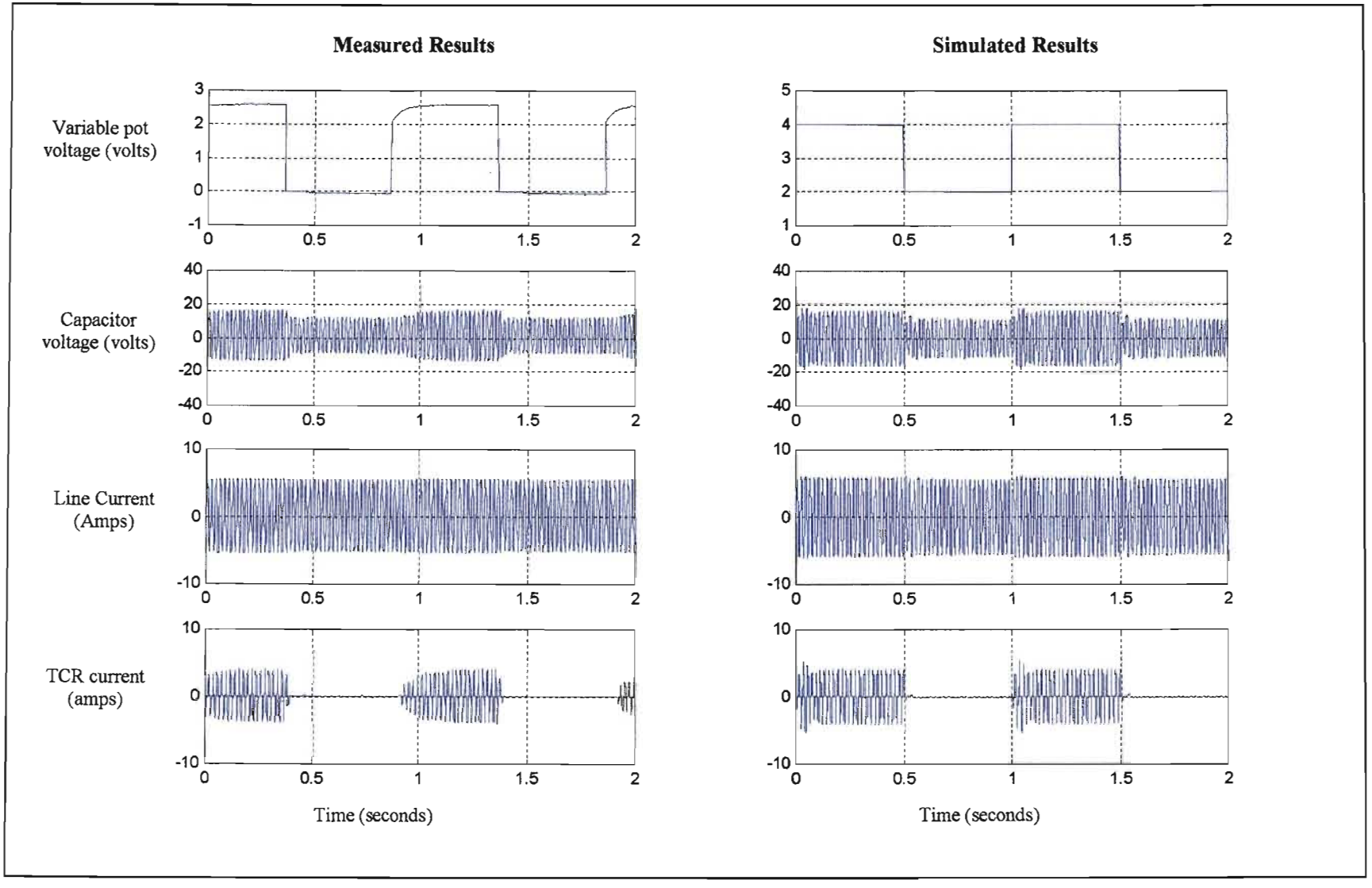

Figure C.10: TCSC response to a two level modulation of reactance order between 1 and 2; Xtcr = 1.2 Ω.

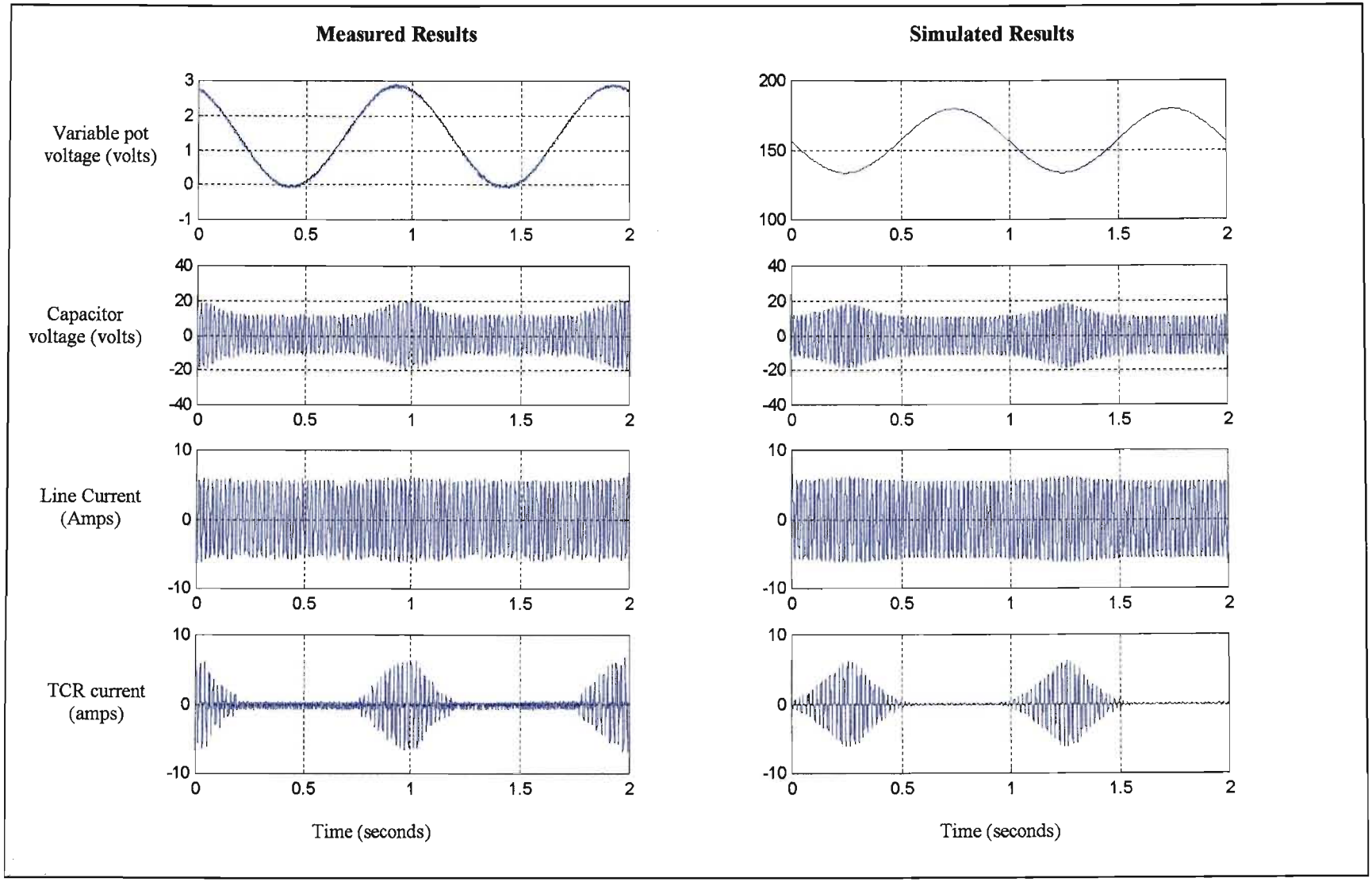

Figure C.11: TCSC response to a 1 Hz modulation of reactance order between 1 and 2; Xtcr = 1.2 Ω.

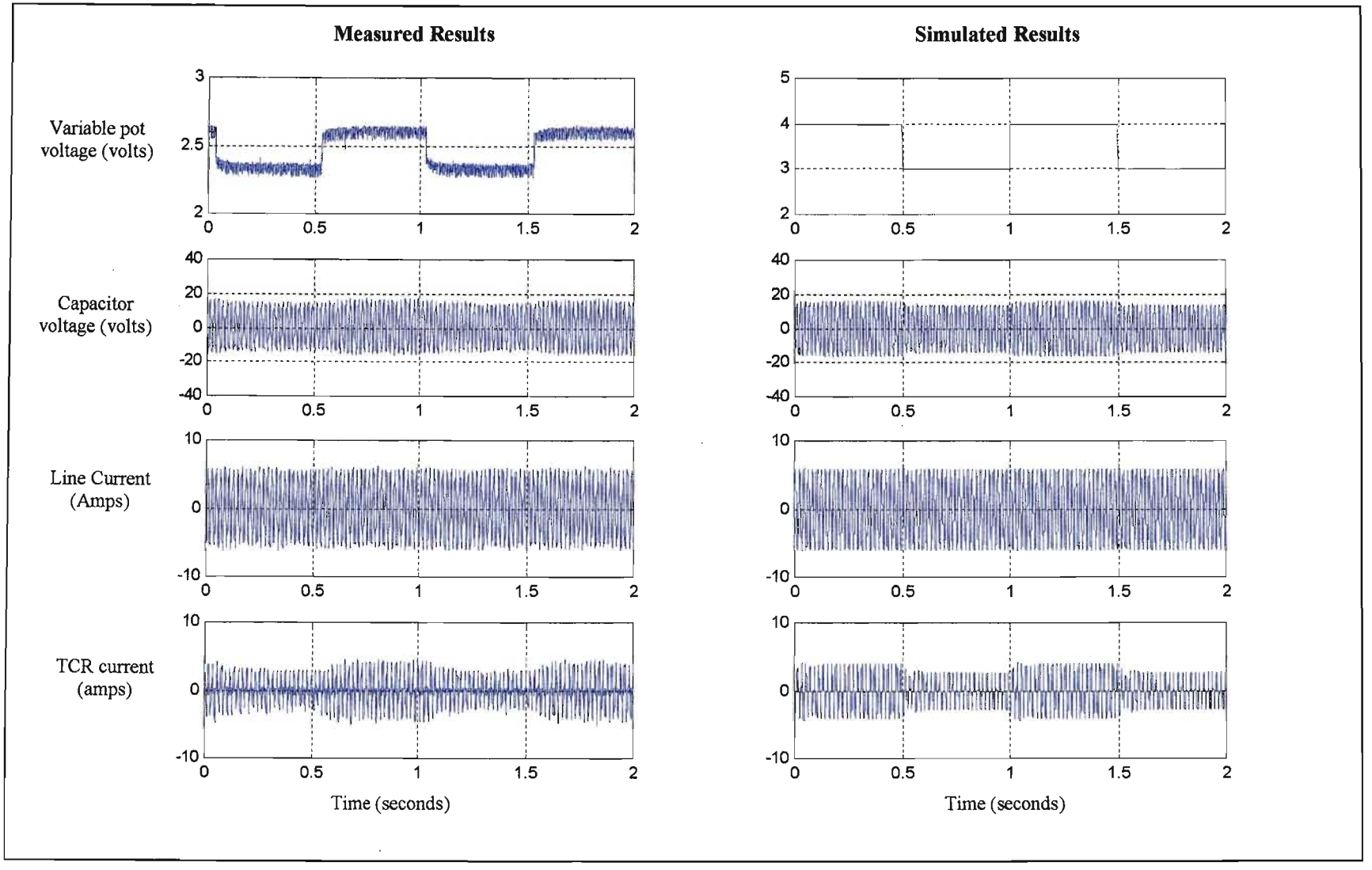

Figure C.12: TCSC response to a two level modulation of reactance order between 1.5 and 2; Xtcr = 1.2 Ω.

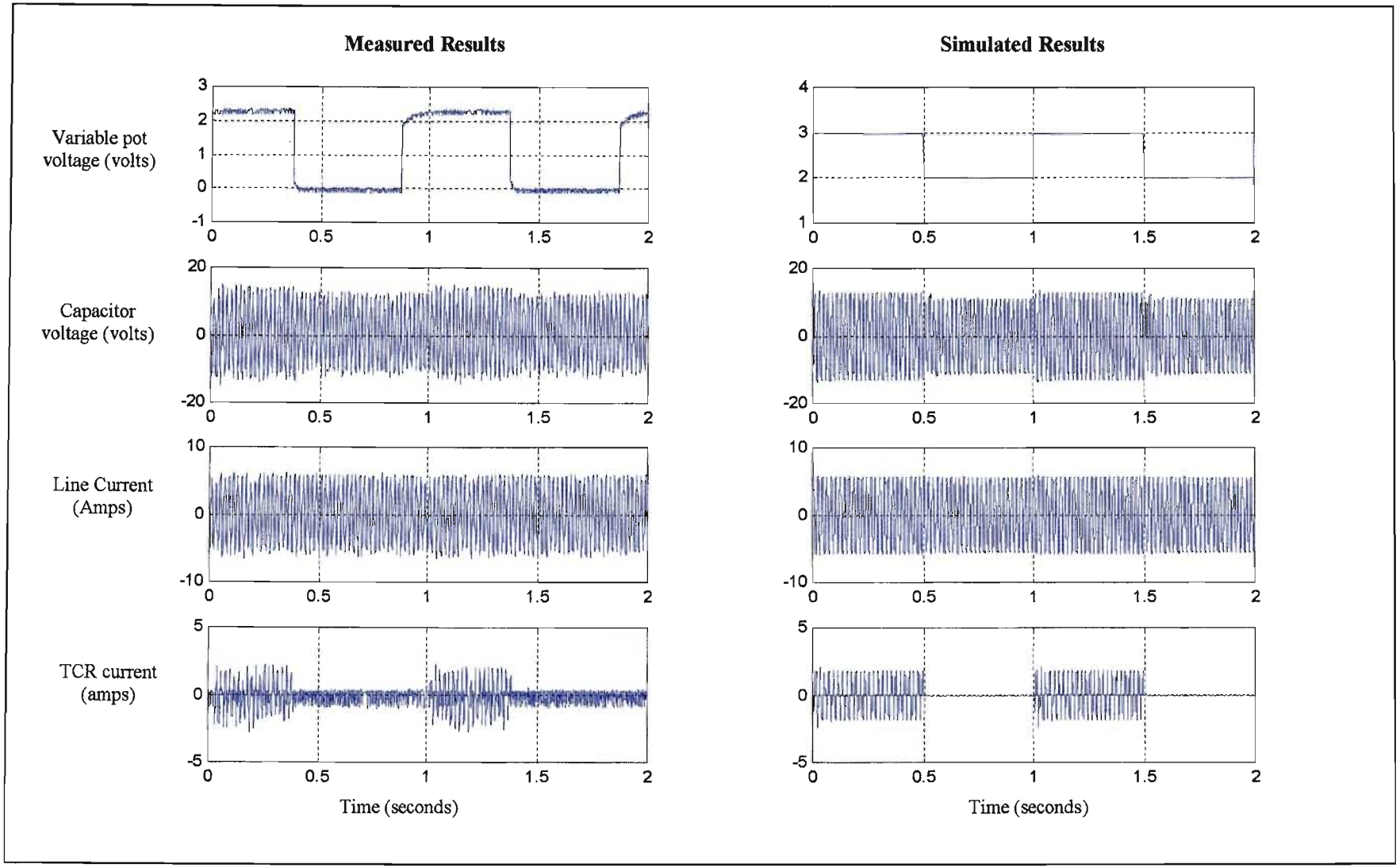

Figure C.13: TCSC response to a two level modulation of reactance order between 1 and 1.5; Xtcr = 1.6 Ω.

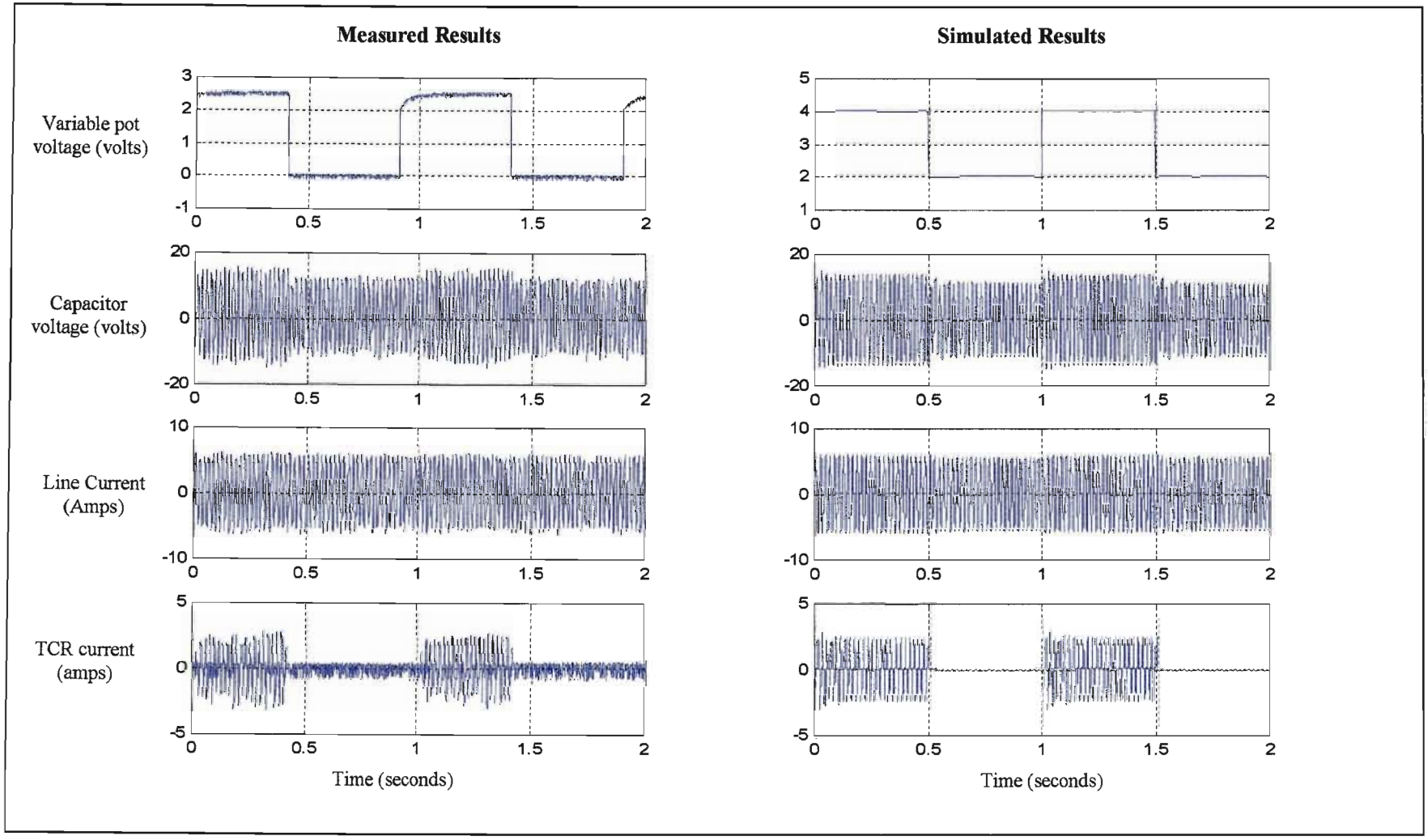

Figure C.14: TCSC response to a two level modulation of reactance order between 1 and 2; Xtcr = 1.6 Ω.

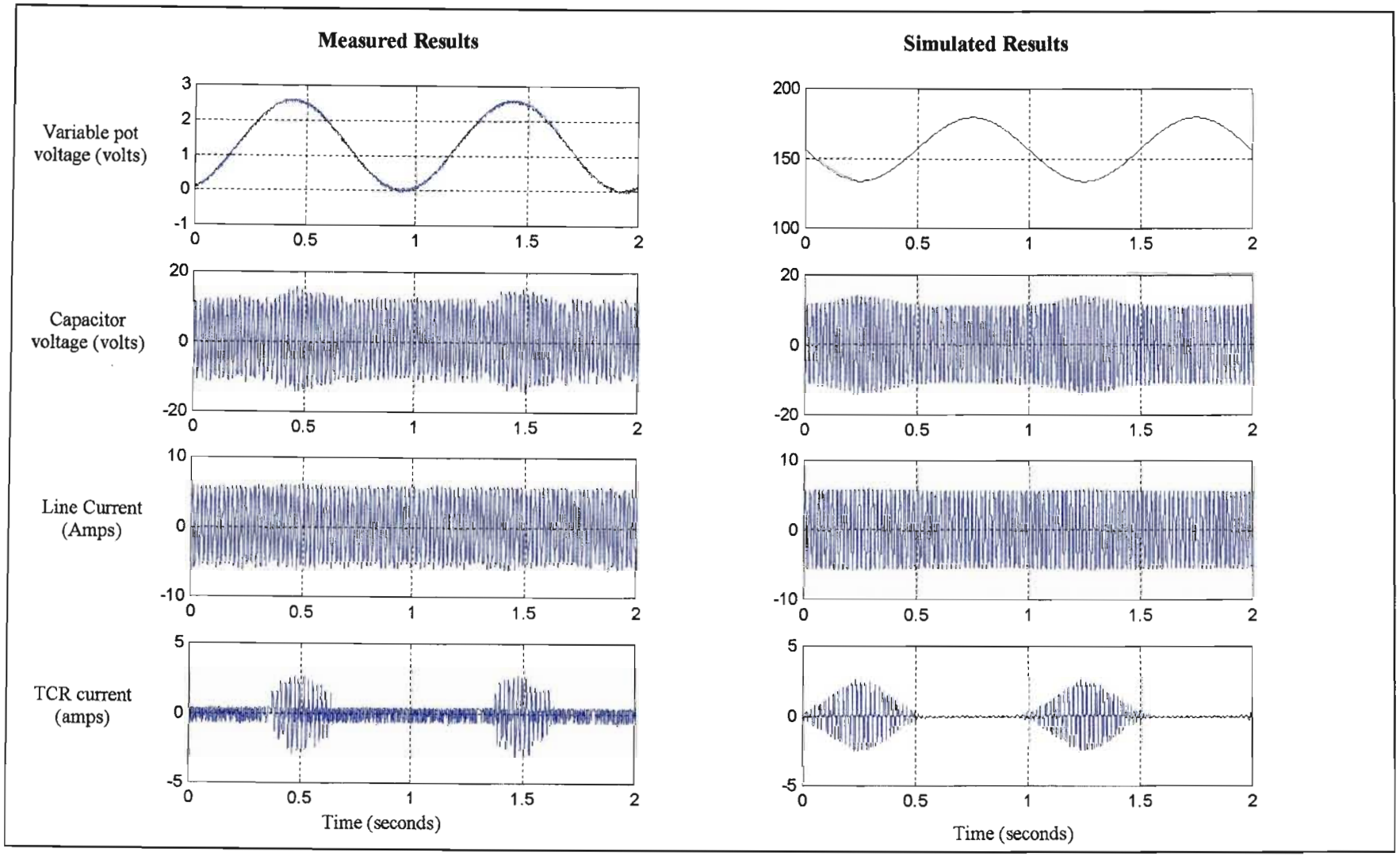

Figure C.15: TCSC response to a 1 Hz modulation of reactance order between 1 and 2; Xtcr = 1.6 Ω.

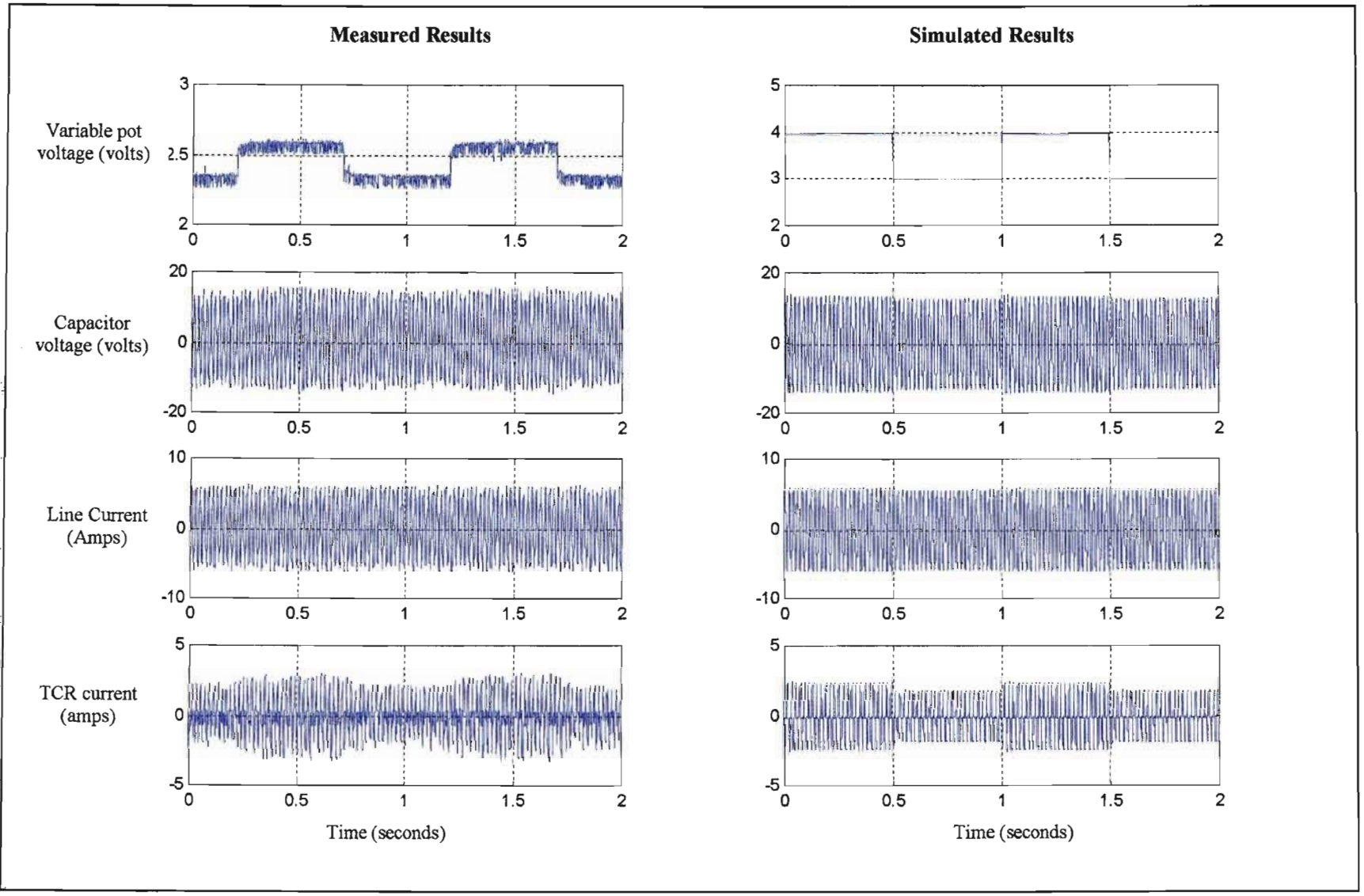

Figure C.16: TCSC response to a two level modulation of reactance order between 1.5 and 2; Xtcr = 1.6 Ω.

APPENDIX D

EMTDC SIMULATION MODEL FOR POWER OSCILLATION DAMPING STUDY

This section introduces the parameters of the EMTDC circuit that was used to investigate power swings damping in Chapter Five.

D.1 Parameters of a Detailed EMTDC Circuit

D.1.1 Generator Parameters (per unit unless stated)

R_a	=	0.006	V_{TO}	=	1.0
X_l	=	0.11	θ_{TO}	=	0.2233 rad
X_d	=	1.98			
R_f	=	0.002			
X_f	=	0.1			
R_d	=	0.0212			
X_{kd}	=	0.125			
X_{mfd}	=	0.0			
X_{mq}	=	1.87			
R_{kq}	=	0.029			
X_{kq}	=	0.257			
Base voltage	=	220 V_{rms} (Line to line)			
Line Current	=	7.873 A_{rms}			
Frequency	=	50 Hz			
H	=	5.68144			

D.1.2 Turbine Model

Number of turbines	=	4
Machine 3 phase MVA	=	0.003 MVA
Electrical base frequency	=	50 Hz
Synchronous speed	=	1500 rpm
Machine initial electrical speed	=	1 per unit
Inertia constant – turbine 1	=	0.37
Inertia constant – turbine 2	=	1.195
Inertia constant – turbine 3	=	1.19
Inertia constant – turbine 4	=	1.222
Inertia constant – generator	=	1.67
Inertia constant – exciter	=	0.0344
Spring constant from turbine 1 to 2	=	3339.5
Spring constant from turbine 2 to 3	=	7960.8
Spring constant from turbine 3 to 4	=	7357.6
Spring constant from turbine to generator	=	8460.3
Spring constant from generator to exciter	=	22148.2

D.1.3 Transmission Line and TCSC Parameters (per phase)

R_L	=	0.397 Ω	$X_{TCSC(MAX)}$	=	-j 4 Ω
X_L	=	j 11.93 Ω	$X_{TCSC(MIN)}$	=	-j 2 Ω
X_C	=	-j 2 Ω			
X_{TCR}	=	j 1.2 Ω			

D.1.4 Infinite Bus-Bar

Base apparent power	=	0.003 MVA
Base voltage	=	220 V_{RMS} (l-l)
Series resistance	=	0.001 Ω

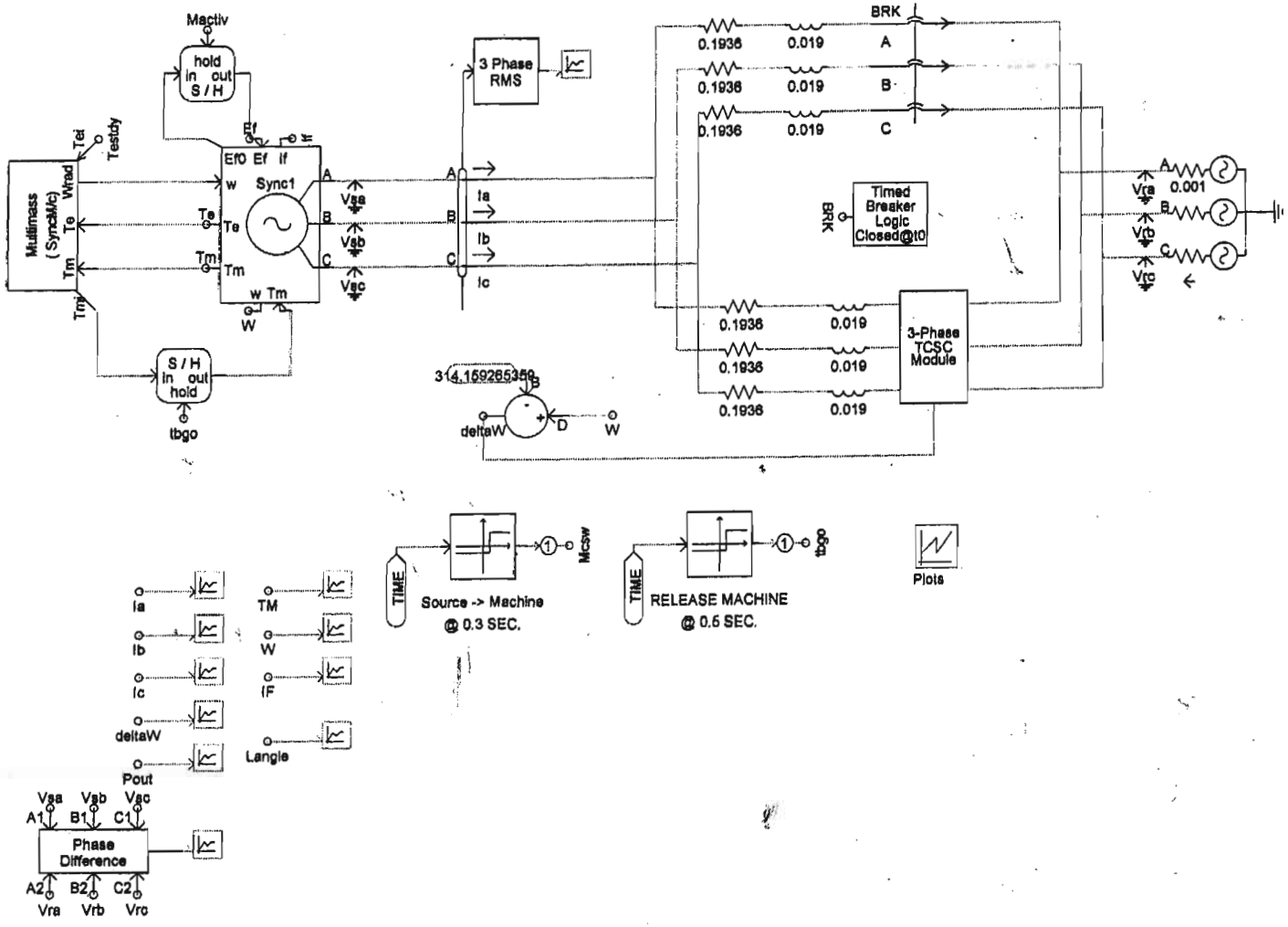

Figure D1: A detailed EMTDC circuit used for damping power swings

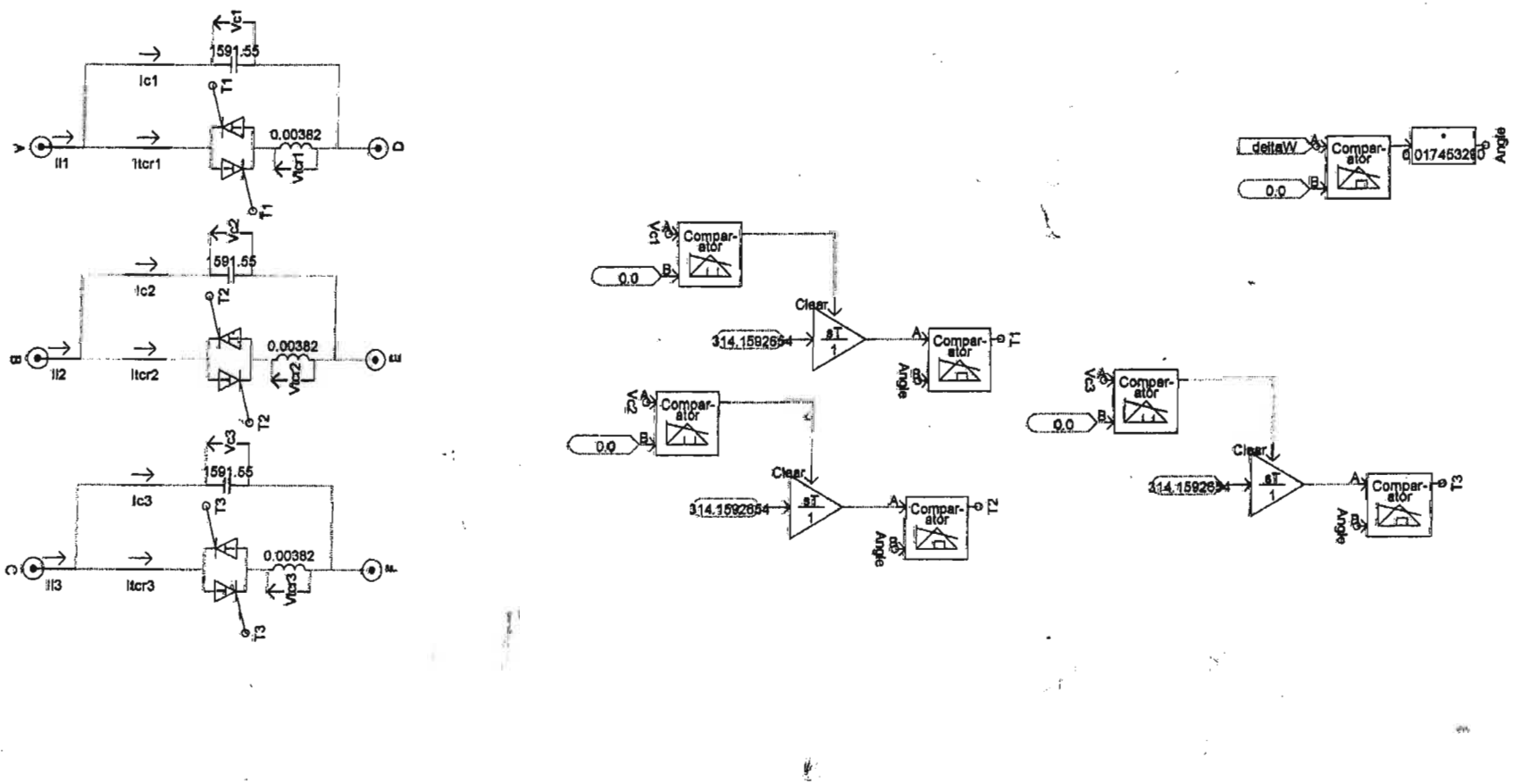

Figure D2: EMTDC model for a three-phase TCSC circuit of Figure D1

REFERENCES

[1]. R. J. Piwko, C. A. Wegner, S. J. Kinney, J.D. Eden, "Subsynchronous Resonance Performance Tests of the Slatt TCSC", *IEEE Transactions on Power Delivery*, Vol. 11, No. 2, April 1996, pages 1112 – 1119.

[2]. V. Venkatasubramanian, C. W. Taylor, "Improving Pacific Inertia Stability using Slatt Thyristor Controlled Series Compensation", *Proceedings of IEEE Power Engineering Society Winter Meeting*, Vol. 2, Jan 2000, pages 1468-1470.

[3]. N. Christl, R. Hedin, R. Johnson, P. Krause, A. Montana, "Power System Studies and Modelling for the Kayenta 230kV Substation Advanced Series Compensation", *IEE International Conference*, London 1991.

[4]. A. T. Hill, E. V. Larsen, E. Hyman, "Thyristor Controller for SSR Suppression: A Case Study", *Proc. EPRI FACTS meeting*, Oct 1994, Baltimore, Maryland.

[5]. S. J. Kinney, W. A. Mittelstadt, R. W. Suhrbier, "Test Results and Initial Operating Experience for the BPA 500KV Thyristor Controlled Capacitor Unit at Slatt Substation", *Proceedings of EPRI FACTS Conference*, 5-7 October 1994, pages 3.1 – 4.15.

[6]. N. S. Chonco, B. S. Rigby, R. G. Harley, "Damping of Power System Oscillations using an Inverter-Based Controllable Series Compensator", *Proceedings of the 9th South African Universities Power Engineering Conference 2000*, pages 192 – 196.

[7]. F. J. Swift, H. F. Wang, M. Li, "Analysis of Controllable Series Compensator to Suppress Power System Oscillation", *Sixth International Conference*, AC and DC Power Transmission, Conference Publication No. 423,

IEE, 29 April – 3 May 1996, pages 202 – 207.

[8]. F. P. de Mello, " Explanatory Concepts on Control of Variable Series Compensation in Transmission System to Improve Damping of Inter-Machine / System Oscillations", *IEEE Transactions on Power Systems*, Vol. 9, No. 1, February 1994, pages 102 - 108.

[9]. P. S. Dolan, J.R. Smith, W. A. Mittelstadt, " A Study of TCSC Optimal Damping Control Parameters for Different Operating Conditions", *IEEE Transactions on Power System*, Vol. 10, No. 4, November 1995, pages 1972 - 1978

[10]. B.S. Rigby, N.S. Chonco, R. G. Harley, " Strategies for Damping Power Swings using Controllable Series Compensator", *Proceedings of the 8th Southern African Universities Power Engineering Conference*, Potchefstroom, January 1999, pages 131-134.

[11]. L. Angquist, B. Lundin, J. Samuelsson, "Power Oscillation Damping using Controlled Reactive Power Compensation - A Comparison Between Series and Shunt Approaches", *IEEE on Power System*, Vol. 8, No. 2, May 1993, pages 687 – 695.

[12]. E. V. Larsen, J. J. Sanchez-Gasca, J. H. Chow, "Concepts for Design of FACTS Controllers to Damp Power Swings", *IEEE Transactions on Power Systems*, Vol. 10, No. 2, May 1995, pages 948 – 955.

[13]. R. Rajaraman, I. Dobson, R. Lasseter, Y. Shern, "Computing the Damping of Subsynchronous Oscillations due to a Thyristor Controlled Series Capacitor", *IEEE Transactions on Power Delivery*, Vol. 11, No. 2, April 1996.

[14]. X. Lombard, P.G. Therond, "Series Compensation and Subsynchronous Resonance Detail Analysis of the Phenomenon and of its Damping by a TCSC",

IEE AC and DC Power Transmission Conference, 29 April - 3 May 1996, pages 321-328.

[15]. J. M. Baylet, "Guide to Harmonic Pollution", *Chauvin Arnoux*, Edition 1, September 1994, pages 1 – 21.

[16]. J. Matsuki, K. Ikeda, "Loop Current Characteristics of a Thyristor-Controlled Capacitor", *Denki Gakkai Ronbunshi*, Vol. 117-B, No. 7, July 1997, pages 991 – 998.

[17]. J. Rico, E. Acha, T.J.E. Miller, "Harmonics Domain Modelling of Three Phase Thyristor-Controlled Reactors by means of Switching Vectors and Discrete Convolution", *IEEE Transactions on Power Delivery*, Vol. 11, No. 3, July 1996, pages 1678 – 1684.

[18]. K. Chu, C. Pollock, "A new PWM-Controlled Series Compensator with Fast Response and low Harmonic Distortion", *IEE AC and DC Power Transmission*, Conference Publication, No.423, 1996, pages 208 – 213.

[19]. B. S. Rigby, C. K. Ndlovu, R. G. Harley, "A Thyristor Controlled Series Capacitor Design for Research Laboratory Application", *IEEE Africon Conference*, 1999, pages 903 – 908.

[20]. S. Jalali, R. Hedin, M. Pereira, K. Sadek, "A Stability Model for the Advanced Series Compensator", *IEEE Transaction on Power Delivery*, Vol. 11, No. 2, April 1996, pages 1128 – 1137.

[21]. B. S. Rigby, R. G. Harley, "A Solid-State Controllable Series Capacitive Reactance for Improved Utilization of High-Power Transmission Lines", *CIGRE Meeting*, Johannesburg, 1998.

[22]. E. Larsen, C. Bowler, B. Damsky, S. Nilsson, "Benefits of Thyristor-Controlled Series Compensator", *CIGRE Proceedings of the 34th Session*, Paris, 1992, pages 14/3738-04/1-8 vol. 2.

[23]. S. G. Helbing, G .G. Karady, "Investigation of an Advanced Form of Series Compensation", *IEEE Transactions on Power Delivery*", Vol. 9, No. 2, April 1994, pages 939 – 946.

[24]. G. G. Karady, T. H. Ortmeyer, B. Pilvelait, D. Maratukulam, "Continuously Regulated Series Capacitor", *IEEE Transactions on Power Delivery*, Vol. 8, No. 3, July 1993, pages 1348 – 1355.

[25]. D. N. Kosterev, W. A. Mittelstadt, R.R. Mohler, W. J. Kolodziej, "An Application Study for Sizing and Rating Controlled and Conventional Series Compensation", *IEEE Transactions on Power Delivery*, Vol. 11, No. 2, April 1996, pages 1105 – 1111.

[26]. N. Martins, H. Pinto, J. Paserba, "Using a TCSC for Line Power Scheduling and System Oscillation Damping-Small and Transient Stability Studies", *IEEE Power Engineering Society Winter Meeting*, Singapore, 23 - 27 Jan 2000, Vol. 2, pages 1455-1461.

[27]. N. Yang, Q. Liu, J. McCalley, "TCSC Controller Design for Damping Oscillations", *IEEE Transactions on Power Systems*, Vol. 13, No. 4, Nov. 1998, pages 1304-1310.

[28]. R.H. Mazibuko, B.S. Rigby, R.G. Harley, "Design of a Three-Phase Thyristor Controlled Series Capacitor", 10th South African University Power Engineering Conference, January 2001, pages 221 – 224.

[29]. IEEE Subsynchronous Resonance Working Group: "First Benchmark Model for Computer Simulation of Subsynchronous Resonance", *IEEE*

Transaction on Power Apparatus and Systems, Vol. PAS-96, Sept./Oct. 1977, pages 1565 – 1572.

[30]. S.G. Jalali, R.H. Lasseter, I. Dobson, "Dynamic Response of a Thyristor Controlled Switched Capacitor", *IEEE Transactions on Power Delivery*, Vol. 9, No. 3, July 1994, pages 1609 – 1615.

[31]. E.W. Kimbark, "How to Improve System Stability Without Risking Subsynchronous Resonance", *IEEE Transactions on Power Apparatus and System*, Vol. PAS-96, No. 5, September / October 1977, pages 1608 – 1619.

[32]. W. Zhu, R. Spee, R.R. Mohler, G.C. Alexandrer, W.A. Mittelstadt, D. Maratukulam, "An EMTP Study of SSR Mitigation Using the Thyristor Controlled Series Capacitor", *IEEE Transactions on Power Delivery*, Vol. 10, No. 3, July 1995, pages 1479 – 1485.

[33]. M. Noroozian, L. Ängquist, M. Ghandhari, "Improving Power System Dynamics by Series-Connected FACTS Devices", *IEEE Transactions on Power Delivery*, Vol. 12, No. 4, October 1997, pages 1635 - –641.

[34]. S.S Choi, F. Jiang, G. Shrestha, "Suppression of Transmission System Oscillations by Thyristor-Controlled Series Capacitor", *IEEE Proceedings on Generation*, Transmission and Distribution, Vol. 143, No. 1, January 1996, pages 7 – 12.

[35]. B.S. Rigby, R.G. Harley, "Resonant Characteristics of Inverter-Based Transmission Line Series Compensator", *30th Annual IEEE Power Electronics Specialists Conference*, Piscataway, NJ, USA, 1999, Vol. 1, pages 412 – 417.

[36]. E.V. Larson, K. Clark, S.A. Miske, Jr., J. Urbanek, "Characteristics and Rating Considerations of Thyristor Controlled Series Compensation", *IEEE Transactions on Power Delivery*, Vol. 9, No. 2, April 1994, pages 992 – 1000.

[37]. Manitoba HVDC Research Centre: "EMTDC V3 Simulation Software", *The Manitoba HVDC Research Centre*, © 1986 1988.

[38]. MathWorks: "MATLAB for Windows User's Guide", *The MathWorks*, Inc., 1991.

[39]. D.J.N. Limebeer, "Analysis and Control of AC Rotating Machines in the Presence of Series Capacitor Compensated Transmission Networks", PhD Thesis, University of Natal, Durban, South Africa, 1980.

[40]. B.S. Rigby, "Analysis and Implementation of a FACTS Series Compensator Based on a Single Voltage-Source Inverter", PhD Thesis, University of Natal, Durban, South Africa, 1997.

[41]. N.S. Chonco, "The Application of Controllable Inverter-Based Series Compensation to Power Oscillation Damping", MSc Thesis, University of Natal, Durban, South Africa, 2000.